

DOCTOR OF PHILOSOPHY

Material and structural properties of a novel Aer-Tech material

Dan-Jumbo, Fubara

Award date:
2015

Awarding institution:
Coventry University

[Link to publication](#)

General rights

Copyright and moral rights for the publications made accessible in the public portal are retained by the authors and/or other copyright owners and it is a condition of accessing publications that users recognise and abide by the legal requirements associated with these rights.

- Users may download and print one copy of this thesis for personal non-commercial research or study
- This thesis cannot be reproduced or quoted extensively from without first obtaining permission from the copyright holder(s)
- You may not further distribute the material or use it for any profit-making activity or commercial gain
- You may freely distribute the URL identifying the publication in the public portal

Take down policy

If you believe that this document breaches copyright please contact us providing details, and we will remove access to the work immediately and investigate your claim.

Material and structural properties of a novel Aer-Tech material

Dan-Jumbo, F.G.

Submitted version deposited in the University institutional repository.

Original citation:

Dan-Jumbo, F.G. (2015) Material and structural properites of a novel Aer-Tech material.
Unpublished PhD Thesis. Coventry: Coventry University.

Copyright © and Moral Rights are retained by the author. A copy can be downloaded for personal non-commercial research or study, without prior permission or charge. This item cannot be reproduced or quoted extensively from without first obtaining permission in writing from the copyright holder(s). The content must not be changed in any way or sold commercially in any format or medium without the formal permission of the copyright holders.

Some materials have been removed from this thesis due to third party copyright. Pages where material has been removed are clearly marked in the electronic version. The unabridged version of the thesis can be viewed at the Lanchester Library, Coventry University.

Material and Structural Properties of a Novel Aer-Tech Material

By

Fubara G. Dan-Jumbo

A thesis submitted in partial fulfilment of the
University's requirements for the degree of doctor
of philosophy

September 2015

Table of Contents

1	Chapter One: Introduction	9
1.1	Introduction	9
1.2	Structure Of Thesis	11
1.3	Research Aim	13
1.4	Research objectives	13
1.5	Research Methodology and methods for data analysis	14
1.6	Literature Review	14
1.6.1	Design laboratory work	15
1.6.2	<i>Analysing the data</i>	16
2	Chapter Two: Literature review	17
2.1	Cellular Concrete	17
2.2	TYPES OF CELLULAR CONCRETE	19
2.2.1	Foam Concrete	20
2.2.2	Gas Concrete	21
2.2.3	Aerated Concrete	21
2.2.4	Non-Fine Concrete	22
2.2.5	Lightweight Aggregate Concrete	23
2.2.6	Aer- Tech Concrete	24
2.3	Comparison and Grading of Types of Cellular Concrete	27
2.4	Preparation Method for Cellular Concrete	28
2.4.1	The Pre-formed foam Method	28
2.4.2	Autoclave Method of Cellular Concrete	30
2.5	Properties and characteristics Of Aerated Concrete	31
2.6	Fresh State characteristics of foam concrete	31
2.7	Consistency of Aerated concrete mix	32
2.7.1	Effect of Varying Water-solid ratio On Consistency of design density	33
2.8	STABILITY OF CELLULAR CONCRETE MIX	36
2.8.1	Effect of Varying Water-Solid Ratio on the Stability Of A Mix	37
2.9	Harden State Properties of Cellular Concrete	39
2.9.1	Physical Properties	39
2.9.2	Density of Aerated Concrete	39
2.9.3	Effect of Density on Cellular Concrete	40
2.10	Cellular Concrete Structure and Air-Void System	41
2.10.1	Effect of Air-Void on Cellular Concrete Structure	42
2.11	DRYING SHRINKAGE	45
2.11.1	Effect of Drying Shrinkage	46
2.11.2	Final values of Drying Shrinkage	46
2.12	Mechanical/Structural Properties Of Cellular Concrete	47
2.12.1	Compressive Strength Of Cellular Concrete	47
2.12.2	Effect Of Fineness Of Filler Type To Compressive Strength Of Cellular Concrete	49
2.12.3	Effect of Density to Compressive Strength Of Cellular Concrete	51
2.12.4	Effect of Water- Solid Ratio to Compressive Strength of Cellular Concrete	53
2.12.5	Effect of Curing on Compressive Strength Of Cellular concrete	54
2.13	Flexural and Tensile Strengths	55

2.14	Shear Strength of Cellular Concrete.....	56
2.15	Modulus of Deformation or Elasticity	58
2.15.1	Effect on E-Value with Different Filler Type.....	61
2.15.2	Effect On E-Values Having Additives Of Fibre Glass Or Polypropylene Fibres. 61	
2.16	Calculation Of Elastic Modulus	62
2.17	Durability Properties Of Cellular Concrete.....	63
2.17.1	Chemical attack.....	63
2.17.2	Physical Stresses	63
2.17.3	Mechanical Assault	64
2.17.4	Water absorption	64
2.17.5	Effect of Replacement of Sand with Fly Ash	65
2.18	Sorptivity of Cellular Concrete	66
2.18.1	Effect of Sorptivity Of Cellular Concrete	67
2.19	Cellular Concrete Resistance To Freeze-Thaw And Chemical Attack	68
2.19.1	68
2.19.2	Effect of Carbonation on Cellular Concrete	69
2.20	Functional Properties.....	71
2.20.1	Thermal Conductivity Of cellular Concrete	71
2.20.2	Thermal Insulation	72
2.21	Acoustical Properties.....	72
2.21.1	Acoustic Insulation	72
2.21.2	Acoustic Absorption	73
2.22	Fire Resistance Properties Of Cellular Concrete.....	74
2.23	Structural Properties of a cellular concrete	74
2.23.1	Effect of fibre reinforcement to concrete	74
2.23.2	Effect of Steel reinforcement to aerated concrete	75
3	Chapter Three: Research Methodology	76
3.1	Experimental Program.....	76
3.2	Aer-Tech Machine.....	77
3.2.1	The Mixing Mechanism of Aer-Tech	77
3.3	Mixes specification	83
3.4	Machine calibration.....	83
3.5	Aer-Tech Plant Batching and mixing Process.....	85
3.6	Aer-Tech Batch Plant	86
3.7	Aer-Tech Global automata: the new formulation method for modeling industrial systems.....	87
	Operation Definition	87
3.8	Modelling of Aer-Tech Machine based on global automata.....	90
3.9	Laboratory Development Of Aer- Tech Material	91
3.10	Material Composition of Specimen.....	91
3.11	Test Procedure.....	92
3.12	Method for making test specimen from fresh concrete.....	93
3.13	Flow table test	96
3.14	Compressive strength test.....	97
3.14.1	Fresh state conditioning of test specimen	98

3.14.2	Measurement Of Aer-Tech Specimen	99
3.15	Compressive test procedure	99
3.15.1	Compressive strength results	100
3.15.2	Assessment of Aer-Tech Failure Mode Type	101
3.16	Machine calibration.....	102
	Numerical Modelling.....	103
3.17	Neural Network Model For Aer-Tech Material	103
3.18	Describing the Neural Network Model	103
3.19	The Basic Strategy Of Neural Network	104
3.20	Types of Neural Network.....	105
3.21	Procedure for Aer-Tech Neural Network.....	105
3.22	Experimental Design.....	109
3.23	Material and mixture composition	109
3.24	Scanning Electron Microscopy	112
3.25	Particle size distribution Test for Aer-Tech material composition	114
3.26	Modulus of elasticity in compression test.....	116
3.27	Demec gauge calibration.....	117
3.28	Modulus of elasticity in compression calculation	117
3.29	Flexural strength test.....	118
3.30	Flexural strength calculation	119
3.31	Reinforced beam test.....	119
4	Chapter four: Analysis and discussion of the results	121
4.1	Introduction	121
4.2	Compressive Strength And Density	122
4.3	Compressive Strength (Mix 4.78 :1 & 5.78:1).....	124
4.4	DENSITY	126
4.5	Effect Of Additives On Compressive Strength.....	126
4.6	Effect of Machine calibration On Compressive Strength	127
4.7	Overall Performance Of Compressive strength	127
4.8	Effect of mixes proportions to the compressive strength.....	128
4.9	Modulus of elasticity.....	129
4.10	Flexural strength.....	131
4.11	Flexural strength and Compressive strength relationship	133
4.12	Structural properties of Aer-Tech reinforced beam	134
4.12.1	Ultimate moment	134
4.12.2	Mathematical theory for Aer-Tech Beam Test	135
4.12.3	Aer-Tech mid span deflection of beam.....	136
4.13	Beam behaviour in service and collapse	140
4.13.1	Deflection Behaviour Of Aer-Tech Singly Reinforced Beam.....	140
4.14	Reinforced Aer-Tech Material Strains and compressive stress	142
4.14.1	<i>Reinforced Aer-Tech beam Ductility Behaviour</i>	145
4.15	Modes of failure	145
4.17	Analysis for the scanning electronic microscopy.....	149
4.17.1	Void Characteristics Of Aer-Tech using the SEM	149
4.17.2	<i>Air-void shape parameter</i>	151
4.17.3	Air-void spacing factor	152

4.1	Particle size Analysis data for Aer-Tech material composition	153
5	<i>Chapter five: Conclusion</i>	155
5.1	Overall Material Behaviour Of Aer-Tech Novel Material	156
5.2	Overall Structural Behaviour Of Aer- Tech Reinforced Beam.....	158
5.3	Over All Scientific contribution of Thesis	159
5.4	Recommendations for future research.....	160
	<i>Reference</i>	162

List of Figures

Figure 2.1 The Pantheon (Andrew and Willaim,1978)	18
Figure2.2 Aerated Concrete (Roji, 1997)	22
Figure 2.3 Non-Fine Concrete (Chung, 1963)	23
Figure 2.4 Lightweight Concrete (Roji, 1997).....	24
Figure 2.5 Aer-Tech Material	27
Figure 2.6 Preformed foam mixing chamber (hpp/cemex.com).....	29
Figure2.7 Density against water solid ratio (Nambiar and Ramamurthy,2008).....	33
Figure2.8 Density against water solid ratio (Nambiar and Ramamurthy, 2008).....	34
Figure 2.9 The effect of foam volume on consistency of base mix (Nambiar and Ramamurthy,2008)	37
Figure 2.10 The effect of varying foam volume to stability (Nambiar and Ramamurthy,2008)	38
Figure2.11 Typical binary images (Nambiar et al, 2006)	44
Figure2.12 Satisfactory Failure Mode (BS EN 12390-3)	48
Figure2.13 Unsatisfactory failure mode (BS EN 12390-3)	49
Figure2.14 Compressive strength as a function of density (Nambiar and Ramamurthy, 2006)	49
Figure2.15 Porosity of cellular concrete (Nambiar and Ramamurthy, 2006).....	50
Figure2.16 Relationship between compressive strength and density (Nambiar and Ramamurthy, 2006)	52
Figure2.17 Ultimate shear stress of reinforced slabs	56
Figure2.18 Comparison between modulus of deformation of concrete and cellular concrete	58
Figure2.19 Relationship between calculated and measured moduli of deformation	59
Figure2.20 Stress-strain relation (INSTRON®,2008)	63
Figure2.21(A-B) Comparison on absorption property (Kolians and Georgious, 2005) ...	65
Figure2.22Comparison of water advancement into base mix and corresponding foam concrete (Nambiar and Ramamurthy, 2005).....	67
Figure3.1 Plan view and side view of the conveyor system arrangement (Patent No. 2330086, 1997)	78
Figure 0.1 Elastic modulus against time	130
Figure 0.2 Sample of the hysteresis effect	131
Figure 0.3 Compressive strength for cube tests and the equivalent cube tests	131
Figure 0.4 Flexural strength against time	132
Figure 0.5 Flexural strength and compressive strength relationship	133
Figure 0.6 Signs of Diagonal failure.....	140

List of Tables

Table 2.1 Comparison and grading on types of cellular concrete(Roji,1997).	27
Table 2.2 Comparison for compressive strength and density(Nambiar and Ramamurthy, 2006)	53
Table 2.3 Reports of few relationships on modulus of elasticity with density and compressive strength.....	62
Table 2.4 Comparison of thermal effect between cellular concrete and concrete	71
Table 4.1(4.78:1 Mix, Specimen CU701-710)	121
Table 4.2(4.78:1 Mix, with 20% water reduction, Specimen CU730 -750).....	121

Abstract

This study critically investigates the material and structural behaviour of Aer-Tech material. Aer-Tech material is composed of 10% by volume of foam mechanically entrapped in a plastic mortar. The research study showed that the density of the material mix controls all other properties such as fresh state properties, mechanical properties, functional properties and acoustic properties.

Appreciably, the research had confirmed that Aer-Tech material despite being classified as a light weight material had given high compressive strength of about 33.91N/mm^2 . The compressive strength characteristics of Aer-Tech material make the material a potential cost effective construction material, comparable to conventional concrete. The material also showed through this study that it is a structural effective material with its singly reinforced beam giving ultimate moment of about 38.7KN. In addition, the Aer-Tech material is seen as a very good ductile material since, the singly reinforced beam in tension showed visible signs of diagonal vertical cracks long before impending rapture.

Consequently, the SEM test and the neural network model predictions, carried out had showed how billions of closely tight air cells are evenly distributed within the Aer-Tech void system as well as the close prediction of NN model for compressive strength and density are same with the experimental results of compressive strength and density. The result shows that the Aer-Tech NN-model can simulate inputs data and predicts their corresponding output data.

Acknowledgement

My sincere gratitude and appreciation go to my Director of study Dr Messaoud Saidani for his constructive guidance, supportive advice and encouragement throughout the research program which had made the completion of my work possible.

Secondly, I am deeply indebted to all members of my beloved family for their saintly patience, priceless sacrifices, love and support especially my wife Mrs Blessing Fubara and our two sons David and Samuel .

I also wish to thank Dr Sam Ngambi who truly was a source of inspiration in surmounting challenges during the study period.

However, I appreciate all the research students who supported me and were a great poll of my enthusiasm to carry on till the end.

Finally, my heartfelt thanks go to Mr Sam George, Chairman of GEM-Tech Limited, for entrusting me to research this topic and giving me the unique opportunity of working on an industry relevant and novel topic. I am deeply grateful for his advice and support throughout the research.

Above all I give God all thanks and glory for a successful start and finish of this research program.

1 Chapter One: Introduction

1.1 Introduction

Aer-Tech material can be said to have evolved out from concrete, but differs greatly in material composition as well as their respective material and structural behaviour. Comparatively, Aer-Tech material apart from its foam constituent, have similar material composition with concrete. (i.e they both contains cement and sand).

Basically, in Aer-Tech material mix, the stone aggregates in concrete is replaced with air-cells, through a mechanical introduction of pre formed foam into a base mix of plastic mortar. This process is facilitated via the Aer-Tech automated machine.

The Aer-tech machine has a mixing system and atomised liquid dosing system which produces a uniform base mix of sand, cement and foam.

Essentially, what happens is that the atomizer injects air cells as small as 20 micron into the mix, as the mixing screw mixes the sand and cement from the hopper with water to produce consistent and evenly distributed material mix.

The final Aer-Tech material shows possession of characteristics, similar to that of geodesic structure, known as the world strongest material.

Precisely, the Aer-Tech material can be defined as a free flowing and self-levelling cementitious material that has more than 10% by volume of foam and

35% by volume of water in its composition of sand, cement and Aer-Tech sol catalyst.

More so, the foam constituent of Aer-Tech is introduced into the mix by a pre formed foam mechanical process. This involves the passing of a dilute surfactant solution known as Aer-Tech sol, with compressed air through a tube.

This process produces high density foam with an expansion factor in the order of 40 to 1 (ATS 10, 2006).

Besides, Aer-Tech material can be describe as a cement – sand bond admixture that comes in various densities than conventional concrete, whose density in practice is within 2200 to 2600 kg/m³. In Aer-Tech material a greater percentage of its constituent is water, as it contains 400 litres of water per cubic metre, and 83 litres of foam per cubic metre, material density of Aer-Tech ranges between 1600-1850 kg/m³.

As the material are produced via an automated machine. The targeted density is achieved through automated data control panel on the Aer-tech machine.

The idea of using lightweight concrete as a structural material is starting to spread among engineers, as the self-weight of the concrete can represent a large percentage of the load on the structure.

It could be noticed that by reducing the self-weight, the cross section of the members will be reduce and yet it is economic and environmentally sustainable.

Appreciably, following the advantage of reducing the self-weight of concrete and stresses concrete structures imposes on the earth mass and the underlying economic and environmental benefit, the use of Aer-Tech material brings to the construction industry. It is apparent, that a large percentage of cost is saved using the material than conventional concrete.

Similar studies have shown that the base mixes of uniform distribution of air-cells in a plastic mortar give a higher strength (Nambiar and Ramamurthy,2006). It is also said that bigger pores in the mix, influences its strength.

This is correct as the pore system in cement-base material is conventionally, classified as a gel pores, capillary pores, macro-pores due to deliberately Entrained air in material structure (Visagie and Keasely,2002).

However, research had shown that the gel pores do not influence the strength of cellular concrete through its porosity, but the capillary pores and other large pores are responsible for reduction in strength and elasticity (Nambiar and Ramamurthy,2006).

1.2 Structure Of Thesis

The first chapter of this thesis gives a brief introduction of Aer-Tech material and its relationship with similar materials, a detailed outline of aim and objectives for the research work, as well as providing the proposed methodology to be followed during investigation.

The second chapter covers extensive reviews of related work carried out in the past by other researchers. This chapter further gives background information for readers of this work. it include contribution and views of researchers of lightweight materials like foam concrete, gas concrete, aerated concrete etc.

The third chapter gives an in-depth coverage on testing programmes that are carried out by the author all in accordance to British standard, the importance of each test, the global automata principle for Aer- Tech machines and some basic mathematical theory to support the test.

Whilst, the fourth chapter covers the discussion of the results and the analysis of the data obtained from the laboratory work, it extensively discusses some of the material properties like compressive strength, flexural strength, elastic modulus, and workability for different mixes. In addition, it investigates the structural behaviour of reinforced Aer-Tech beam and comparing it to that made with normal concrete, along with discussing the advantage of using fibre mesh with this material.

The last chapter includes a summary of the main findings, the contribution to knowledge this research had brought and some recommendation for future researchers. A complete list of references and bibliography is provided at the end of the thesis followed by an appendix that contains tables and information needed for the research.

1.3 Research Aim

The overall aim of this research is to investigate the material and structural capability of Aer-Tech novel material. The Aer-Tech novel material can be said to have evolved out from concrete, but differs greatly in material composition, as well as their respective material and structural behavior.

This research had extensively investigated the material and structural behavior of Aer- Tech novel material through series of experimental test.

1.4 Research objectives

Below are the specific objectives:

- Carry out experimental program for an in dept analysis on material properties of Aer-Tech material with regards to density, compressive and flexural strengths.
- Carry out structural testing of $1500 \times 180 \times 75$ reinforced beams made from Aer-Tech and compare their performance with similar elements made from conventional reinforced concrete.
- Determine the relationship between compressive strength and flexural strength of Aer-Tech material.
- Investigate the effect of fibre glass and plasticizer in the material.

- Critically assess the consistency and workability of Aer-Tech material.

1.5 Research Methodology and methods for data analysis

The research program consists of both experimental testing as well as numerical modeling. The experimental program consists of carrying out the following tests:

- Compressive strength test
- Flexural Strength
- Elastic Modulus
- Drying shrinkage (In-house method)
- Effects of adding Fibre glass to the mix,
- Effects of super plasticizers in the mix

Whilst, the numerical programme consist of;

- The neural network
- SEM (scanning electronic microscopy
- Particle size Analysis.

1.6 Literature Review

The literature search was carried out throughout all phases of the project.

The literature review was concentrated on the following keywords:

- Lightweight concrete.

- Aerated concrete.
- Cellular concrete.
- Gas concrete.
- Foam concrete.
- Concrete properties, such as compressive strength, flexural strength, elastic modulus and workability.

Because, Aer-Tech is a new concept, most of the information that was found is related to the subject in some aspect, but most of the research conclusion will depend on analysing the results data from the laboratory work.

1.6.1 Design laboratory work

With a clear understanding of the research objectives, the author to ensure critical assessment of Aer-Tech material carried out over 75 mix run of Aer-Tech material, with a specimen output of about seven hundred (700) Aer-Tech specimen. These specimens were produced majorly in cubes, then mini beams and reinforced beams.

All Aer-Tech specimens are air-cured to be tested for compressive strength, elastic modulus and flexural strength at seven, fourteen, twenty-eight days and fifty six days. In addition, workability and reinforced beam behaviour will be tested. Some of the mix has fibre mesh and plasticizers in it, and the reason for choosing this mix is to study the effect of these additives in Aer-Tech mix.

More so, Aer-Tech laboratory works are structure in accordance to the British Standards (BS EN 12390-3:2000-2003). This had help designing the laboratory

work and choosing the right machines for the tests, as it explain how to perform the best tests and it explain the way to analysis the data coming from each individual test. Plus, using the Standards, the reinforced beams could be designed and then the result could be checked against the laboratory results.

The Standards that are going to be used in this research are listed in the table below according to their specification:

BSI reference Title

BS 8110-1: 1997 Structural use of concrete – Part1: Code of Practice for Design and Construction.

BS EN 12390-3:2003

Testing hardened concrete – Part3: Compressive strength of test specimens.

BS EN 12390-4:2000

Testing hardened concrete – Part4: Compressive strength – Specification for testing machines.

BS EN 12390-5:2000

Testing hardened concrete – Part5: Flexural strength of test specimens.

BS EN 13412:2006 Products and systems for the protection and repair of concrete structures –Test methods – Determination of the modulus of elasticity in compression

1.6.2 Analysing the data

Following the volume of results obtained from laboratory experiment and need for effective analysis of data's, a matlab software programme was used to construct a numerical model for predictions of results in comparison to experimental results.

2 Chapter Two: Literature review

2.1 Cellular Concrete

Precisely, the cellular concrete is a class of lightweight concrete, which is defined as “ cement-bonded material that is manufactured by blending a very fluid cement paste(slurry) or mortar with a separated manufactured foam (resembling shaving leather) in to a grey mousse with high fluidity.

It is defined by (Tikalsky, 2004) as a concrete composed of cementitious mortar surrounding disconnected random air bubbles, with the air typically occupying more than 50% of the volume. The air bubbles are a result of gas formed within the mortar or foam introduced into the mortar mixture.

Specifically, the volume between the slurry and the foam determines the density of the foam concrete. The presence of the cement causes the material to be cohesive (strength/stiffness) after hydration of the cement. Its overall matrix can be described as a pore structure surrounded by cement slurry” (Foam Concrete Limited, 2008).

Cellular concrete can be describe as a type of concrete whose components includes an expanding agent that increases the volume of the mixture while giving additional qualities such as reduced dead weight (Lazim,1978).As defined by (American Concrete Institute, 2009): “*cellular concrete is referred as a low density, product consisting of Portland cement- pozzolan, or lime silica pastes*

containing blinds of these ingredients and having a homogeneous void or cell structure, attained with gas-forming chemicals or foaming agents”.

Cellular concrete is lighter than conventional concrete, with a dry density of 300 kg/m³ up to 1840 kg/m³ (87 to 23% lighter). It was first introduced by the Romans in the second century where ‘The Pantheon’ has been constructed using pumice, the most common type of aggregate used in that particular year (Roji,1997). From there on, the use of lightweight concrete has been widely spread across other countries such as USA, United Kingdom and Sweden.

The main specialties of cellular concrete are its low density and thermal Insulation properties. Comparatively, the advantages are apparent as uses of cellular concrete leads to reduction of dead load, faster building rates in construction and lower haulage and handling costs. The building of ‘The Pantheon’ of lightweight concrete material is still standing eminently in Rome until now for about 18 centuries as shown in figure 2.1.It confirms that the lighter materials can be used in concrete construction and has an economical advantage.

This item has been removed due to third party copyright.
The unabridged version of the thesis can be viewed at
the Lanchester library, Coventry university.

Figure 2.1 The Pantheon (Andrew and Willaim,1978)

In accordance to (Orchard,1979) cellular concrete could be produced in the following ways:

1. By mixing normal air entraining agents with cement or cement and sand in special high speed or whisking mixers.
2. By mechanically entraining foam in a plastic mortar.
3. By making foam separately and subsequently adding a given quantity to a known density plastic mortar.
4. The formation of air bubbles through the addition of calcium carbide (CaC_2)
5. By adding hydrogen peroxide (H_2O_2) to a base mix.
6. By adding aluminum powder or zinc powder to the cement mortar

2.2 TYPES OF CELLULAR CONCRETE

Cellular concrete can be prepared either by injecting air in its composition or by aerating a plastic mortar. The former and latter are said to have been prepared by two major method of preparing cellular concrete. They are; preformed foam method and autoclave or mixed method, details of the said methods will be discussed later in this chapter.

Particularly, cellular concrete can be categorized into five groups:

- Foam concrete
- Gas concrete
- Aerated concrete
- Non-fine concrete
- Lightweight aggregate concrete

2.2.1 Foam Concrete

Generally, foam concrete is defined as concrete created by uniform distribution of air bubbles throughout the mass of concrete” (<http://www.ibeton>). It is produced by mechanically mixing of foam prepared in advance with concrete mixture and not with help of chemical reactions.

Intrinsically, foam concrete could be describe as free flowing, self- leveling , material that does not require compaction. Its main advantage over more traditional fill or sub base material is ability to flow around pipes and cables in situation where crowded excavation would make it difficult to adequately compact other materials. It is also a useful material to apply where the side stability of trenches is poor or where there is undercutting of the adjacent carriage. The lack of compaction also helps towards the reduction of white knuckle syndrome (<http://www.ibeton>).

The foam concrete is a low density cementitious material, due to replacement of aggregate by air voids from air entraining or foaming agent.

The mix of this material is restricted to comply with the 28 days compressive strength. Thus the maximum permitted strength for all foam concrete mixes is 10N/mm^2 . Therefore care should be taken not to exceed the maximum values for two reasons, firstly above 14N/mm^2 it starts to behave more like structural concrete and may crack and produce reflective cracking.

2.2.2 Gas Concrete

This is another form of lightweight concrete, which is produced from different mixture of silica, sand, cement, lime, water and aluminum cake which produces gas. However, it is said to be produced by a chemical process of the above constituent material mix. The gas concrete is five times lower than the usual concrete material. In addition, the heat transfer that exists in gas concrete is reduced fivefold by the bubbles inside. It is sometimes called autoclaved aerated concrete '(AAC)', this is due to air bubbles arising in the chemical reaction. More so, according to research, the gas concrete exhibits an extraordinary properties of the heat insulation at high or low outside temperature. In accordance to (Autoclave aerated concrete, 1993), gas concrete is a form of aerated concrete produced by the formation of microscopic air gas bubbles within the mass during the liquid or plastic phase. The said air bubbles are uniformly distributed and are retained in the matrix on setting and later hardening to produce a cellular structure.

2.2.3 Aerated Concrete

Aerated concrete is a form of cellular concrete without a coarse aggregate, and can be regarded as an aerated mortar. Typically, aerated concrete is made by introducing air or other gas into a cement slurry and fine sand. In commercial practice, the sand is replaced by pulverized fuel ash or other siliceous material, and lime maybe used instead of cement (Roji,1997).

Particularly, there are two methods to prepare the aerated concrete. The first method is to inject the gas into a plastic mortar by means of a chemical reaction. The second method, air is introduced either by mixing-in stable foam or by whipping-in air, using an air-entraining agent. The first method is usually used in precast concrete factories where the precast units are subsequently autoclaved in order to produce concrete with a reasonable high strength and low drying shrinkage. The second method is mainly used for in-situ concrete, suitable for insulation roof screeds or pipe lagging. Figure 2.2 shows the aerated concrete.

This item has been removed due to third party copyright. The unabridged version of the thesis can be viewed at the Lanchester library, Coventry university.

Figure 2.2 Aerated Concrete (Roji, 1997)

2.2.4 Non-Fine Concrete

This is another form of cellular concrete composed of cement, fine aggregate and uniformly distributed voids formed throughout its mass. Besides the main characteristics of this type of lightweight concrete is it maintains large voids and not forming laitance layers or cement film when placed on the wall. **Figure 2.3** shows an example of No-fines concrete.

This item has been removed due to third party copyright.
The unabridged version of the thesis can be viewed at the
Lanchester library, Coventry university.

Figure 2.3 Non-Fine Concrete (Chung, 1963)

2.2.5 Lightweight Aggregate Concrete

The lightweight aggregate can be natural aggregate such as pumice, scoria and all of those of volcanic origin and the artificial aggregate such as expanded blast-furnace slag, vermiculite and clinker aggregate.

The main characteristic of this lightweight aggregate is its high porosity, which results in a low specific gravity (Chung, 1963).

The lightweight aggregate concrete can be divided into two types according to its application: one is partially compacted lightweight aggregate concrete and the other is the structural lightweight aggregate concrete.

The partially compacted lightweight aggregate concrete is mainly used for two purposes that is for precast concrete blocks or panels and cast in-situ roofs and walls. The main requirement for this type of concrete is that it should have adequate strength and a low density to obtain the best thermal insulation and a low drying shrinkage to avoid cracking (Roji, 1997).

Structurally lightweight aggregate concrete is fully compacted similar to that of the normal reinforced concrete of dense aggregate. It can be used with steel reinforcement as to have a good bond between the steel and the concrete. The concrete should provide adequate protection against the corrosion of the steel. The shape and the texture of the aggregate particles and the coarse nature of the fine aggregate tend to produce harsh concrete mixes. Only the denser varieties of lightweight aggregate are suitable for use in structural concrete (Roji,1997). Figure 2.4 shows the feature of lightweight aggregate concrete.

This item has been removed due to third party copyright. The unabridged version of the thesis can be viewed at the Lanchester library, Coventry university.

Figure 2.4 Lightweight Concrete (Roji, 1997)

2.2.6 Aer- Tech Concrete

It may be defined as a cementitious material with more than 10% by volume of foam mechanically entrained in the plastic mortar.

Aer-Tech is a cement-sand bond admixture that comes into various densities than normal concrete which is made by aggregates. In practice, the density of normal concrete lies within the range of 2200 to 2600 kg/m³. The lower bulk density of Aer-Tech is produced by using a special machine that produces

cellular concrete using special foam, and could produce concrete in various densities. In theory the cellular concrete that is produced by Aer-Tech is not concrete in the traditional form as there is no aggregate present in the mix.

The basic principle of Aer-Tech concrete is to reduce the density of concrete by introducing Billions of air voids within the hardened cement paste. Although, this principle was used before by the use of gas, aerated and foam concrete. However, Aer-Tech is aimed at producing a more controlled and constant mix using this technology.

Consequently, it is obvious that the Aer-Tech material is similar to other light weight material in principle of which this research is expected to clear. However, in spite of its similarities, the Aer-tech product should not be confused with the other lightweight aerated product, considering the fact that some of these products had been in used for about 30 to 40 years. And for many reason until now, foam concrete has been considered only suitable for low quality application. These light weight aerated product are characteristically associated with low strength products in the construction industries (up to a maximum compressive strength of (6to 10 N/mm²).Which obviously not capable of being used for high strength applications or uses.

More so, in a similar fashion , the Aer- tech products is a unique process of producing a lightweight cementitious material capable of achieving strengths

comparable with normal concrete. Aer-Tech has been tested and has shown proven compressive strengths of 32N/mm^2 (4640 p.s.i.)

The Aer-Tech process is a patented machine which has been designed to achieve a homogenous mix with efficient blending and uniform mixing with consistency of ingredients such as cement, sand, water and air cells to reduce material content. The end product is closer to consistency of steel rather than concrete. All the ingredients including the air cells are evenly distributed throughout the mix and remain so when pumped from the machine through the delivery mechanism. The remarkable consistent distribution of the air cells creates a geodesic structure, the second strongest structure in the world. When Aer-Tech has cured, the billions of air cells are enraptured within the material, whereby they cannot and do not collapse, but coalesce when force is applied.

Aer-Tech has greater potential than any other previous basic construction material. Properly developed, it will create in the industry a deeper and wider existing building material. It provides a process and end product that places cementitious building material at the leading edge over other construction material or product. With a focus objective on this research work, the under listed test will be carried out to ascertain the claims on the Aer-Tech products. Figure 2.5 shows an example of Aer-Tech material.



Figure 2.5 Aer-Tech Material

2.3 *Comparison and Grading of Types of Cellular Concrete*

Table 2.1 Comparison and grading on types of cellular concrete(Roji,1997).

This item has been removed due to third party copyright. The unabridged version of the thesis can be viewed at the Lanchester library, Coventry university.

2.4 Preparation Method for Cellular Concrete

Cellular concrete can best be prepared by two distinct methods known as;

- Preformed foam Method
- Autoclave Method

2.4.1 The Pre-formed foam Method

It is a mechanical process, where special devices such as a foam generator, which produces foam by exerting a high shearing force on a diluted foaming agent in the presence of (compressed) air. The foaming agent is a surfactant typically made from animal proteins.

Sand, fly ash, stone dust or other fillers may be added to save money or achieve particular properties. (Concrete Limited, 2003). The fresh foam has a paint-like viscosity, making it easy to convey via pumps and hoses. The foam generator produces foam concrete with different densities based on requirements and specification. Hereto the preformed foam method comprises of water and small quantity of foaming agent named as listed below;

- a) Saponified wood resins
- b) Saponified vinsol resins
- c) Certain sodium compounds of aliphatic and aromatic sulphates
- d) Protein based compounds.

Using this method, the foam concrete product is achieved by blending together already a mortar mix and foam in a substantially closed chamber. The mortar mix

includes all the component of the eventual foam concrete. For mix constituent blending, the mix is introduced into a closed chamber. Where each of the chambers is occupied by a rotary mixer, which occupies majorly the entire space defined by the chamber, each mixer being substantially disc shaped but being provided with projections extending out of the plane of the disc. On rotation of the mixers, the projection on the walls of the chambers helps greatly in producing a uniform mix. This conforms to analogy of (Dyson, 1983) that this arrangement ensures efficient blending of the walls of the chambers

Besides, it is important to know that foam concrete made by this method, is highly homogeneous in the sense that the gas bubbles are discrete and of a uniform size are such they are homogeneously spread throughout the foam concrete. Figure 2.6 shows a diagram of inner chamber of a preformed machine. More so, preformed foam machines could produce foam concrete with different densities ranging from 200kg/cub.m to 1600kg/cub.m

This item has been removed due to third party copyright. The unabridged version of the thesis can be viewed at the Lanchester library, Coventry university.

Figure 2.6 Preformed foam mixing chamber (<http://cemex.com>)

2.4.2 Autoclave Method of Cellular Concrete

Interestingly, this method of foam concrete was first developed in Sweden in the late 1920s. It is mostly called the Autoclave cellular concrete (ACC), due to its harden state material (lightweight concrete) is cured under elevated pressure inside a special kilns called autoclaves (Portland Cement Association,2009).

The basic raw materials for autoclave are Portland cement, limestone, aluminum powder, water and a large proportion of a silica-rich material, usually sand and fly ash. During this period once the raw material are mixed into slurry and poured into greased moulds, the aluminum powder reacts chemically to create millions of tiny hydrogen gas bubbles. These microscopic, unconnected cells cause the material to expand to nearly twice its original volume (similar to the rising of bread dough) showing clear properties of lightweight autoclave concrete ACC.

After the setting time ranging from thirty minutes (30min) to four hours, the foam like material is hard enough to be wire cure into the desired shapes and moved into an autoclave oven for subsequent curing.

The autoclave uses high- pressure steam of about 356°F(180°) to accelerate hydration of the concrete and spur a second chemical reaction that gives ACC its strength, rigidity and dimensional stability.

Autoclaving can produce within eight to fourteen hours of mix a concrete strength equal to strengths product of lightweight air cured 7days,that are usually shrink

wrapped and transported directly to the construction site. The autoclave cellular concrete is one fourth of the weight of conventional concrete.

2.5 Properties and characteristics Of Aerated Concrete

Considering the significant importance, the material and structural properties of cellular concrete, posed on its characteristics performance.

The author had extensively classified these properties into two basic state, they are the fresh and harden state properties (Ramamurthy and Kinhamandan, 2009).

Subsequently, the fresh state properties are subdivided into the consistency and stability properties.

While the harden state properties are further classified into the physical properties which consist of (density, drying shrinkage, porosity and air-void system, absorption and sorption properties), mechanical properties are (the compressive strength, modulus of elasticity), the durability properties and functional characteristics (thermal conductivity, acoustical properties and fire resistance).

2.6 Fresh State characteristics of foam concrete

According to (Kunhanandan, Nambiar, and Ramamurthy, 2006), unlike normal concrete, cellular concrete cannot be subjected to any type of compaction or vibration that would affects its design density.

The fresh state characteristics are said to be outstanding for cellular concrete due to self-identity tendency of flow ability and self –compatibility. It could also be describe as the plastic state of freshly prepared aerated concrete.

Consistency and Stability properties are the two basic fresh state characteristics of cellular concrete. These properties are determining function of design mix ratio.

Preliminary studies by (Nambiar and Rammamurthy, 2006a) show that design densities are achieved only by a particular consistency of base mix. This is expressed in terms of water – solid ratio, which varies with filler type.

Consequently, the consistency of foam concrete is either lower (mixture is too stiff causing the bubbles to break) or higher(slurry becomes too thin to hold the bubbles resulting in segregation) as this leads to increase in density.

2.7 Consistency of Aerated concrete mix

The idea of consistency of cellular concrete is describe as a measure of uniformity in its material composition or a measure of spreadability of material mix. This can be measured by flow %and time, determined by use of a standard flow cone. (ASTM, Specification for flow, 1998) and the flow time using marsh cone.

The later involves filling a portion of an aerated base mix into a cone, then lifted and an average flow of the mix is measured without raising and dropping on the

flow table (Nambiar and Ramamurthy, 2006), because doing this may affect foam bubbles entrained in the mix.

As concluded by (Nambiar and Ramamurthy, 2008) consistency of base mix is defined as that water solid ratio at which design density is attained. This is an important factor, which has significant effect on the stability of the mix.

On the other hand the fluidity of aerated concrete is measured using the marsh cone test (Jones et al., 2003). In this test, the flow time which is an indication of plastic viscosity (ranged between 210 and 10s) are then measured with different mixes by varying mixture parameters.

2.7.1 Effect of Varying Water-solid ratio On Consistency of design density

Considerably, consistency of a mix is affected by the introduction of foam or any filler material to the wet mix of cellular concrete. These disruption in the consistency contribute significantly in determination of the mix design density.

-

This item has been removed due to third party copyright. The unabridged version of the thesis can be viewed at the Lanchester library, Coventry university.

Figure 2.7 Density against water solid ratio (Nambiar and Ramamurthy, 2008)

This item has been removed due to third party copyright. The unabridged version of the thesis can be viewed at the Lanchester library, Coventry university.

Figure 2.8 Density against water solid ratio (Nambiar and Ramamurthy, 2008)

Figure 2.7 and Figure 2.8 shows a level of variation on density ratio (measured fresh density divided by design density) with water-solid ratio for mixes with different filler type for each design densities.

According to (Nambair and Ramamurthy, 2006), at lower water-solid ratios, ie at lower consistency, the density ratio is higher than unity. The mix is too stiff to mix properly thus causing the bubbles break during mixing resulting to increased density. Whilst at higher water-solid ratio there is also an increase in density ratio, which causes mix slurry too thin to hold the bubbles, resulting in segregation of the foam from the mix along with the segregation of the mix itself, there by leading to increase in density.

Furthermore, consistency of a cellular concrete, depends also on the filler type (Nambiar and Ramamurthy, 2006). With reference to filler type replacement, sand with fly ash, it is observe that fly ash exhibit characteristics of higher surface area than sand mix due to fineness property of fly ash. The resultant effect of fly

ash larger surface area leads to relatively higher water- solid ratio requirement, compared to mixes with sand.

Secondly, cellular mix with fly ash requires less foam volume due to the low specific gravity (2.09) compared to that of sand whose specific gravity is (2.52).

Ultimately, the effect on the behavioral pattern of cellular concrete due to replacement of sand with fly ash show that water-solid ratio of a fly ash mix has a marginal increase, while its subsequent volume of foam requirement has a steep reduction.

Appreciably, observation made by (Nambiar and Ramamurthy, 2008) recommended ways to avoid the effects of breaking bubbles and excessively thin slurry in cellular mix. A higher water-solid ratio is required and the use of super plasticizer, which reduces considerably the water demand.

This is attributed to (i) reduced self-weight and greater cohesion resulting from higher air content (ii) adhesion between the bubbles and solid particles in the mix increase stiffness of the mix.

Although, reduction in the water content achieved is relatively lower at higher foam volume. This show that there is a bit of interaction between the foam volume in the mix and super plasticizer dosage.

Quantitatively, consistency values are modified by the foam content (i.e. volume of air in the mix).

However, subsequent reduction in the consistency of mix in the presence of foam maybe attributed to reduced self-weight and greater cohesion resulting from higher content (Karl and Worner,1994).

2.8 STABILITY OF CELLULAR CONCRETE MIX

The word stability which is often referred as a measure of consistency of any given mix, is defined as the consistency at which the density ratio is nearly one

(i.e. a measure of design density) without any segregation and bleeding.(Nambiar and Ramamurthy,2006).

Consequently, the design density is said to be of higher than unity at both lower and higher consistencies, this further buttresses the fact that consistency of base mix is a major determining factor to the stability of the mix.

More so, as reported by (Nambia and kamamurthy, 2009) stability of a base mix can be measured by comparing (i) The calculated and actual quantities of foam required to achieve a plastic density within 50kg/m^3 of design value, and (ii) calculated and actual water-cement ratio.

In view of this inherent link between stability and consistency of a mix, there is need for determining the water-solid ratio which would satisfy both stability and consistency of a mix.

2.8.1 Effect of Varying Water-Solid Ratio on the Stability Of A Mix

Basically, the direct and indirect effect on consistency of cellular concrete has a corresponding effect on the stability of the mix. This is so because, consistency which is a measure of flowability and spreadability, acts integrally as a function of stability. Investigation made by (Nambiar and Ramamurthy,2009) on the different filler-cement ratio is shown in illustrations of Figure 2.9 and Figure 2.10, shows their findings for fly ash replacement level and varying foam volume percentage in mix, this confirms that for every cellular concrete mix there is a band of water - solid ratio within which a stable mix can be produced.

This item has been removed due to third party copyright. The unabridged version of the thesis can be viewed at the Lanchester library, Coventry university.

Figure 2.9 The effect of foam volume on consistency of base mix (Nambiar and Ramamurthy,2008)

Figure 2.9 shows the water–solid ratio of a cellular concrete mix with fly ash increases due to increase in surface area of fly ash as against sand.

This item has been removed due to third party copyright. The unabridged version of the thesis can be viewed at the Lanchester library, Coventry university.

Figure 2.10 The effect of varying foam volume to stability (Nambiar and Ramamurthy,2008)

Figure 2.10 Shows effect on stability of a mix with fly ash by varying foam volume. Intrinsically, from the figure it is apparent that increase in foam volume result to increase in water-solid ratio of cellular concrete mix. This occurs because there is an increase of adhesive force which exists between the solid material and foam volume, there by causing the mix to be stiffer.

This stiffness further affect stability of cellular concrete, due to breaking of air bubbles during mixing. To avoid this, higher water-solid ratio is required in the base mix. Ultimately, this effect confirms the importance of mix stability to the fresh state characteristics of cellular concrete.

2.9 Harden State Properties of Cellular Concrete

Fundamentally, the harden state of cellular concrete is characterized by dry state product of a freshly prepared cellular concrete .The harden state is an important state of cellular concrete, as it determines the following properties; the physical properties, mechanical properties, durability properties and acoustical properties.

2.9.1 Physical Properties

2.9.2 Density of Aerated Concrete

Density is defined as mass per cubic volume of a material. The use of density in aerated concrete , is of immense importance to its formation .This is so, because the idea of cellular concrete originate from pressing concern on bulk density reduction in conventional concrete.

Besides, the effect of density of a cellular concrete is apparent in either fresh or harden state. The fresh state density is required for mix design and casting control purposes. Essentially, many physical properties of foam concrete are dependent upon its density in the harden state.

However, in specifying density of material a close definition of its degree of dryness is needed, this will help describe the moisture condition of material (Valore, 1954).

In addition, density can be measured by taking the overall weight of material per the unit volume of the material.

2.9.3 Effect of Density on Cellular Concrete

Since, density in cellular concrete is a function of solid material with air bubbles. It can be controlled by the amount of reduction or increase made on water solid – ratio or air-water solid ratio during mixing.

In accordance to (ACI Committee 213, 2003), density properties of cellular concrete are predominantly influenced by cement, water and air content.

For this reason, density effect is intense in determining aerated freshly state properties such as material mix consistency and stability.

Intrinsically, for aerated concrete, the higher the density of solid in a mix, the lower the consistency, because the mix becomes too thick, leading to breaking of air bubbles.

(McCarmick, 1967) studied the effect of types of fine aggregates, aggregate gradation, types of foam and sand-cement ratio on wet density of aerated concrete, whilst he reported that wet densities within 5% of the design densities can be achieved by using solid volume calculations.

In addition the cement-sand based non-autoclaved preformed aerated concrete has relatively higher density, than autoclaved aerated concrete.

Further investigation made by (Nambia and Ramamurthy,2009), on comparative studies with different mix of sand or fly ash, confirms that replacement of sand with fly ash helps in reducing the density with increasing strength (Durack, 1998).

Ultimately, replacement of sand with fly ash due to lower specific gravity of fly ash with sand results in reduction of volume requirement of foam and a subsequent increase in strength absorption properties.

2.10 Cellular Concrete Structure and Air-Void System

Precisely, the structure of cellular concrete is characterized by pores formed during chemical process (hydration) that occurs between hydrogen gas, air and water at casting and rising stage (Comite' Euro-international du Beton,1978).

These formed pores are also classified as the air-void system, which fundamentally remains the main basis of cellular concrete. The air-void system, are introduced through the use of foam as a constituent material or entrained air in material mix.

Considerably, pores sizes and other physical characteristics subdivide the pores system into micro pores and macro pores. Which implies that the micro pores are classified as capillary active pores, whilst the remaining pore volumes are considered as the macro pores. Clearly, (Visagie and Keasely, 2002) stated that the pore structure of cellular concrete, consist of gel, capillary pores and air voids.

Besides, the pore structure of cellular concrete is mostly predetermined by its porosity, permeability and pore size distribution. These are very important characteristics of cementitious material. All these significantly contribute to influences its behavioral properties on strength, durability, thermal conductivity, capillary and frost resistance of a cellular concrete.

2.10.1 Effect of Air-Void on Cellular Concrete Structure

The air void system in cellular concrete is mainly characterized by a few parameters like volume size, size distribution, shape and spacing between air-void.

According to (Ramamurthy et al, 2009) air-void distribution is one of the most important micro properties influencing strength of the cellular concrete. By this analogy, study shows that cellular concrete with narrow air-void distribution gives higher strength.

Similar investigation was carried out on different filler type, such as replacing sand with fly ash. Results, proved that fly ash helps in achieving more uniform distribution of air-void by providing uniform coating on each bubble and thereby prevent merging of bubbles (Ramamurthy et al, 2009).

Appreciably, at higher foam volume, the merging of bubbles resulted in wide distribution of voids sizes leading to lower strength (Nambiar and Ramamurthy, 2007).

Parameters like, the air void size and its distribution, the compressive strength, sorption and absorption characteristics are greatly affected by the (void/paste ratio, spacing of air-voids, number of air-void (volume).

Subsequently, study on air-voids system of cellular concrete made of cement together with granulated blast furnace slag mixture, are designed to achieving a high strength-to-weight ratio, an air –void system with a spacing factor, air-void size and air content of 0.04mm,0.12mm and 42% respectively were reported to be optimal (Wee,2006).

Essentially, the paste/void ratio has an enormous effect on characteristics properties of cellular concrete, several study had shown that, a mix with sand gives less paste, due to higher foam volume resulting to lesser presence of capillary pores, evidence of lower sorptivity and absorption. but a mix with fly ash gives higher paste , due to less volume of foam taken in a given water/solid ratio increase in paste , result to more capillary pores presence in the mix.

This item has been removed due to third party copyright. The unabridged version of the thesis can be viewed at the Lanchester library, Coventry university.

Figure 2.11 Typical binary images (Nambiar et al, 2006)

However, (Nambiar et al., 2006) concluded the following by using typical binary images as shown in figure 2.11.

- (1) “For a given mix type sorptivity and water absorption are mainly controlled by capillary porosity, while the reduction in strength with density is mainly governed by volume of entrained air voids”
- (2) (Nambiar *et al*, 2006) concluded that “out of the air-void parameters investigations shows that volume, size and spacing have influence on the strength and density.”

Mixes with a narrower air-void size distribution showed higher strength, whilst at higher foam volume, merging of bubbles seems to produce larger voids, which results in wide distribution of voids sizes and lower strength.

2.11 DRYING SHRINKAGE

Short and Kinniburgh (1978) defined drying shrinkage “as the difference between the length of a specimen which has been immersed in water and the length when subsequently dried, all under specified conditions, expressed as a percentage of the length of the specimen”.

Precisely, the cellular concrete possesses high drying shrinkage due to absence of aggregate. This property of cellular concrete exhibiting clear sign high drying shrinkage, comparable to conventional concrete, it is observed to be ten times more (Valore, 1954).

More so, several investigation had shown that autoclaving cellular concrete produces results of very reduced drying shrinkage significantly by 12-50% of moist-cured concrete, due to change in mineralogical composition) (Schubert,1983).

This conforms to the studies of (Andrew and William,1978)as they stated that cellular concrete, which are aerated rich mortar, has very high shrinkage unless the products are high-pressure steam-cured and by this treatment changes of a physicochemical nature take place in cement minerals, which in turn lead to reduction in drying shrinkage.

2.11.1 Effect of Drying Shrinkage

Drying shrinkage is described as a process which results to water loss from the cellular material, thus a subsequent rewetting causes swelling (RILEM, Recommended Practice, 1993).

Further research has shown, that a cellular concrete exposed to carbon dioxide (CO_2), lead to the material undergoing two types of drying shrinkage (1) the carbonation shrinkage and (2) the hygral shrinkage, which is a superimposed by carbonation shrinkage.

Drying shrinkage depends on the mineral binding agent. Whilst dry shrinkage of cellular concrete reduces with density (Jones and McCarthy, 2003), this effect is caused by lower paste content affecting the shrinkage in the low- density mixes.

In view of comparative study on shrinkage behaviour having sand or fly ash as filler type, foam concrete with sand report shows smaller drying capacity as compared to fly ash particles (Jones and McCarthy, 2003)

2.11.2 Final values of Drying Shrinkage

The final values of drying shrinkage are almost independent of the materials dry density. The final shrinkage from vapour saturated state as a function of relative humidity.

Appreciably, a considerable amount of shrinkage of cellular concrete is not reversible after it is dried for the first time.

The hygral final equation is written as:

$$E_{hf} = \alpha_h \Delta H \text{-----} (2.1)$$

In this equation E_{hf} denotes the final hygral strain in equilibrium, ΔH stands for the difference in relative humidity (%), while α_h stands for coefficient of linear hygral dilatation.

2.12 Mechanical/Structural Properties Of Cellular Concrete

2.12.1 Compressive Strength Of Cellular Concrete

According to (RILEM, 1993) compressive strength is the overall resisting capability of a cellular concrete on application of axial compression.

More so, the compressive strength for cellular concrete is dependent on its density. This is such that's light increase in density leads to corresponding increase in compressive strength (RILEM,1993).

In addition compressive strength decreases exponentially with a reduction in density of cellular concrete (Kearsley, 1996).

Ultimately, compressive strength is measured through the compressive strength test using cubes or cylinders specimens.

Previous research has indicated that, the specimen size and shape, the method of pore formation, direction of loading age water content characteristics of ingredient used, specimen planes or cap piling material and method of curing are reported to influence the strength of cellular concrete (Valore,1954).

Comprehensively, other parameters that influence the strength of cellular concrete are cement-sand, water cement-sand and water cement ratios, curing pattern and particles size distribution of sand and type of foaming agent used.

Generally, “strength is influenced by both the water- cement ratio of the mix and by the volume of induced voids (Niville, 1995).

In addition BS EN 12390-3 specifies that there are modes of failures that are accepted and some that are not as shown in Figure 2.12 and Figure 2.13.

This item has been removed due to third party copyright. The unabridged version of the thesis can be viewed at the Lanchester library, Coventry university.

Figure2.12 Satisfactory Failure Mode (BS EN 12390-3)

This item has been removed due to third party copyright. The unabridged version of the thesis can be viewed at the Lanchester library, Coventry university.

Figure2.13 Unsatisfactory failure mode (BS EN 12390-3)

2.12.2 Effect Of Fineness Of Filler Type To Compressive Strength Of Cellular Concrete

Previous studies as presented in Figure 2.14 has shown that for a given density, a mix with fine sand resulted in higher strength, than mix with coarse sand.

Also, this clear variation in strength is higher at higher density. Comparatively, Figure 2.14 clearly illustrates that the compressive strength with additive shows higher value than the mix without additive.

This item has been removed due to third party copyright. The unabridged version of the thesis can be viewed at the Lanchester library, Coventry university.

Figure2.14 Compressive strength as a function of density (Nambiar and Ramamurthy, 2006)

Considerable binary images obtain from scanning electronic microscopy (SEM) as shown in figure 2.15 had proved that for fine sand , the uniformly distributed pores act strongly as a function to higher strength display for specimen with fine filler, whereas the pores appear irregular for mixes with coarse sand. This indicates that coarse sand causes clustering of bubbles to form irregular large pores.

This item has been removed due to third party copyright. The unabridged version of the thesis can be viewed at the Lanchester library, Coventry university.

(A) Coarse Mix Specimen (B) Fine Mix Specimen
Figure 2.15 Porosity of cellular concrete (Nambiar and Ramamurthy, 2006)

(Nambiar and Ramamurthy, 2006) concluded that “fine sand results in uniform distribution of bubbles and hence result in higher strength than coarse sand at a given density.

Furthermore, on replacement of sand with fly ash, report by (Keasely and Visagie, 1999) had shown that the use of fly ash filler type result in strength increase for given density, whilst a mix with sand gives lower strength. The

reason for strength increase is summarized as evidence of fly-ash retainability and pozzolanicity of this filler material.

Importantly, the reduction in foam volume requirement for fly ash mix due to lower specific gravity. This leads to increase in strength, following corresponding reduction in pore volume (Nambire and Ramamurthy, 2006)

Similarly, (Durack and Weigius, 1998), observed enhancement in strength using fly ash was attributed to development of strong inter particle bond between the gel matrix and the fly ash particles.

2.12.3 Effect of Density to Compressive Strength Of Cellular Concrete

The effect of density to compressive strength is one of the most important parameters that can clearly control the compressive strength of cellular concrete (Kan and Ramazan, 2009)

Comparatively, compressive strength is more sensitive to density than tensile strength. In addition as stated earlier compressive strength decrease exponentially with decrease in density of foam concrete.

(Ramamurthy et al, 2009) reported that for density of foam concrete between 500 and 1000 Kg/m³, the compressive strength decreases with an increase in void diameter, whilst for densities higher than 1000Kg/m³, it depends purely on bulk density of mix. This is so because the air-voids are far apart to have influence on

compressive strength. Intrinsically, higher density of constituent material leads to higher strength.

This item has been removed due to third party copyright. The unabridged version of the thesis can be viewed at the Lanchester library, Coventry university.

Figure 2.16 Relationship between compressive strength and density (Nambiar and Ramamurthy, 2006)

Figure 2.16 gives an illustration of density relationship with compressive strength. Whereas, table 2.2 shows comparison of strength to density ratio for different mixes from which, Nambiar and Ramamurthy (2006) drew the following conclusions:

- “For a given mix , the strength to density ratio increases with an increase in design density”

- “Out of the four types of design investigated, cellular concrete with fly ash as filler has a higher strength to density ratio for all design density values “(i.e. finer filler results in higher strength to density ratio)”.

Table 2.2 Comparison for compressive strength and density(Nambiar and Ramamurthy, 2006)

This item has been removed due to third party copyright. The unabridged version of the thesis can be viewed at the Lanchester library, Coventry university.

2.12.4 Effect of Water- Solid Ratio to Compressive Strength of Cellular Concrete

Essentially, water and moisture content of the cellular concrete contribute to compressive strength .Studies by (Nambiar and Ramamurthy, 2006) concluded that there are marginal increase in strength of a cellular concrete following reduction of water content. While, investigation shows increase in foam volume causes reduction in strength to excess porosity present in the specimen.

2.12.5 Effect of Curing on Compressive Strength Of Cellular concrete

Curing which is the process of strength activation of cellular concrete, often follows a defined curing duration of 7,14,21,28 and 56 days. This process has a lot of effect on the strength of concrete.

Following variation in curing process, (Orchard, 1979) stated that strength of cellular concrete developed after it is stored in water. Its strength development is estimated to be between 0.74 to 0.9 times the strength of air-cured cubes.

(Neville,1995) stated that cellular concrete are considered as moist cured material by means of steam atmospheric pressure (autoclaving process).

Comparatively, autoclaving method of curing cellular concrete increases the compressive strength, more than other forms of curing.

In general, compressive strength of water- cured cellular concrete is reported to be higher than that cured in air (Hamidah and Azmi, 2005)

Similarly, higher strengths are reported for humid air curing of a specimen (Keasely and Booyens, 1998).

However, the low cost of moist – curing is of economic attraction and a simpler alternative in many application (Tam and Lim,1987), But strength development is rather slow.

2.13 Flexural and Tensile Strengths

The flexural and tensile strength are important properties of a cellular concrete.

It is defined as the maximum fibre stress developed in a specimen just before it cracks or break in a flexure test (INSTRON, 2008).

Appreciably, (Andrew and William, 1978) stated that modulus of rupture is a resultant effect, due to tensile strength failure. (This represents the tensile stress at which a standard 10×40×40cm cellular concrete prism breaks when subjected to a bending test.

In general, the ratio of flexural strength to compressive is $1/4 - 1/6$. (Comite' Euro- international du Beton, 1978). This conforms to the work conducted by (Valore, 1954), which states that the ratio of compressive strength is ranging from 0.25-0.35.

More so, flexural strength measurement is known to be even more sensitive to the test condition than compressive strength measurement. The splitting cylinder test (Brazilian test) is commonly used to measure tensile strength.

Apparently, the moisture gradient, density and curing method within the specimen has a strong influence on the test result. (Comite' Euro–international du Beton, 1978).

2.14 Shear Strength of Cellular Concrete

Shear strength is describe as the tensile rapture and therefore depends on the distribution stresses in the test. (Comite' Euro-International due Beton, 1978)

Several researchers (e.g. Andrew and Willian,1978) had proved that the shear rapture strength of a pure punching shear with a cylindrical piece over a hole of a same diameter is assured to be 25%-30% of the compressive strength.

Moreover, in absence of any other information the value for pure shear can be taken as direct tension.

Besides, in a reinforced slab without shear reinforcement, its ultimate shear strength depends only on the concrete quality (strength), and subsequently on the span ratio a/h . Figure 2.17 illustrates the ultimate shear stress of reinforced slab.

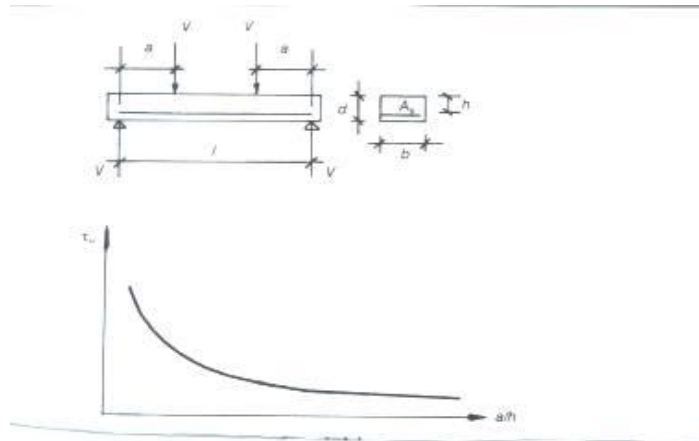


Figure2.17 Ultimate shear stress of reinforced slabs

With conditions;

$$\begin{aligned} 2.3 \leq f_k \leq 6.0, \\ 0.12 \leq h/a \leq 0.6, \\ 0.12 \leq \mu \leq 0.8 \end{aligned}$$

This can be calculated with the equation;

$$T_u = 0.035f_k + 1.163\mu h/a - 0.053 \text{ MPa} \text{ -----(2.2)}$$

Where ($T_u = V_u/(b.h)$), is the nominal characteristics value of the ultimate shear stress (MPa), V_u is the ultimate shear force, in failure (N), F_k is the characteristics compressive strength of AAC (MPa) $\mu = (100A_s / (b.h))$ is the percentage of tensile reinforcement(%) and A_s is the area of tensile reinforcement (mm^2)

Whereas, in a reinforced beam with shear reinforcement the ultimate shear strength depends on the total percentage of shear reinforcement, in addition to concrete quality(strength) the span ratio (a/h) and the amount of longitudinal tensile reinforcement(RILEM,1993)

This ultimate shear strength can be calculated from the following expression.

$$T_u = 0.077f_k + 0.719\mu h/a + 0.001P_{wt,yw} - 0.142 \text{ -----(2.3)}$$

Where, $T_u = V_u/b.h$ is the nominal value of ultimate shear stress MPa,

V_u = ultimate shear force in shear failure

F_k = is characteristics compressive strength

μ = % of tensile reinforcement = $100A_s$

2.15 Modulus of Deformation or Elasticity

This is a mechanical property of cellular concrete, which could be caused by mainly, the application of uni-axial or transverse load on cellular concrete specimen.

Comparatively, studies confirms that modulus of deformation of cellular concrete in general is lower than, the conventional concrete (Andrew and willaim,1978).

Thus, Figure 2.18 shows that the E-Value of cellular concrete ranges between one third and two third of the E- value of conventional concrete. In this case the modulus of deformation increases with the cube strength and depends on the aggregates used.

Modulus of deformation against density graph

This item has been removed due to third party copyright. The unabridged version of the thesis can be viewed at the Lanchester library, Coventry university.

**Figure2.18 Comparison between modulus of deformation of concrete and cellular concrete
(Andrew and William, 1978)**

Appreciably, in accordance to (Andrew and William, 1978) the modulus of deformation increases with the density (w) of cellular concrete. This fact is proved theoretically by applying a correction factor for density of concrete whereby;

$$E_c = (w/2400)^2 \times 9100u^{1/3}, \text{ MPa. -----(2.4)}$$

The relationship between the E-value calculated with this equation and measured values obtained at the Building Research station is shown in Figure 2.19.

The figure indicate that cellular concrete ranges from about 10×10^3 to 30×10^3 MPa for different strengths and aggregate under short term loading(Andrew and willaim,1978).

This item has been removed due to third party copyright. The unabridged version of the thesis can be viewed at the Lanchester library, Coventry university.

**Figure2.19 Relationship between calculated and measured moduli of deformation
(Andrew and William, 1978)**

More so, this figure shows the relationship between the calculated and measured modulus of deformation for various lightweight concrete.

In addition (Andrew and William, 1978), stated that modulus of deformation is of special importance for structural lightweight concrete construction because of its effect on the deflections of flexural members, on the distribution of internal forces in the cross-section of compression members and the critical load in the case of members liable failure due to elastic instability, where a lower E- value of light weight concrete has an unfavorable influence. On the other hand, the resistance of lightweight concrete to impact loads may be enhanced by their lower modulus of deformation.

Further works by (Ramamurthy et al., 2009) state that the static modulus of elasticity of cellular concrete is reported to be significantly lower than that of the normal concrete.

Similarly, (Jones and McCarthy, 2005), says their values are varying from 1.0 to 8.0 KN/mm², for dry densities between 500 and 1500kg/m³, respectively.

(ACI COMMITTEE213, 2003), also explained that “modulus of elasticity of lightweight concrete depends on the relative amount of cement paste and aggregates and the modulus of elasticity of its components.

Ultimately, other related studies by (Svanholm,1983) “shows that modulus of elasticity is affected by the measure of moisture content comparable to the influence of compressive strength, though of lesser influence”.

The MPa of modulus of elasticity ranges between 1.7 and 3.5MPa.

2.15.1 Effect on E-Value with Different Filler Type

Previous research has shown that cellular concrete with fly ash as fine aggregate is reported to exhibit lower E-value than that of cellular concrete with sand. This variation is attributed to the high amount of fine aggregate in the sand mix compared to fly ash mix, which contains entirely paste with no aggregates (Jones, 2001).

2.15.2 Effect On E-Values Having Additives Of Fibre Glass Or Polypropylene Fibres.

Previous investigation carried out by (Jones and Mc Carthy,2005), shows that the E –values of cellular concrete is increased by two to four times, when there are presence of polypropylene fibres as additive . This analogy supports the use of fibre mesh as a strength improvement additive.

Considerably, at low temperature, an increase in compressive strength is accompanied by an increase in stiffness, which was observed to be more in the higher density range (Richard, 1977).

Table 2.3 Reports of few relationships on modulus of elasticity with density and compressive strength.

Author(s) and year	Relationship	Remarks
Tada (49)	$E=5.31 \cdot w-853$	Density from 200 to 800kg/m ³
Mc Cormick (3f)	$E= W^{1.5} J F_c$	Pauw's equation
Jones and Mc Carthy (9)	$E= 0.42 F_c^{1.18}$ $E=0.99 F_c^{0.67}$	Sand as fine aggregate Fly ash as fine aggregate

Where

W—density of concrete (Kg/m³)

F_c— Compressive Strength (N/mm²)

E— (KN/mm²)

2.16 Calculation Of Elastic Modulus

According to (Instron, 2008) web site, elastic modulus is the rate of change of strain as a function of stress. The slope of the straight line portion of a stress-strain diagram “as shown in **Fig 2.17**. Tangent modulus of elasticity is the slope of the stress- strain diagram at any point. Secant modulus of elasticity is stress divided by strains at any given value of stress or strain. It is also called stress-strain ratio. Where tangent and secant modulus of elasticity are equal, up to the proportional limit of a material modulus of elasticity which may be reported as compressive modulus of elasticity (INSTRON,2008).

This item has been removed due to third party copyright. The unabridged version of the thesis can be viewed at the Lanchester library, Coventry university.

Figure2.20 Stress-strain relation (INSTRON®,2008)

2.17 Durability Properties Of Cellular Concrete

According to (Andrew and William, 1970) the durability of cellular concrete is defined as the ability of this cellular concrete to with stand the effects of its environment.

Essentially, the author has classified this peculiar characteristics ability to withstand; into three categories ;(i) chemical attack (ii) Physical Stress and(iii) Mechanical assault.

2.17.1 Chemical attack

This is the behavioural stability of the material itself, in presence of moistures, which defines its permeability properties.eg water absorption and sorptivity.

2.17.2 Physical Stresses

This is the durability response to physical stresses caused principally by frost action, shrinkage and temperature stresses.

2.17.3 Mechanical Assault

These are described as effect from abrasion or impact on cellular concrete, it can also be the effect of excessive loading of flexural members.

Appreciably, having discussed earlier the impact of mechanical assault, efforts are focus on the chemical attack and physical stresses properties of cellular concrete.

2.17.4 Water absorption

Water absorption is said to be comparatively lower for cellular concrete than conventional concrete. Though, cellular concrete are more porous material than normal concrete , but investigation had shown that not all the artificial pores are taking part in the water absorption, this indicates they are not inter connected.

Precisely, water- absorption is a function of capillary pores, which is dependent on the paste content.

(Nambiar and Ramamurthy, 2007) reported that as foam volume increases, the volume of entrained air pores increases reducing the paste content and causing a reduction in the volume of capillary pores. This effect is followed by a decreasing trend of water absorption.

In addition, it is known fact that water absorption of base mixes (before adding foam) were higher than that of a corresponding foam concrete mixes, which

further buttress the influence of the paste content on water absorption(Kolians and Georgious,2005).

This item has been removed due to third party copyright. The unabridged version of the thesis can be viewed at the Lanchester library, Coventry university.

Figure2.21(A-B) Comparison on absorption property (Kolians and Georgious, 2005)

2.17.5 Effect of Replacement of Sand with Fly Ash

According to (Nambiar and Ramamurthy, 2007) there are appreciable variations in the water absorption on cellular concrete mix with fly ash than sand.

As illustrated in Figure 2.21(A-B), for a given density of foam concrete, the water absorption is relatively higher in mixes with fly ash as compared to sand.

Thus from the figures, it is seen that the water absorption is lower at lower densities.

This is so because, for a cellular concrete with fly ash, there is lower requirement of foam volume due to lower specific gravity. Thus attributes higher paste content to a mix with sand.

Consequently, water absorption is on the increase since, there are evidence of higher paste content, with higher capillary pores in the mix.

2.18 Sorptivity of Cellular Concrete

(Nambiar and Ramamurthy, 2007). Describe Sorptivity as measure of transport mechanism within cellular material.

According to (Ramamurthy et al, 2009) “ the moisture transport phenomenon in the cellular material is a measurable property called” sorptivity.

While (Hall C,1989) define sorptivity phenomenon as a mechanism based on unsaturated flow theory.

Considerably, sorptivity of cellular concrete is reported to be lower than the corresponding base mix and the value reduces with increase in foam volume (Nambiar and Ramamurthy, 2007).

This actually conforms to the observations made by (Prime and Wittman, 1983),(Tada and Nakano,1983) and (Goual et al.,2000) In aerated concrete and (Jones and Mc Carthy,2005), (Madjoud et al.,2002) and (Grannakou and Jones,2002).

2.18.1 Effect of Sorptivity Of Cellular Concrete

Previous, research has shown comparison of sorption properties of cellular concrete and corresponding base mixes (mix without foam) .

Ultimately, a typical foam concrete mix exhibits lower sorptivity, this illustrates clearly the effect due to paste content in the mix as compared to corresponding base mix. This confirms evidence of lower paste content due to foam.

In addition, the cellular concrete mixes exhibit a longer linear behavior with reduced moisture in take which is comparable to the corresponding base mix.

As such visual examination after the test, showed the presence of water on the top surface of the base mix specimen, while such behavior was not observed on cellular concrete specimen.

This is specifically attributed to increased average path water migration due to an increase in the entrained air voids.

This item has been removed due to third party copyright. The unabridged version of the thesis can be viewed at the Lanchester library, Coventry university.

Figure 2.22 Comparison of water advancement into base mix and corresponding foam concrete (Nambiar and Ramamurthy, 2005).

Figure 2.22 shows the comparison of cellular concrete and base mix which assumes that the discrete unconnected entrained air voids deviates the path of

capillary flow of water. Thus the entrained air voids (macropores) create an increasing tortuous path for the capillary flow in proportion of foam volume and dampen the transport phenomenon.(Nambiar and Ramamurthy, 2005).

2.19 Cellular Concrete Resistance To Freeze-Thaw And Chemical Attack

According to (RILEM, 1993), cellular concrete usually possesses good resistance to freezing, which is proved by unimpeded buildings, suited in areas where frequent freeze/thaw cycles occur, as they remain undamaged.

The reason behind this peculiar property of a cementitious material is that the introduced big spherical pores are almost closed, the material has comparatively very brittle capillary suction and therefore, the moisture content does not normally reach the critical degree.

Comparatively, cellular concrete mixture which is designed at low density, with consideration of initial depth penetration, and absorption rate provide good freeze- thaw resistance (Tikalsy and Pospisil, 2004).

On the other hand, sulphate resistance of cellular concrete reveals that cellular concrete has good resistance to chemical attack (Jones and McCarthy,2005). Though for concrete cement product are attacked to some extent by soluble sulphate.

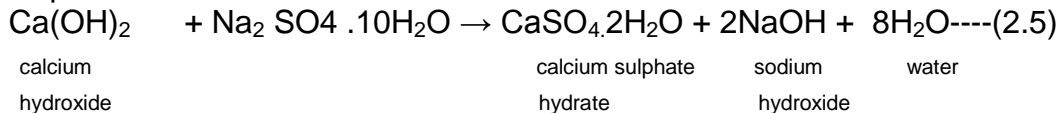
2.19.2 Effect of Carbonation on Cellular Concrete

(Jones and Mc Carthy,2005) in their study on accelerated carbonation of cellular concrete indicated that lower density cellular concrete proves to carbonate at a relatively higher rate .They compared performances of mixes with sand or fly ash. Mixes with fly ash were found to exhibit higher carbonation than sand.

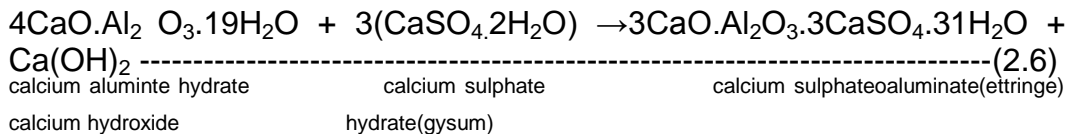
Consequently, the presence of carbonation in a fly ash, further support the analogy posed by cellular concrete mix with fly ash, that increasing carbonization of the cellular concrete leads to higher compressive strength and tensile strength (Andrew and William,1978).

As written by (Andrew and William,1978), sulphate solution attack Portland cement in two ways;

- They react with calcium hydroxide in the set cement to form calcium sulphate



- They react with calcium aluminate to form calcium sulphoaluminate



Considerably, cellular concrete as an impervious cementitious material exhibit a more corrosive resistance than, conventional concrete (K Ramamurthy et al,2009).

More so, report of investigation by (Kearsley and Booyes,1998) reveals that cellular concrete performances is equivalent to that of normal concrete with enhanced corrosion resistance at lower density, during accelerate chloride ingress test. This is so because the air –voids appears to act as a buffer preventing rapid penetration.

Appreciably, the conversion of calcium hydroxide to calcium sulphate is known to be more than double the solid volume.

Likewise, the formation of highly-hydrated sulphoaluminate occurs with doubling the solid volume.

Apparently, it is this solid volume expansion, which cause disruption of concrete that are exposed to sulphate attack.

However, the presence of tricalcuim aluminate content in Port land cement, increase the resistance of cement to sulphate attack.

Ultimately, cellular concrete due to its imperviousness are said to be more vulnerable to sulphate attack.

2.20 Functional Properties

2.20.1 Thermal Conductivity Of cellular Concrete

According to (Andrew and William,1978), thermal conductivity is a measure of ability of a cementitious material to conduct heat, and in metric unit is expressed as heat flow(in watts) through a square metre of material when a temperature difference of 1°C is maintained between opposite surface of a metre thickness of the material.

The thermal conductivity k is expressed in flowing metric dimensions:

$(\text{w/m}^2) \times (\text{m}/^\circ\text{C})$ or $\text{w/m } ^\circ\text{C}$

The said thermal conductivity of cellular concrete depends primarily on density and other factor like moisture content, temperature level, raw material, pore structure.

Since, cellular concrete are less dense material, they are relatively low thermal conductors as compared to conventional concrete.

Table 2.4 Comparison of thermal effect between cellular concrete and concrete

Bulk density(kg/m³)	(lb/ft³)	3% moisture(exp)	5% moisture(pro)	3% moisture(prot)	5% moisture(expo)
400	25	0.15	1.16	1.03	1.10
500	31	0.17	0.18	1.17	1.24
600	38	0.19	0.20	1.31	1.38
700	44	0.21	0.23	1.45	1.59
800	50	0.23	0.26	1.59	1.80
900	56	0.27	0.30	1.87	2.07
1000	63	0.30	0.33	2.07	2.28

This illustrates the relationship of bulk density with thermal conductivity. Appreciably, this is so because, the pore structure of cellular concrete contains higher thermal insulation volume of air-voids. Whilst air originally is a poor conductor of heat, it thus reduces the thermal transfer of the heat.

2.20.2 Thermal Insulation

Considerably, cellular concrete has excellent thermal insulating properties that are known to be more or less proportional to the density of concrete (Shrivastava, 1977).

Similar studies by (van Deijk, 1991) confirmed that alteration on mortar/foam ratio affects density, which has enormous impact on cellular concrete insulation capacity.

Ultimately, the volume of air void in cellular concrete is advantageous to its insulating capacity.

Thus, increasing foam volume leads to higher thermal insulating properties (Weigher and Karl, 1980).

2.21 Acoustical Properties

2.21.1 Acoustic Insulation

The acoustic insulation property of cellular concrete restricts the usage in areas where the nuisance caused by transmitting noise through walls is of immense importance.

According to (Valore,1954) cellular concrete does not possess unique or significant sound insulation characteristics.

It further confirms the findings of (Taylor, 1969), that cellular concrete is less effective than dense concrete in resisting the transmission of air-borne sound. This is so because the transmission, loss of air- borne sound is dependent on mass law, which is a product of frequency and surface density of the components.

In reality the mass law principle applies, as it gives acoustical performances based on bulk density and thickness. Consequently, as a lightweight material it's less dense composition gives it a weak reflecting property, but a better acoustical absorption property.

Research by (Wit,1969) conforms to this analogy, that dense concrete tends to deflect sound, and cellular concrete has higher sound absorption capacity.

2.21.2 Acoustic Absorption

(Andrew and William, 1978) reported that sound absorption is quite different property from sound insulation. Thus sound absorbing material reduces sound reflection from the surface, while sound insulating material reduces the sound passing through.

This is so because the air-void structure in cellular concrete, frequently leak sound through imperfect formation of joints (Andrew and William,1978)

2.22 Fire Resistance Properties Of Cellular Concrete

The fire resistance of the cellular concrete characteristics makes an outstanding, material when compared to conventional concrete.

Reviewing earlier studies on fire resistance (Jones and McCarthy,2005) summaries that for lower densities of cellular concrete , the proportional strength loss on exposure to fire, is far less, when compared to conventional concrete. This is so because, the air – void contained in cellular concrete are poor conductors to heat transfer, as such a better thermal insulators, than conductivity of heat.(Valore,1954) reported that, along with thermal conductivity and diffusivity, foam concrete has better fire resistance properties.

2.23 Structural Properties of a cellular concrete

2.23.1 Effect of fibre reinforcement to concrete

Fibre reinforcement improves the mechanical properties of concrete, as (Reinhardt et al.,1992) stated that “*Most notable among the improved mechanical characteristics of fibre reinforced concrete (FRC) are its superior fracture resistance and resistance to impact and impulsive or dynamic loads. Secondly they impart additional strength under all modes of loading which include, direct tension, shear, flexural and tensional loading*”.

2.23.2 Effect of Steel reinforcement to aerated concrete

The bonding effect of steel reinforced aerated concrete can effectively be assisted by provision of anchorage elements placed at the ends of steel bars or intermediately at intervals along the bars. Appreciably, by providing end hooks pull out strength can be increased by as much as 30 per cent compared with straight bars. More so, the bonding is so strong after slip had taken place, which enhances mechanical anchorage due to corrugated surface, formed due to contact between aerated concrete and steel. However, failure then takes place due to shear in concrete along the bars or splitting of aerated concrete.

3 Chapter Three: Research Methodology

3.1 *Experimental Program*

The experimental program was designed to achieve the research aim and objectives. The program gives in-depth understanding on the material and structural behavior of Aer-Tech novel material. The research program consists of both experimental testing as well as numerical modeling. The experimental program was compiled by carrying out the following tests:

- Consistency of Aer- Tech material mix.
- Compressive strength test for 300 cubes of $(100 \times 100 \times 100) \text{ mm}^3$
- Flexural Strength test for 20 mini beams of $(500 \times 100 \times 100) \text{ mm}^3$
- Elastic Modulus 10 mini- beams of $(500 \times 100 \times 100) \text{ mm}^3$
- Drying shrinkage (In-house method) for density test on 200 cubes of $100 \times 100 \times 100$
- Effects of adding Fibre glass to the mix, on 50 cubes of $(100 \times 100 \times 100) \text{ mm}^3$
- Effects of super plasticizers in the mix on 40 cubes $(100 \times 100 \times 100) \text{ mm}^3$
- Test for ultimate moment and deflection on 3 singly reinforced beam $(1500 \times 180 \times 75)$

Whilst, the numerical program is

- The neural network simulation for compressive strength and density – this involves the training of over 300 cube results for input and output data through a NN-model.

3.2 Aer-Tech Machine

3.2.1 The Mixing Mechanism of Aer-Tech

The Aer-Tech mixing process is made possible by a specially designed automated machine, patented solely for production of Aer-Tech mix with Patent number (No. 2330086, 1997).

The Aer-Tech automated machine is separated into three basic unites. These unites are clearly shown in figures 3.1, 3.2, and 3.3.

More so, background discussions with reference to the above stated figures are as given below;

Figure 3.1 represents the first unit of the Aer-Tech machine, it majorly comprises of two conveyer systems for feeding solid materials to the mixing chamber.

The solid materials are sand and cement placed in an endless conveyor belt (52, 53). These belts have cross members (54) that are upstanding from conveying runs (52A, 53A). The cross members (54) are spaced on the belts by a pre-determined amount selected according to the desired rate of feed and speed of the belt.

Each belt passes around rollers (56,57), and a driver motor (58) drive the roller (56), so both conveyors would be driven at the same speed as assigned in the automated control panel in Figure .

Consequently, the higher the automated speed of the driver motor in the machine the greater the quantity of solid mix delivered per minutes into the mixing chamber becomes, whereas the lower the speed of the driver motor the lesser the quantity of solid mix delivered into the mixing chamber per minutes.

Figure 3.2, has shown clearly the interior mechanism of the Aer- Tech process. Specifically, this unit is described as one of the most important section of the Aer-Tech automated machine. It is made up of the central mixing chamber vessel (10), this central mixing chamber (10) is where all Aer-Tech material constituent are collated and mixed.

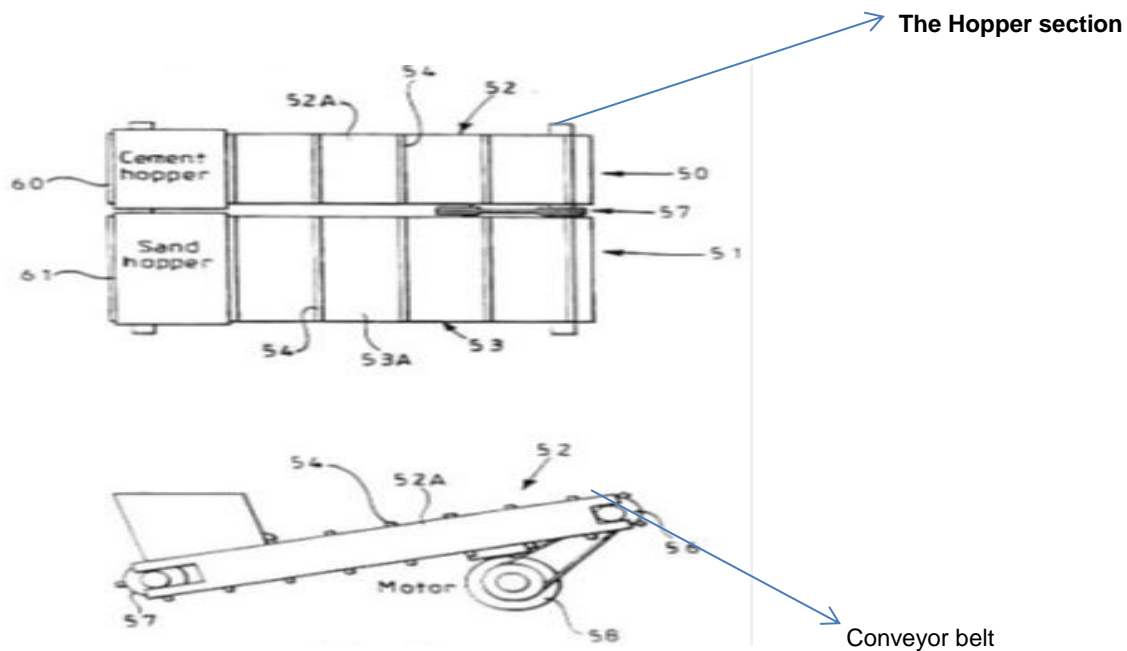


Figure3.1 Plan view and side view of the conveyor system arrangement (Patent No. 2330086, 1997)

Interestingly, this part of the machine receives the solid material that have been delivered by the conveyor belts through hopper (14), this hopper acts like a

collection point for the solid materials as they are driven to the cylinder mixing vessel (10).

The cylinder mixing vessel has a central longitudinal axis inclined to the horizontal by thirteen degrees, so the initial end (11) is lower than the outlet end (12). The reason that this vessel is inclined is that when the material is being mixed, it tends to flow back to the initial end of the mixing vessel, by having this action the material is mixed in a more consistent form.

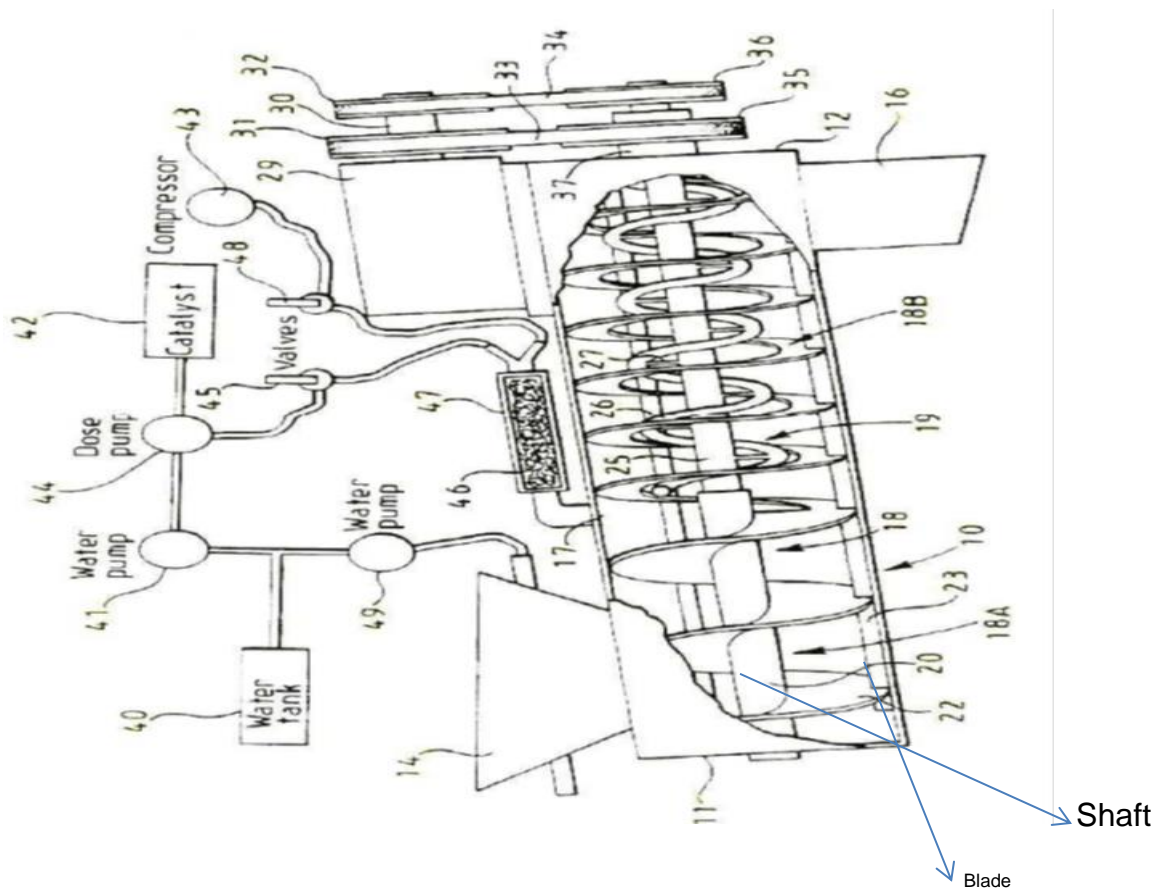


Figure 3.2 Side elevation of mixing apparatus with part of the mixing vessel broken away to show the interior (Patent No. 2330086, 1997)

Also in Figure 3.2 the arrangement of the liquid material as water and foam is shown. The liquid material has two access points to the mixing vessel, the first access is for water from the water source (40), as it is pumped directly to the hopper (14) using a pump (49).

The second access for liquids is inlet (17) that introduces the foam to the mixing vessel. The feeding arrangement of the foam includes a source of water (40), a water pump (41), a source of foaming agent (42) and a source of compressed air (43). The water pump (41) pumps the water from the water source (40) to the dosing pump (44) and the foaming agent from the foaming agent source (42) is pumped to the dosing pump. The dosing pump mixes the water and the foaming agent in the desired proportions and conveys the mixture towards a valve (45) from which the mixture is directed towards a chamber (47). In chamber (47) the mixture of water and foam agent is mixed with compressed air. The compressed air is directed to valve (48) by a compressor (43), valve (48) controls the supply of compressed air to the chamber (47), as the water and foam agent enter the chamber with the compressed air, the mixture is caused to foam producing a large quantity of small bubbles in a form of foam which is directed to the inlet (17) and into the central mixing chamber vessel (10).

More so, inside the central mixing chamber vessel (10) there are two mixing elements (18,19). Mixing element (18) extends between the inlet from the hopper (14) and the outlet (16), this element contains hollow shaft (20), around the shaft

a spiral plate (22) is located, which extend between the inner surface of the central mixing chamber vessel (10) and the shaft (20) with a clearance of 5 mm.

The spiral plate (22) extend beyond the liquids inlet (17) towards the outlet (16) but it diminishes in its radial direction so that it extends from the inner surface of the central mixing chamber vessel (10) to accommodate the inner mixing (19).

The inner mixing element (19), contains a spirally extending bar (26) spaced from and supported on the shaft (25) by extending connectors (27). Shaft (25) has a smaller radius than shaft (20) and extends through shaft (20) from one end of the vessel (10) to the other.

Both shafts rotate around their axis by a driving motor (29). Having this arrangement in the mixer insure that the mixing elements are carefully mixed and the foam is evenly distributed so that a homogeneous mixture is discharged. After the mixture has been discharged from the vessel it would be conveyed by a peristaltic pump to the point at which it is to be used.

Finally, Figure 3.3 represents the third unite and most powerful unit of the Aer-tech automated machine, without this unit no other unites could be operated. Indeed, it is apparent that the function of the other two unites of Aer-Tech machine are solely dependent on the control instructions received from this unite. Furthermore, this is also known as the control panel of the Aer-Tech automated machine. It consist of a system PC, automated control software, UPS, daily

records for Aer-tech material produced and a panel where data's are inputted for a specified mix ratio.

In addition, this unit of the Aer-Tech machine gives the machine a unique feature, wherein It is described as a fully automated Aer-Tech material productions on computer.

This item has been removed due to third party copyright. The unabridged version of the thesis can be viewed at the Lanchester library, Coventry university.

Figure 3.3 A model of Aer- Tech operation(<http://batchingplantprocessing>)

Appreciably, the inventor of Aer-Tech material realises all his machine processes by using CAD programs in his young and dynamic Innovation, which is targeted to reach high sensitivity and precision in the production process. The newly designed and invented Aer-Tech machine, works with special computer programs.

3.3 Mixes specification

There had been well over twenty three mix ratio carried for this research. As clearly specified in the mix ratio, some of the mixes are with plasticizers, fibre glass and varying foam and water content.

3.4 Machine calibration

Especially, for purposes of consistency in results obtained, this research had carried out extensive recommendation on calibration and recalibration of the Aer-tech Machine following early machine problems experienced.

Apparently, the Aer-Tech Machine problems are majorly caused by two basic engineering problems. Firstly, on commencement of laboratory production of Aer-Tech material.

The Aer-Tech machine produces a heterogeneous mix, which caused urgent modification of the Aer-Tech machine.

However, after these modifications were effected, the engineering company unknowingly forgot the re-calibration of machine, which in turn diminishes the specified flow rate of water and catalyst.

Therefore, the mixing water flow rate and the foam flow rate have to be re adjusted as stated below; mixing water to be set at 3.06 Litres per minute 12% reduction on the machine foam flow rate to be set at 0.219 Litres/minute, solution water to be set at 0.01400 Litres per minute, while the catalyst to be set

at 0.00346 Litres per minute.

Consequently, the significance of not recalibrating machine had shown a marginal decrease in densities composition of an Aer-Tech design mix ratio.

This effect continues and became more apparent when mixing Aer-Tech materials at lower densities such as 1600 Kg/m³ and 1400 Kg/m³. During this period produced densities of Aer-Tech material were calculated, results show that the produced densities were much lower than the densities set on the Aer-Tech Machine.

Table 3.1 Comparison between expected densities and actual densities

Mix	Expected density (kg/m ³)	Lower range (Kg/m ³)	Upper range (Kg/m ³)	Variance
1	1810	1631	2092	11%
2	1810	1411	1702	26%
3	1400	1028	1255	36%

In addition an acknowledgement of drying shrinkage effect on air cured Aer-Tech material, evidence of reduction on calculated densities from wet density of material. As Aer-Tech material after being air cured, its density became approximately 3.9% lower.

It was observed that the lower the density set on the Aer-Tech machine, the difference in the actual density was greater. It then became obvious the machine settings were not correct and it suggested too much foam was added to the mixes. Table 2.6 shows the actual flow rates for the catalyst, solution

water and foam that have been used in the mix.

Table 3.2 Effect on expected density by actual flow rate of water, catalyst & foam

Mix	Expected density (kg/m ³)	Solution water (L/Min)	Catalyst (L/Min)	Foam (L/Min)
1	1810	0.1330	0.0090	1.9000
2	1600	0.2250	0.0158	4.2000
3	1400	0.3550	0.0295	5.2000
4	1810	0.1330	0.0090	1.9000

The second problem experienced, are error in measurement of constituent material. Laboratory checks show excessive delivery of the sand against cement design ratio.

Following design specification Aer-Tech material composition was meant to be 10 Kg/Min with a ratio of 3:1 sand to cement. But after checking the quantity of sand and cement used, it was discovered that the actual combined quantity of sand and cement was 11.463 Kg/Min, as 2.866 Kg/Min of cement and 8.597 Kg/Min of sand.

3.5Aer-Tech Plant Batching and mixing Process

The Aer-Tech mixing plant which is a major part of this research is depicted in figure 2.25. Batching is the process of weighing and introducing into the mixer the ingredients for a batch of Aer-Tech material. All raw materials, cement, sand, foam, water and admixtures are weighted and batched, at the aggregate and cement weigh hoppers and at the admixtures reactor respectively. The plant has two main feeder bin. The cement feeder bin and the sand feeder bin. Admixtures, which are in liquid form, have also three different types of tanks separately.

Water is controlled using a meter system measuring the volume required. For the mixing process a twin shaft mixer is used to ensure that Aer-Tech is mixed thoroughly until there is a uniform appearance and all ingredients are evenly distributed. Finally, the freshly mixed Aer-Tech material is deposited into moulds as specimen.

3.6 Aer-Tech Batch Plant

Ultimately, most crucial factor concerning Aer-Tech material in relation to its mechanical, chemical and structural properties is the precision in materials proportion.

Comparatively, other essential parameters such as material hierarchy – regarding the input sequence in the mixer, the mixing time are considered in order to ensure the quality objective. In addition, Figure 3.3 shows that all Aer-Tech parameters are machine regulated, in accordance to their varying percentage of mix.

The whole process commences as soon as the Aer-Tech machine starts, all the major constituent and additives begin to collate in the revolving mixer blade point in accordance to automated quantity discharge. Prior, to the commencement, the Aer-Tech system operator has to choose the desired recipe and insert the wanted quantity of Aer-Tech material through the SCADA graphic user interface

panel on the side of the Aer-Tech plant. Then, the batching process starts for the three different kinds of materials (there is no need for batching water), and the process continues to the next step, which is the mixing process, only when all ingredients are batched properly. Mixing process starts simultaneously with the material induction in the mixer.

Mixing timer starts counting mixing time after all ingredients are placed into the mixer and when time elapses, after the Aer-Tech mixed material are put in the moulds for testing

3.7 Aer-Tech Global automata: the new formulation method for modeling industrial systems

The Aer-Tech machine is an automated machine, which applies the principle of global automata. Global automata, as introduced in (Deligiannis, Manesis, and Lygeros, 2007), are a generalised formal method for modelling industrial production systems. They are based on automata philosophy bridging the gap between academic methods and real application systems, being suitable for modelling a large variety of industrial systems. As a method, global automata introduce additional formulation parameters to those of the conventional methods. The formal definition of global automata is given here

Operation Definition

A global automaton is defined by the tuple $A = \langle X, Z, Q, \Sigma, Init, Flow, L, S, W, E, R_X, R_Z \rangle$, where:

- The set of real-valued variables $X = \{x_1, x_2, x_3, \dots, x_m\}$ and the set of discrete or binary variables $Z = \{z_1, z_2, z_3, \dots, z_k\}$ comprise system's variables.
- Set of states $Q = \{q_1, q_2, q_3, \dots, q_n\}$.
- Alphabet or set of events: $\Sigma = \{\sigma_1, \sigma_2, \sigma_3, \dots, \sigma_\lambda\}$, which can be discrete variables, conditions over the real-valued variables and any combination of them.
- Initial conditions: *Init*, regarding all system variables and the initial state.
- Flow conditions, $F_i(X, X) = 0$ and $Z_{j+1} = G_i(Z_j)$, according to which system variables fluctuate between the limits given by the invariant conditions $L = \{\ell_1, \ell_2, \ell_3, \dots, \ell_n\}$.
- The set of events to be ignored, $W = \{w_1, w_2, w_3, \dots, w_n\}$ with $w_i \subseteq \Sigma$, until the satisfaction of restrictions: $S = \{s_1, s_2, s_3, \dots, s_n\}$.
- Set of transitions: $E \subseteq Q \times Q \times E \times R_X \times R_Z$ with reset table for each transition concerning the relative system variables: $X = R_X$ and $Z = R_Z$.

More so, each set $(q, q', \sigma, r_X, r_Z)$ represents a transition from state q to state q' , which is caused by the event $\sigma \in \Sigma$. Set $r_X \subseteq R_X$ gives the real-valued variables to be reset during this transition, while set $r_Z \subseteq R_Z$ gives the discrete variables.

From Figure 2.26 each state q_i has a corresponding set of parameters, according to the definition. Here it has to be pinpointed that each state has a set of active events: $\Sigma_i \subseteq \Sigma$. Set Σ_i has, by definition, ξ elements, each one of which belongs to set Σ . $\Sigma_i = (\sigma^{j,k}_i)$, where i is the present state, $k = 1, 2, \dots, \xi$ and $j \in (1, \lambda)$. Index k also denotes transitions priority caused by different events. If two events occur

simultaneously and cause two different transitions, transition with the lower index k will take place, while the other will be ignored.

Comparatively, global automata are based on automata theory and hence their main feature is the control graph with a number of states and transitions between those states. The prime definition of states in automata theory implies that a state of a system is the set of all discrete and continuous variables, which is all the knowledge needed to calculate system's behaviour in an input sequence (Deligiannis, Manesis, and Lygeros, 2007).

This item has been removed due to third party copyright. The unabridged version of the thesis can be viewed at the Lanchester library, Coventry university.

Figure 3.4 A simple global automaton model with two states
(V. Deligiannis, J. Lygeros, 2007).

Appreciably, in global automata state takes a more general description definition, rather than operation mode or location, putting aside its former definition. Consequently, in this research, the generalised form of states is used under the title *state*.

Considerable measures are taken for effective control task. Firstly, this is seen in steps taken to the control set of flow conditions in a state. For example, the most common control algorithm in industrial use today, PID controller, can take its common form using a flow condition. Global automata provide two very useful tools in modelling industrial systems, especially large ones, which are state aggregation and composition (Deligiannis, Manesis, Lygeros , 2007). State aggregation is the merging of two or more states in order to construct a new hyper-set, which has the same behaviour as all merged states without losing any kind of data. Examples of state aggregation are shown in (Deligiannis, Manesis, and Lygeros , 2007), whereas in (Deligiannis and Manesis ,2005) composition examples are given. Composition allows the construction of large system models using simple models of all system's components. Small models demand less effort and by putting into practice composition, whole system's model arises. Combination of state aggregation and composition is an extra tool for engineers who have to deal with contemporary industrial systems. (Deligiannis, Manesis, Lygeros, 2007).

3.8 Modelling of Aer-Tech Machine based on global automata

Fundamentally, in modeling the Aer-Tech automated machine, a simple approach had been used, which implies the use of several automata each one modeling a specific part of the overall system. First of all, an automaton describing the recipe mechanism has to be constructed. This automaton plays the role of the supervisor controller feeding all the other controllers with specific

set-points in order to achieve the desired proportion of raw materials. The panel section represents the supervisor controller.

The main purpose of the Aer-Tech automated machine is to feed mixer with all the ingredients and control the mixing process. Here, it must be noted that in the given approach, mixing timer starts simultaneously with the mixing process, but as shown in Figure 3.3, timer starts when all components are discharged into the mixer. In this case, we have a slightly diversified approach where mixing time includes the time needed for mixer feeding.

3.9 Laboratory Development Of Aer- Tech Material

The experimental program in this chapter, had holistically considered an overall specification of material used for specimen, outline mixing process used, classification of test specimen, the test set up for material and structural assessment of the material, instrumental calibration, as well as calculation that was used for each test.

3.10 Material Composition of Specimen.

The constituent material used to produce Aer-Tech material were comprised of : Pro- Chem. Cement conforming to BS8110, pulverized river sand finer than 300 μ (specific gravity 2.5) and foam produced by aerating a foaming agent (Aer-Sol)

dilution ratio (1:5) by weight using an indigenous Aer-Tech designed machine, calibrated to a density of 1810kg/m^3 .

Appreciably, for this experiment three different types of mixes were used (1) several specimen were composed of Pro-chem cement, pulverized river sand, distil water and foam (2) a good number of specimen were composed of pro-chem cement, pulverized river sand, distilled water, foam and plasticizer and (3) the third type of specimens are composed of Pro-chem cement, water, foam and fibre glass. Different mixes of Aer-Tech material were made varying the filler-cement ratio of 4.78:1 and 5.83:1 design mixes.

The mixing sequence consisted of a well calibrated Aer-Tech machine, which passes the constituent material from its internally built in conveyor to a mixing chamber, which is designed like a mini batch plant. This process continues until a uniform homogenous base mix was achieved.

The higher air content eliminate any tendency to bleed and with good insulation properties, as the mix temperature increases during setting the air expands slightly, which ensures good filling and contact in confined voids.

3.11 Test Procedure

With a clear objective of assessing the compressive strength and flexural performance of Aer- Tech, the author had considered the use of cubes and mini beam moulds. The samples are then leveled to achieve good finished surface,

left for 24 hours, after which the moulds are uncoupled and carefully placed for air curing in accordance to BS8110 testing procedures. The air-curing period are 7 days, 14 days, 28 days, 56 days and 6 months period as the case may be.

On completion of air curing period in compliance with test requirements, a compressive strength test is carried out to ascertain the Aer-Tech resistance capability, which is particularly, targeted to confirm the general material resistance tendency of the Aer-Tech material.

3.12 Method for making test specimen from fresh concrete

Consideration for research specimen has been focused on production of eight different types of mix ratio, three basic sample specifications. Table 3.1 gives a summary of varying Aer –Tech mix ratio.

Essentially, following focus on adequate critical assessment of material and structural properties of Aer-Tech material, production of specimen are categorized into three state samples specification. The first specimen type are the (100 × 100 × 100) mm³ cubes. For this specimen a lot of work had been done as over seven hundred cubes samples was produced for wide assessment, the second type are the (500 X 100 X 100) mm³ mini-beams, and the third type are an (1500 X 180 X 75) mm³ reinforced beam; the detail for the reinforced beam is shown in figure 3.4. Table 3.3 shows the amount of specimen made for each mix.

Table 3.3 Overall mix ratio for Aer-Tech 1% P= 1% complast SP430 plasticizers,

MIX	Date	Specimens	Sand [kg]	Cement [kg]	Water [l]	Foam [l]	Catalyst [l]
4.78 20% water reduction	10-6	301 to 310	11.34	2.37	2.62	0.2	0.0032
4.78P1% complast SP430	10-6	401 to 410	11.702	2.008	2.62	0.2	0.0032
5.83	26-6	320 to 329	11.34	2.37	2.008	0.2	0.0032
5.83P1% Complast SP430	26-6	420 to 429	11.34	2.37	2.008	0.2	0.0032
4.78	30-6	330 to 339	11.34	2.37	2.8	0.2	0.0038
4.78 20% water reduction	30-6	430 to 439	11.34	2.37	2.8	0.2	0.0038
4.78 20% water reduction	2-7	440 to 449	11.34	2.37	3.15	0.2	0.0038
4.78P1%	2-7	450 to 459	11.34	2.37	2.80	0.2	0.0038
4.78P1%	6-7	460 to 469	11.34	2.37	2.98	0.2	0.0038
4.78Fiber/cement.20%	8-7	500 to 509	11.34	2.37	3.05	0.2	0.0038
4.78Fiber/cement.20%	8-7	510 to 519	11.34	2.37	2.8	0.2	0.0038
4.78Fiber/cement.30%	10-7	520 to 529	11.34	2.37	2.63	0.2	0.0038
4.78Fiber/cement.50%	10-7	530 to 539	11.34	2.37	2.63	0.2	0.0038
4.41Fiber/cement.50%	16-7	540 to 551	11.4625	2.5975	2.63	0.2	0.0038
4.41Fiber/cement.50%	20-7	560 to 569	11.4625	2.5975	3.06	0.2	0.0038

Table 3.3 shows that 700 specimens were prepared, with about 180 average test results was derived from these specimens, although early samples poured in the steel cube moulds were discontinued.

Basically, the researcher discontinued the use of steel mould due to leaking problems and difficulties in cleaning steel moulds, to the use of disposable cubes.

Prior to discontinuing steel moulds, the moulds were cleaned, sealed with oil on every joint and surrounding of mould, to prevent water leakages. The cellular concrete were poured to the moulds by a pumping technique in the same way it been discussed in section 3.2 as shown in figure 3.2. After the moulds were filled with concrete the material were levelled with the top of the moulds using a plasterer's float and covered. Afterwards the specimens were left for three days and then the moulds were taken out and the specimens were left to be air-cured

It is observed that mix with high density faces bleeding as shown in figure 3.2,a situation where water in the mix raises to the surface of the freshly prepared Aer-Tech material. These defects had resulted to rejection of some of the samples taken.

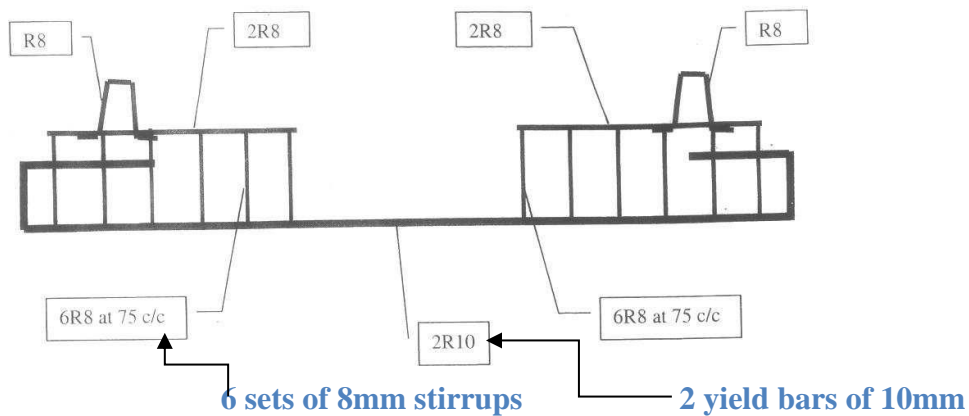


Figure 3.4 Reinforcement details



Figure 3.5 Bleeding of Aer-Tech material

Table 3.4 Summary of Specimen taken

Specimen Type	Quantity Taken	Sizes
Cubes	700	(100×100×100)
Mini beam	54	500×100×100
Reinforce beam	3	1500×180×75

3.13 Flow table test

The flow test is simple test to measure the flowability and spreadability of the material, the result of this test represents the workability of the material.

On this research programme, the flow test is carried out in accordance to BS1881: part 105, with specific difference using a steel ring as shown in figure3.1 (with diameter188 mm) instead of a cone as specified by BS1881 code. This test uses a flow table as shown in figure 3.6, the steel ring was placed in the middle of the flow table, and filled with the Aer-Tech concrete.

After that the ring were lifted vertically over a period of 3 to 6 seconds. Then the table was stabilised by standing on the toe board at the front of the flow table.

After that the table top was raised using the handle till it reached the upper stop. The table top was then allowed to fall freely to the lower stop and this cycle was repeated five times. At the end of this process the concrete spread was measured in two directions with a roller and the arithmetic mean of both diameters was found.

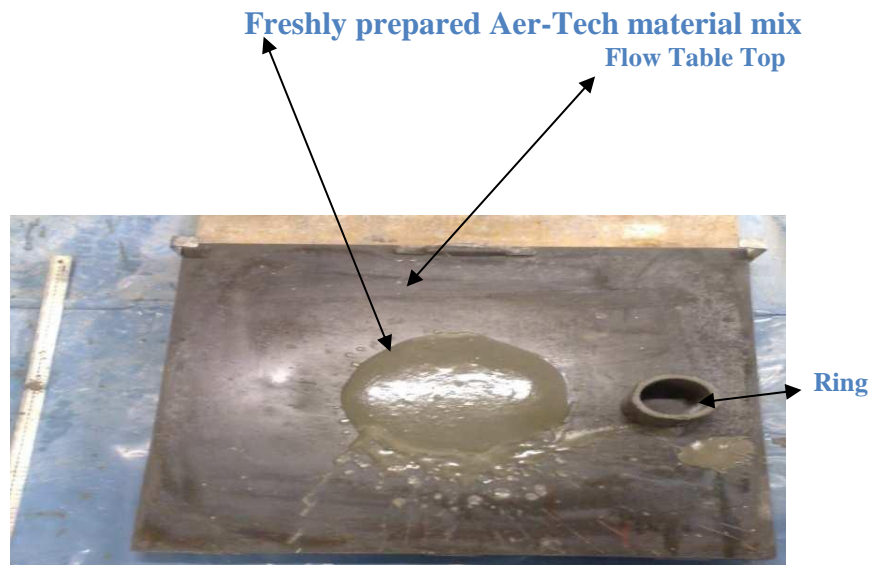


Figure 3.6 Flow Test Apparatus

3.14 Compressive strength test

This test is a simple uniaxial compression test for cubes, it is determined as the ratio between the rupture load in axial compression and the cross-sectional area of the test specimen perpendicular to the loading direction, in accordance to BS EN 679: 2005 .The specimen size used is 100mm cube.

Appreciably, compressive strength test specifically designed to determine the concrete strength in compression is widely used in the industry.

According to (Newman *et al.*, 2003), the compressive strength testing machine do consider the under listed factors in order to give accurate result (Figure 3.7).

- Load indication.
- Lateral and axial stiffness of frame.
- Spherical seating design
- Machine platen shape and hardness etc.
- Auxiliary platen shape and hardness.
- Specimen location.

This item has been removed due to third party copyright. The unabridged version of the thesis can be viewed at the Lanchester library, Coventry university.

Figure 3.7 Problems with force transfer to specimens (Newman *et al.*, 2003)

Ultimately, since the specimen for compressive strength are to be air cured, it is specified that ten specimen be taken for any given mix.

3.14.1 Fresh state conditioning of test specimen

The test specimen straight from Aer-Tech machine is poured into 100 mm cube disposable mould at a temperature not exceeding 60°C. After 24hrs the specimen is de-moulded and air cured for a period of 7,14,21,28 and 56 days.

Prior to testing of specimen it was ensure that specimen was in a dried state. Measures are taken such that the weighing error did not exceed 0.1% of the mass.

3.14.2 Measurement Of Aer-Tech Specimen

The harden Aer-Tech specimen, length, width and height of the specimen was measured to an accuracy of 0.1 mm, using callipers.

This measurement allows the determination of the volume V of a specimen with an error not exceeding 1%.

3.15 Compressive test procedure

Considerably, the mass of each specimen is again checked just before testing and accurately recorded. The platens of the testing machine are wiped clean, and the test specimen is centred in the testing machine. Then compression load of about 2000KN Avery Denison machine gradually drops load ranging from 10-50KN which is applied axially and perpendicularly to the direction of rise (figure 3.6).

This test specimen is loaded gradually and without shock at a constant rate corresponding to a stress increase of (0.1 ± 0.05) MPa per sec, until rapture of the test specimen occurs or until no greater load can be sustained by the specimen in compression. More so, the Aer-Tech specimens are loaded at such rate that

failure occurs within 25-35s. Thus the load at which each individual specimen fails is noted.



Figure 3.8 2000KN Avery Denison Compressive strength machine

3.15.1 Compressive strength results

The compressive strength f_{ci} , in MPa, of the test specimen i is determined as follows:

$$F_{ci} = F_i / A_{ci} \text{ -----(3.2)}$$

where $i = 1, 2, 3$

F_i is the maximum load failure, in Newton's;

A_{ci} is the cross- sectional area to which the load is applied.

Thus, the compressive strength of the product f_c , in Mega Pascal's is defined as the mean value of the compressive strength f_{ci} of the three test set specimen.

$$f_c = (f_{c1} + f_{c2} + f_{c3}) / 3 \text{ -----(3.3)}$$

The compressive strength of the product, f_c , is expressed to the nearest 0.1 MPa(BS679:2005)

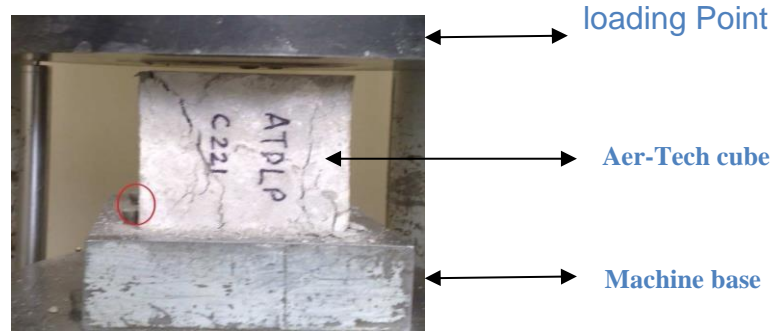


Figure 3.9 Cube sample positioned in Avery-Dimension machine

In addition to the (100×100×100)mm cubes that have been tested, an equivalent compressive strength tests have been performed for the beams that been tested for flexural using steel cap as shown in figure 3.10.



Figure 3.10 Equivalent compressive Strength Test

3.15.2 Assessment of Aer-Tech Failure Mode Type

In accordance to BS EN12390-3 clause 6.3, the test has shown that most of the Aer-Tech test specimen had produced satisfactorily compression mode with a few unsatisfactory mode. Specifically, figure 3.8 shows the failure mode that most of the specimens undergo.

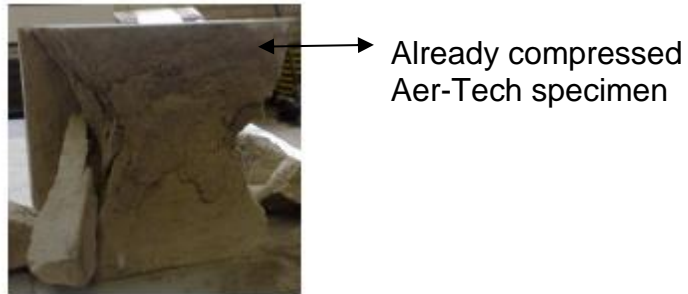


Figure 3.11 Failure Mode for Aer-Tech specimen

The main problem encountered by carrying out this test was that some specimens were so weak that the machine would squeeze the specimen without undergoing a large load drop and this had subsequently lead to reduction of load drop on cube specimen from 50kN to 10kN.

3.16 Machine calibration

Avery-Denison 200kN was upgraded in a way that it could measure the deformation in the specimen, and that would allow the user to calculate the elastic modulus of specimen.

The elastic modulus using this machine were calculated for all the samples, and then it calculated elastic modulus using another test that will be described later, the results shows that the elastic modulus using this machine is actually much lower than the elastic modulus using the other test that been used, as the other test is similar to the test that is described in BS EN 13412:2006, the modulus of elasticity using this machine was ignored.

The reason for this difference could be because the deformation gauge for the machine is not actually attached to the plate that is transferring the load to the spacemen, instead it is attached to another plate that move along with this plate.

Numerical Modelling

3.17 Neural Network Model For Aer-Tech Material

In order to find the best combinations of materials and their relative proportions, an experimental laboratory programme was carried out. Mixes with different proportions of Aer-Tech material was carried out. Their respective compressive strength and density for 56 days test was taken for design of an effective model using the concept of neural networks (NN).

The neural network tool tested to optimize the mixture ingredients to achieve the highest compressive strength. In order to obtain the final proportion for each binary or ternary binder, a simple but effective experimental design was made. The compressive strength and density of several mixes with different proportions was evaluated to ascertain the influence of various proportions on the strength.

3.18 Describing the Neural Network Model

An Artificial Neural Network (ANN) is one of the artificial intelligence techniques used as information processing systems, capable of learning complex cause and effect relationships between input and output data (Demuth, Beale and Hagan, 2008). It was further defined by (Fanchou and Pellinen, 2005) that neural network

is a functional abstraction of the biological neural structures of the central nervous system.

Apparently the NN as it often known, can exhibit a surprising number of human brains characteristics, for example, learning from experience and generalizing from previous examples to new problems. The neural network can provide meaningful answers even when the data to be processed include errors or are incomplete, and can process information extremely rapidly when applied to solve real world problems.

What happens in Neural network software is that the neural computing architect had built into the physical hardware (or machine) a neural software languages that can think and act intelligently like human beings.

The neural network approach to modelling process involves five main aspects: (a) data acquisition, analysis and problem representation; (b) architecture determination; (c) learning process determination; (d) training of the networks; and (e) testing of the trained network for generalization evaluation (Ahmet, Murat and Bhatti, 2004).

3.19 The Basic Strategy Of Neural Network

The basic strategy for developing a neural network model for material behaviour is to train a neural network on the results of a series of experiments using that material. If the experimental results contain the relevant information about the material behaviour, then the trained neural network will contain sufficient

information about material behaviour to qualify as a material model, these strategy conforms to works of (Lee, 2003).

Consequently, training a network with fewer samples often leads to early convergence.

3.20 Types of Neural Network

Considerably, there are two types of ANN architectures which can be used in performing higher level human task such as diagnosis, classification, decision making, planning and scheduling. They are; the feed-forward networks designed to have their neurons arranged in layers. Also it is known that these layers have connections to the layers on either side. Secondly, the Elman ANN has a loop from the output of the hidden layer to the input layer.

Particularly, for this work the feed forward network which applies the back propagation processes had been used. The Back propagation algorithms is one of the most popular training algorithms for multilayer perception, it uses the gradient descent technique to minimize the error.

3.21 Procedure for Aer-Tech Neural Network

With a clear objective of producing an effective ANN model of Aer-Tech material. The researcher had focus on training the network properly.

Appreciably, in the training of an ANN model, a function is mapped from known inputs to known outputs. This process is classified as a supervised learning. The

training process involves passing a reasonable input of experimental data(mix constituent of Aer-Tech material) and their respective resultant compressive strength and density for training. In addition, to minimise errors weights between the neurons are adjusted.

Specifically, the researcher had used the Matlab Neural Network Toolbox to construct and train the networks.

Interestingly, the Matlab toolbox has pre-programmed training functions. The Matlab tool box is different from other computational software because its operation is not programmed but is taught.

Primarily, the network is trained on the relationship between mix proportions of Aer-Tech material, its compressive strength and density.

Besides, the Aer-Tech material neural network model can be describe as mapping function represented in simple mathematical models defining a function $F: X \rightarrow Y$. Each type of ANN model corresponds to a class of such functions.

The Aer-Tech neural network F consist of the nodes in which data are transmitted from one neuron to another and second also consists of a set of rules upon which the transformation of data within each neuron is based. The behaviour of an ANN depends on both the weights and the input–output function (transfer function) that is specified for the units. In all the layers in the present study there are i inputs, j outputs, and k neurons. Inside each neuron, a weighted

sum of the inputs is calculated and this value, called NET, is transformed by a hyperbolic tangent function. The transformed result is sent to neurons in the next layer.

The input values are forwarded after multiplying by the weights associated with each neuron that diagram of neuron in ANN is shown in [Figure 3.9](#).

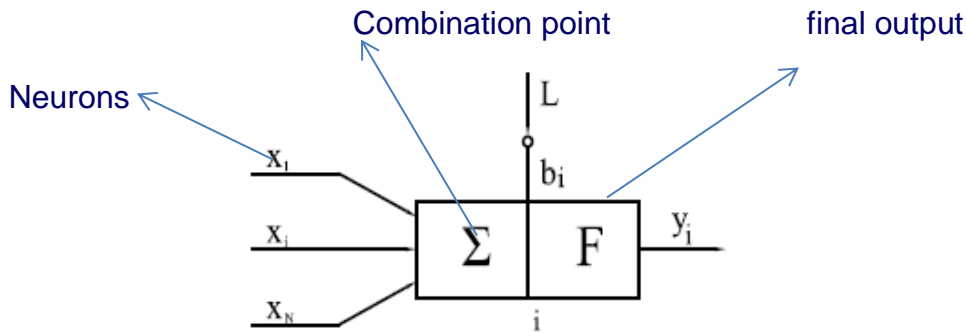


Figure 3.12 Diagram of neuron in ANN

Each training pattern contains an input vector of 5 elements such as; cement content, sand, water, foam, catalyst ratios and two output data compressive strength and density. Furthermore, ANN are highly non-linear, and can capture complex interactions among input and output variables. This characteristic is likened to what happens in human brains. In the case of ANN the neuron is connected to other neurons through links that produce a stimulus to the entry and exit as a response, in addition, they have the ability to communicate among themselves. Whilst, the ANN has a finite number of neurons distributed in the input layer for input data and a corresponding output layer for the target output data, also it has the intermediary layers called hidden layers, which establishes a network of relationships between layers of input and output values.

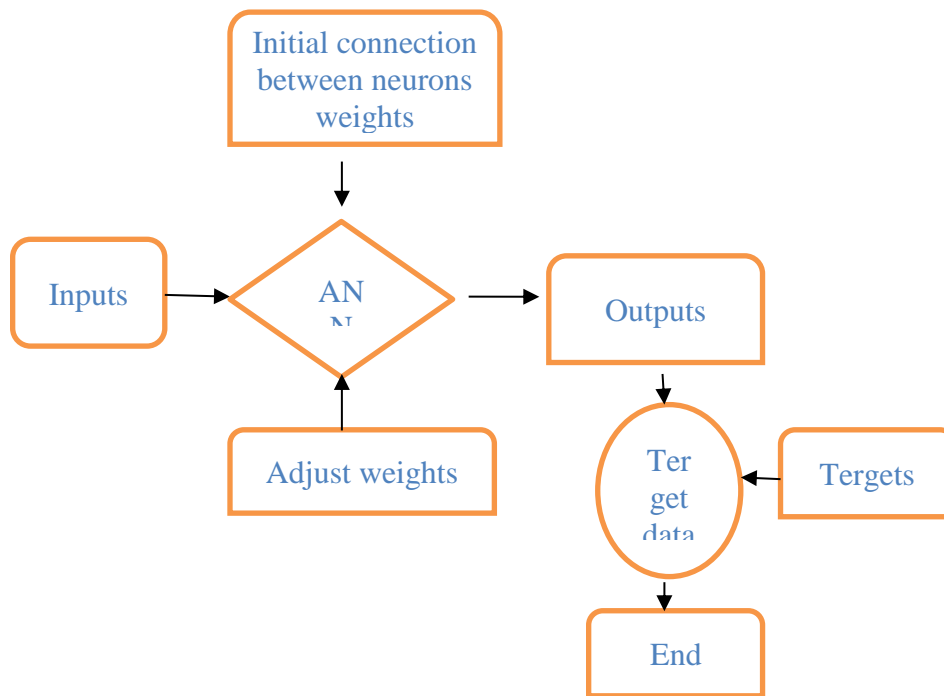


Figure 3.13 Training back-propagation algorithm of the neural network method

From figure 3.13 one can deduce what happens in the neural network, it is obvious that entrance to a neuron is a numeric value defined as a scalar p , which in turn is multiplied by a weight w and finally generate a product wp , which is scalar as well. In order to generate a scalar output in a neuron, it is necessary to evaluate a function known as transfer function f , which may sometimes be influenced by a bias defined by a scalar b . The transfer function f , usually corresponds to a step, linear or sinusoidal function, which uses n as an argument and generates a scalar output.

3.22 Experimental Design

The Aer-Tech neural network model is developed by training matlab programme with experimental results of material composition, compressive strength and density, which is obtained from about 81 different mix ratio of Aer-Tech material. More so after the network had been trained by the said experimental result, the model is simulated to predict compressive strength of Aer-Tech material and density for 56 days.

The predicted results are compared with experimental result to verify the effectiveness of the neural network model. The error incurred during the learning can be expressed as root-mean-squared (RMS) one and is calculated.

$$RMS = \sqrt{(1/p) \sum_j |t_j - o_j|^2} \quad \text{-----}(3.4)$$

Also, for a more holistic look on error, the absolute fraction of variance (R^2), the mean absolute percentage error (MAPE) and sum of the squares error (SSE) are calculated using the following equation:

$$R^2 = 1 - (\sum_j (t_j - o_j)^2 / \sum_j (o_j)^2) \quad \text{-----}(3.5)$$

$$MAPE = (o - t / o) * 100 \quad \text{-----}(3.6)$$

$$SSE = \sum_j (o_j - t_j)^2 \quad \text{-----}(3.7)$$

Where t is the target value, o is the output value and p is the pattern.

3.23 Material and mixture composition

The constituent material used to produce Aer-tech material were comprised of: Pro-chem cement conforming to BS8110, pulverized river sand finer than 300 μ (specific gravity 2.5), Aer-Tech catalyst and foam produced by aerating a foaming

agent (Aer-Tech Sol) (dilution ratio 1:5 by weight) using an indigenously Aer-tech machine calibrated to a density of 1810kg/m^3 . Figure 3.10 give the linear value of constituent material composition that was transform to a nonlinear value into the matlab.

Below are values of parameters used in this model;

- Number of input layer = 5
- Number of hidden layer = 2
- Number of first hidden layer unites=4
- Number of second hidden layer unites= 1
- Number of output layer unites=2

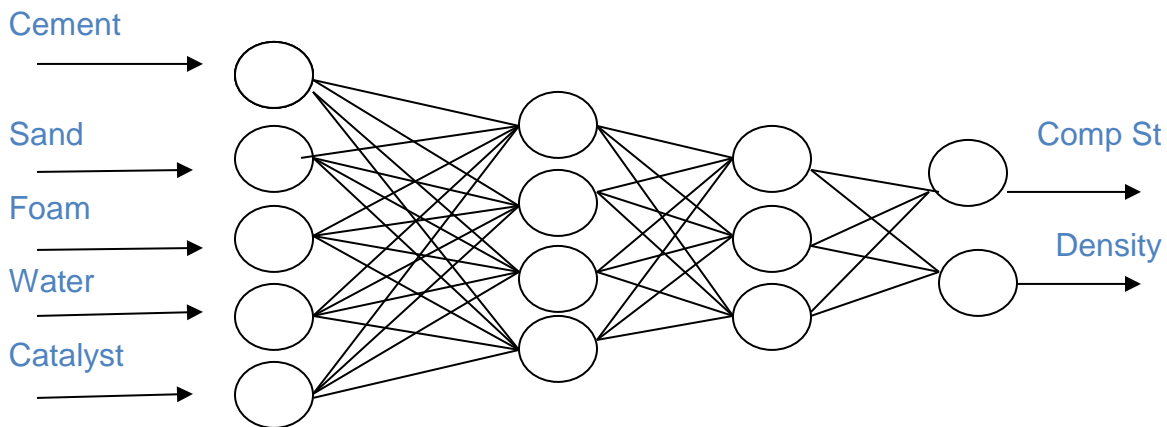


Figure 3.14 Proposed Aer-Tech Neural Network Model

The Aer-Tech neural network model was constructed and trained using the neural network toolbox of Matlab®. To train the network the numerical physical model was run several times in order to obtain enough input vectors and the corresponding target vectors.

Consequently, for effective and accurate training, all the inputs and outputs were normalized between -1 and +1 in order to avoid the influence of the scale of the physical quantities. In the same way, to feed the neural network it is necessary to normalize the data. A linear relationship was used to find the equivalence between the real coordinate system and the natural system (-1 to +1).

Below is figure 3.12 which shows the relationship between real and normalized. The corresponding constants to normalize the input experimental data are:

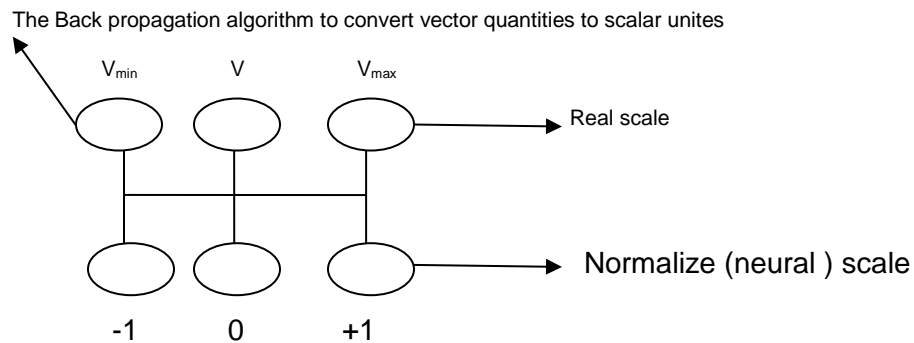


Figure 3.15 Relationship between real and normalized scales

$$U = \frac{2(V_i - V_{avg})}{(V_{max} - V_{min})} \text{-----(3.7)}$$

3.24 Scanning Electron Microscopy

In order to critically access the pore structure of Aer-Tech material a scanning electronic microscopy test was carried out on two basic mix samples, they are the mix sample with fibre glass and sample without fibre glass.

In accordance to experimental method in session 3.3 a two slice specimen of mix with fibre mesh and the mix without fibre mesh were shape to a sizable dimension to fit properly into the SEM machine. The SEM machine is a microscopy tool used to observe real-time objects as a stereographic magnified image. During this test, an electron beam is focused on the Aer-Tech specimen in machine. This causes surface and sub-surface atomic reaction within the specimen. Specific electrons are released from the material. These are detected and converted to electrical signals which are amplified to produce a real-time image.

More so, higher level magnifications are achieved through accurate manipulation of the electron beam and the system can be used for topographical, composition and elemental analysis.

Imaging was performed in high vacuum with the application of a conductive coating. The samples were made conductive. Figures 3.13 and 3.14 shows samples with a carbon and gold layer. The accelerating voltage of the scanning electron microscope was 15 k.

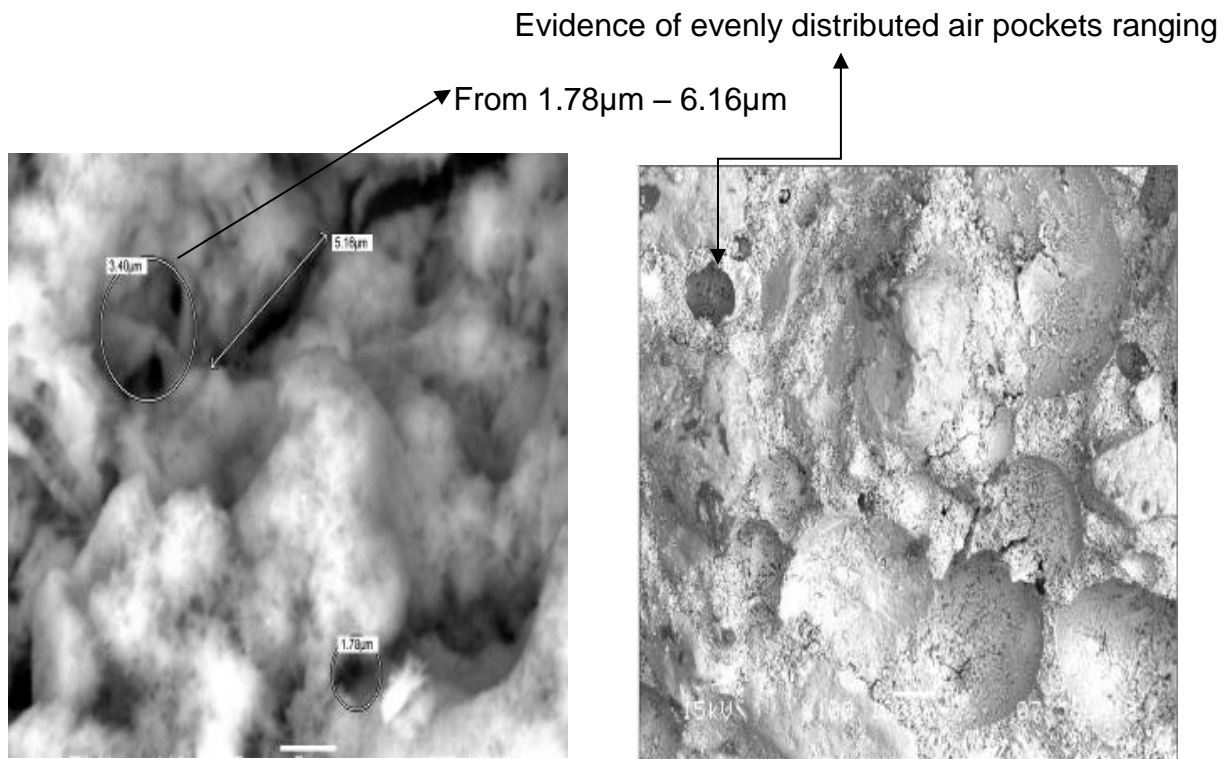


Figure 3.16 Aer Tech material SEM images without fibre glass

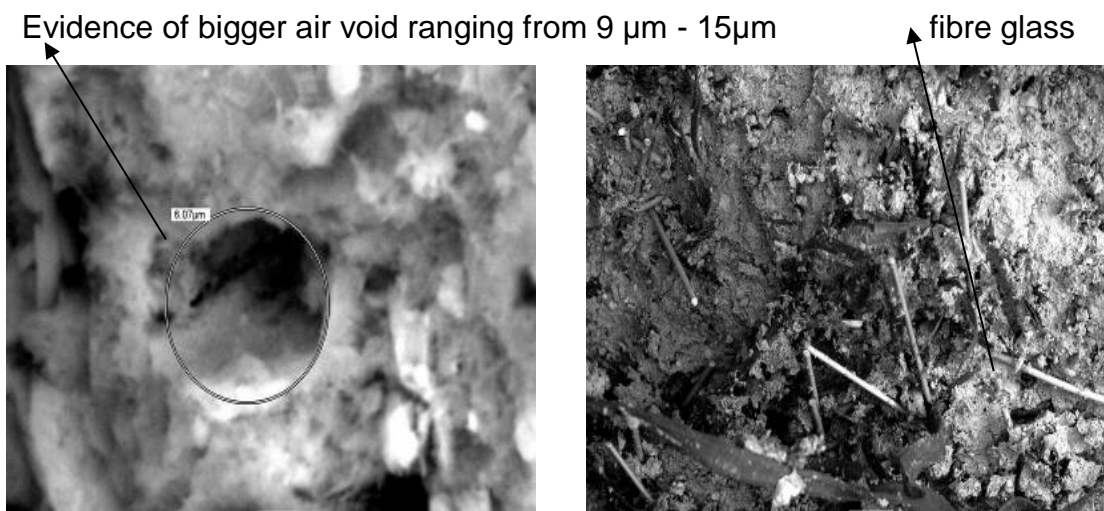


Figure 3.17 Aer-Tech SEM images with fibre glass

Comparatively, the above figures have shown microscopic capillary structure of two different mix of Aer-Tech material. The mix without fibre glass and the mix with fibre glass, the microscopic pictures which had capture the stereographic

images of Aer-Tech novel material had given opportunity to truly confirm the real state of specimen micro structure.

Table 3.3 below gives the number of visible voids within a measured area of the specimen.

Table 3.5 Determining the number of visible voids within a measured area

Specimen	Measuring Area Of Specimen(mm ²)	Numbers of visible voids	Original Specimen density
Cu301	0-100	6	1805
Cu401	100-150	9	1810
Cu501	150-200	11	1803
Cu601	200-250	15	1807
Cu701	250-300	18	1800

3.25 Particle size distribution Test for Aer-Tech material composition

The **particle-size distribution (PSD) test of Aer-Tech specimen** without fibre glass and a specimen with fibre glass is granulated into power form and passed through the particle size distribution machine. The outcome of the particle sieve or a mathematical function that defines the relative amount, typically by mass, of particle sieve is recognized as the particle seize distribution analysis.

The way PSD is usually defined by the method by which it is determined. The most easily understood method of determination is sieve analysis, where powder is separated on sieves of different sizes. Thus, the PSD is defined in terms of

discrete size ranges: e.g. "% of sample between 45 μm and 53 μm ", when sieves of these sizes are used. The PSD is usually determined over a list of size ranges that covers nearly all the sizes present in the sample. Some methods of determination allow much narrower size ranges to be defined than can be obtained by use of sieves, and are applicable to particle sizes outside the range available in sieves. However, the idea of the notional "sieve", that "retains" particles above a certain size, and "passes" particles below that size, is universally used in presenting PSD data of all kinds.

The PSD may be expressed as a "range" analysis, in which the amount in each size range is listed in order. It may also be presented in "cumulative" form, in which the total of all sizes "retained" or "passed" by a single notional "sieve" is given for a range of sizes. Range analysis is suitable when a particular ideal mid-range particle size is being sought, while cumulative analysis is used where the amount of "under-size" or "over-size" must be controlled.

The way in which size is expressed is open to wide range of interpretations.

A simple treatment assumes the particles are spheres that will just pass through a square hole in a sieve. In practice, particles are irregular – often extremely so, for example in the case of fibrous materials- and the way in which such particles are characterized during analysis is very dependent on the method of measurement used.

3.26 Modulus of elasticity in compression test

In this test, 50 x 10 x 10 cm mini beams specimens were used, the specimens have been tested using the Avery-Denison 500 kN machine.

This is a compression machine which allows the beams to be tested in full compression as the assumed force system is shown in figure 3.8, the machine has a computerized system that allows the loading process to be controlled with a specified loading rate, most of the specimens were tested with a loading rate of 0.09 kN/s.

Four demec points have been attached to each specimen, in line with procedure. The demec points are glued in two opposite sides of the specimen, to ensure that the specimens are in full compression failure as shown in figure 3.20.

Each beam was tested with three different loads, for each load increment, the strain was measured using an strain electronic gauge as shown in figure 3.20 plus the zero reading was measured as well, and after loading the beam to the maximum tested load the load was decreased and the strain was measured again for the same loads, by carrying that out any inertial damage in the specimens will be indicated.

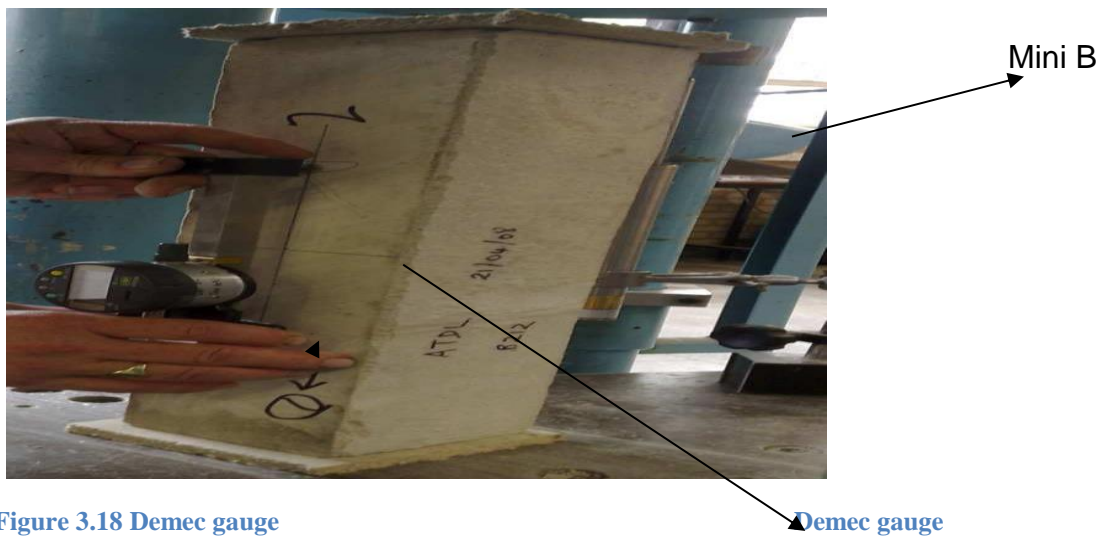


Figure 3.18 Demec gauge

3.27 Demec gauge calibration

The gauge has a strain factor of 0.403×10^{-5} for each 0.001 division, this strain factor has been calibrated using a wood beam, the demec gauge were set for a zero reading when the demec points were 200 mm apart,

then one of the points were shifted 5 mm, and the demec reading were taken to be 6.203, using that reading it could be shown that the strain is 0.025, as the zero reading were 200 mm apart and one of the points where shifted 5 mm using $\Delta\epsilon/\epsilon_1$ the stain could be found to be 0.025.

3.28 Modulus of elasticity in compression calculation

The analysis and calculation for this test are simple; first the strain was found (such as from figure 3.21) using the following equation:

$$\Delta\epsilon, = \text{demec gauge reading} \times 10^8 \times \text{strain factor} \text{-----}(3.8)$$

Second the modulus of elasticity was plotted in a graph to fulfil the following equation:

$$\text{Modulus of elasticity} = \Delta\sigma/\Delta\varepsilon$$

Where

- $\Delta\varepsilon$ = strain change due to the load.
- $\Delta\sigma$ = is the stress change due to the load in N/mm^2 .

By finding the secant modulus equation as described in chapter 2, the modulus of elasticity is the first number before the x in the equation.

3.29 Flexural strength test

In this test, the 50 x 10 x 10 cm mini beams specimens that been used in the modulus of elasticity were reused used again. The specimens have been tested using the Avery-Denison 150kN machine. This machine performs a two point load test that is described in BS EN 12390-5:2000 as shown in figure 3.19. The machine is upgraded with a computerized program that allows controlling the load and the load rate

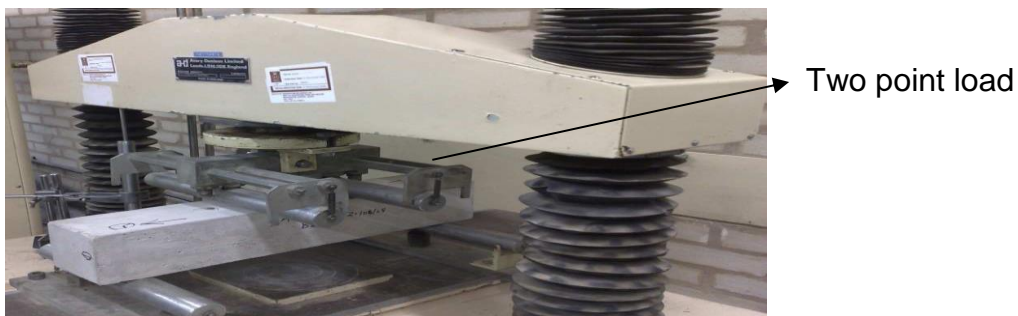


Figure 3.19 Two point flexural test Avery-dimension machine

3.30 Flexural strength calculation

The important of this test is that, using the result of maximum failure load of the specimen, the flexural strength could be calculated using the following equation:

$$F_{cf} = \frac{F \times L}{D_1 \times D_2} \text{-----(3.9)}$$

Where

- f_{cf} = flexural strength, in mega Pascal's.
- F = maximum load, Newton's.
- L = the distance between the supporting rollers, in millimetres.
- D_1 and D_2 = the lateral dimension of the specimen, in millimetres

3.31 Reinforced beam test

By making this experiment the behaviour of a reinforced Aer-Tech beam when tested to failure was investigated. Deflection and its strain were also measured through the experiment.

Then the experimental values of deflection, strain and the behaviour of the beam were compared with its theoretical values of normal reinforced concrete beam, this experiment allows one to discuss how reinforced Aer-Tech beams behave in service and at collapse. It further allows us, to carry out design calculations for the preliminary stages of reinforced Aer-Tech material design.

In order to test the beam, it was set-up into the loading machine in the configuration as shown in figure 3.20, and 10 demec points were glued to the specimen as showed in figure 3.21 shows. The zero deflection reading was measured using deflection gauge that were installed under the midpoint of the specimen, then the load was increased in equal increments of 3kN, each time there is a deflection at the various increments. The varying beam behaviour on all increments was noted.

As the increment was measured, the demec readings were taken too at each weight increment. This procedure continues until the first cracks appear onto the beam. When the first cracks appeared, the loading continued to attain point where the beam snaps or failed. Consequently, the mode of failure, the failure load, the deflection and the demec readings were noticed.

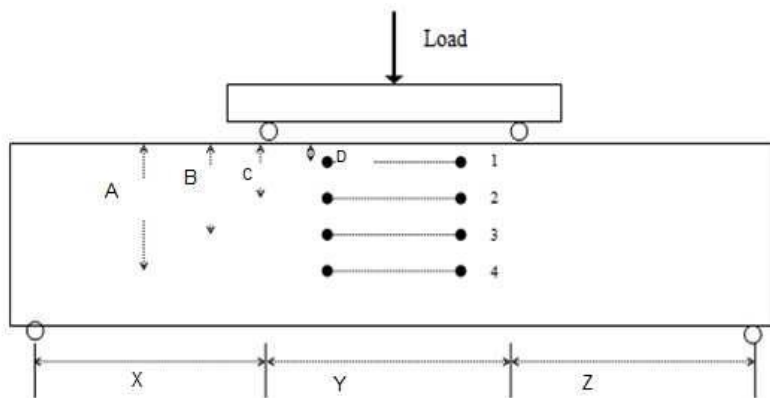


Figure 3.20 Reinforced beam test configuration



Figure 3.21 Demec point on reinforced beam

4 Chapter four: Analysis and discussion of the results

4.1 Introduction

This chapter provides discussion for the analysis of the results. It includes the results, analysis and discussion. Precisely, the chapter is structured in line with the analysis of test results from chapter 3. Intrinsically, the chapter has focused on detailed discussion about the material behaviour of Aer-Tech novel material and the structural behaviour of Aer-Tech reinforced beams.

Below, are tables (4.1 to 4.7) of result for compressive strength and density with duration. These results are experimental values of different mixes of Aer Tech material mix.

Table 4.1(4.78:1 Mix, Specimen CU701-710)

Duration(days)	7	14	28	56
Density(Kg/mm ³)	1907	1888	1845	1824
Com.Stgth(N/mm ²)	11.5	16.0	25.7	28.71

Table 4.2(4.78:1 Mix, with 20% water reduction, Specimen CU730 -750)

Duration(days)	7	14	28	56
Density(Kg/mm ³)	1829	1824	1817	1806
Com.Stgth(N/mm ²)	12.41	17.13	27.97	33.34

Table 4.3 (5.78:1 Mix, Specimen CU760-780)

Duration(days)	7	14	28	56
Density(Kg/mm ³)	1890	1864	1843	1826
Com.Stgth(N/mm ²)	13.1	16.93	19.41	23.40

Table 0.4 (5.78:1 Mix, with 1% fibre glass, Specimen CU790-810)

Duration(days)	7	14	28	56
Density(Kg/mm ³)	1917	1880	1867	1851
Com.Stgth(N/mm ²)	9.79	13.9	15.49	18.10

Table 0.5(20% water reduction 4.78:1 Mix, with 1% plasticizers Specimen CU830-839)

Duration(days)	7	14	28	56
Density(Kg/mm³)	1816	1830	1808	1718
Com.Stgth(N/mm²)	11.43	14.56	17.30	18.38

Table 0.6(20% w/c reduction from 4.78:1 Mix, with 1% fibre glass, Specimen CU840-849)

Duration(days)	7	14	28	56
Density(Kg/mm³)	1832	1819	1795	1781
Com.Stgth(N/mm²)	5.66	9.30	10.14	12.33

Table 0.7 (20% w/c reduction from 4.78:1 Mix, Specimen CU850-859)

Duration(days)	7	14	28	56
Density(Kg/mm³)	1835	1814	1805	1800
Com.Stgth(N/mm²)	15.19	20.5	28.21	33.91

4.2 Compressive Strength And Density

Figures 4.1 and 4.3 Show density and compressive strength time relationship of Aer-Tech material base mix for mixes 4.78 :1 and 5.78:1. Obviously, both figure 4.1 and 4.3 shows that Aer-Tech material density decreases with increase in time, though both represents different mix of 4.78:1 and 5.78:1. Their corresponding drying shrinkage characteristics behaviour, remains the same as it conforms to the analogy reported in literature that mix design ratio is a key function of density composition in any given mix.

(4.78:1 Mix, Specimen)

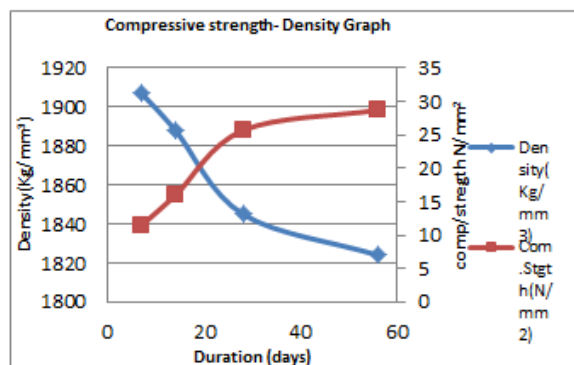


Figure 4.1

(5.78:1 Mix, Specimen)

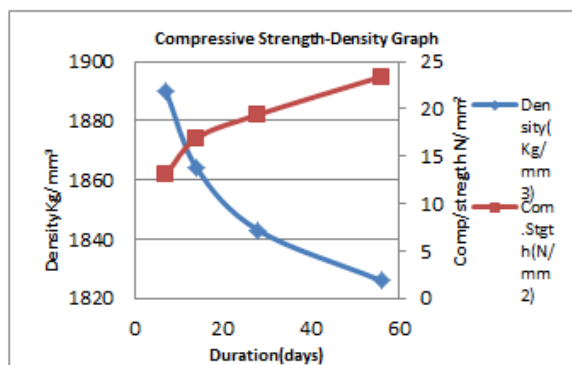


Figure 4.3

(4.78:1 Mix, with 20% water reduction)

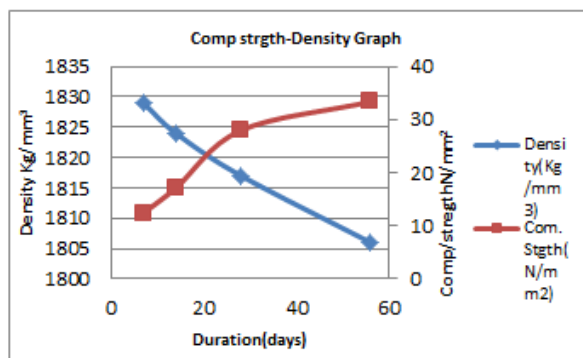


Figure 4.2

(5.78:1 with 1% Fibre Glass Mix)

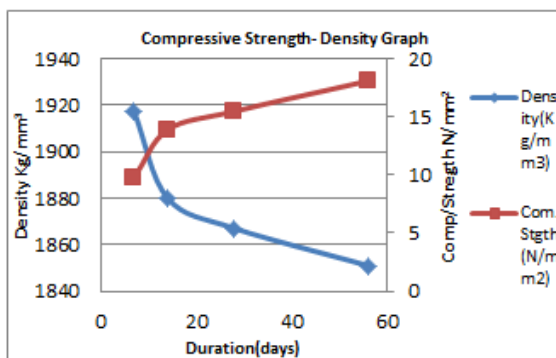


Figure 4.4

Comparatively, the results of both mix shows that achieved Aer-Tech material density is far higher than design density of 1810kg/m³ as output density spans up to 1890 to 1909 kg/m³ in the two mix.

However, the higher the difference in density output the more invalid the specimen taken from mix is, as results exceeds 1-7% tolerable limits between actual density and automated computerized density as specified by BSEN 1810.

Objectively, Aer-Tech material as a lightweight material is designed to showcase a display of low range density material against the over weighing density of conventional concrete. In addition, results had shown evidence of inconsistency in design mix ratio which is a fundamental factor to achieving an acceptable design density.

4.3 Compressive Strength (Mix 4.78 :1 & 5.78:1)

The excellent performance of Aer-Tech material in figure 4.1, 4.2, 4.3 & 4.4 are clear indication that the material Aer-Tech increases in strength as age increases, which is similar to reports in literature, that curing of Aer-Tech material further improves material compressive strength.

Considerable, measure were taken to bridge gaps observed, from experimental defaults of mix(5.78:1). These measure are similar to researchers position as reported in literature that density ratio of unity or nearly unity is achieved only at a particular consistency.(ie) at low consistency, the density ratio is higher than unity. The mix is too stiff to mix properly, thus causing bubbles to break during mixing resulting in increased density. Whilst at higher water-solid ratio there is also an increase in density ratio, whereby higher water content makes the slurry too thin to hold the bubbles resulting in segregation of the foam from the mix along with segregation of the mix itself, thereby causing an increase in measured density. Emphatically, to strike a balance to this effect, a percentage reduction of water content in mix ratio, where abducted for all subsequent mix.

More so, figure 4.3 differs from figure 4.1 via water reduction ranging from of 5-20% was used to all Aer-Tech material mix ratio.

Figure 4.3 shows fall in compressive strength with time as against figure 4.1.

This is as a result of more foam content in Aer- tech mix ratio.

Intrinsically, discrepancies of material behaviour on fall in strength conforms to the works of Nambiar and Ramamurty that says mixes with higher foam content are prone to give lesser strength value.

4.78:1 Mix 20% Water-Redtn with 1% Pls

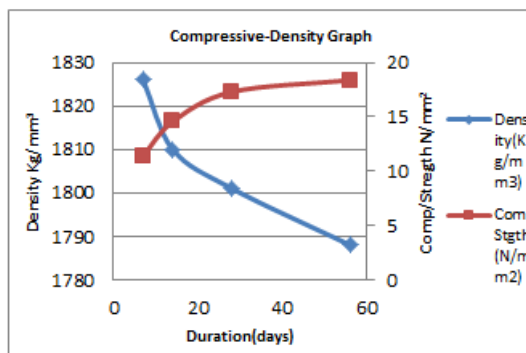


Figure 4.5

4.78:1, 20 % Mix water-R with fib-Gls

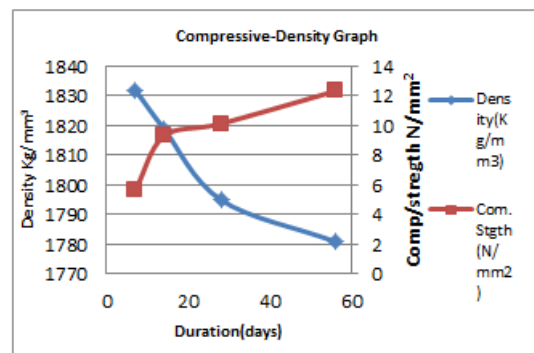


Figure 4.6

4.78:1 mix with 20% water-Reduction

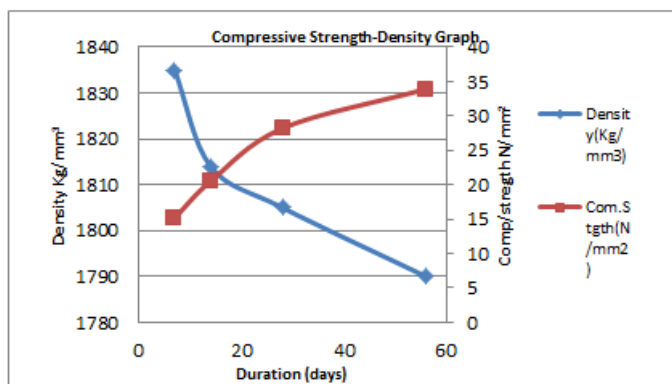


Figure 4.7

4.4 DENSITY

Appreciably, figure 4.5 - 4.7 whose mix ratio is 4.78:1 with 20% water reduction, with fibre glass and plasticizers shows incredible results, whereby density in this case clearly drops with time increase.

Ultimately, though results shows tremendous improvement in density as compared to results of figure 4.1 – 4.4.

4.5 Effect Of Additives On Compressive Strength

Figure 4.1 to 4.7, shows that the Aer-Tech material gain strength along with dropping density. This in a way confirms that Aer-Tech material hydration process continues as material ages.

More so, figure 4.5 and 4.6 which contains 1% plasticizer and 1% of fibre mesh (additive) shows no significant increase in strength, due to reaction between plasticizer and water, thereby making it inactive.

It was thought that dispersed glass fibres would reinforce the material structure but on testing, failure of the whole structure occurred at once because the fibres transmitted the load throughout, thereby preventing steady, progressive collapse. Fibre addition does not therefore improve compressive strength but it does allow the foam to sustain increasing load post fracture. Subsequently, distortion caused by presence of fibre glass in Aer-Tech material mix leads to low compressive strength.

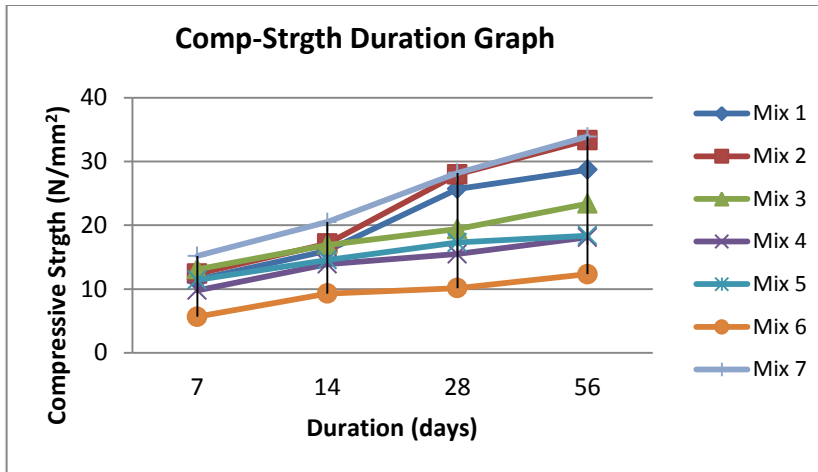


Figure 4.8

4.6 Effect of Machine calibration On Compressive Strength

Considerably, Figure 4.8 had shown that mix 1- 7 displays reasonable increase in strength as age increases.

Intrinsically, findings prove that all the irregularities in strength from Aer-Tech material specimen are caused by non précised material composition, due to machine default.

4.7 Overall Performance Of Compressive strength

Comparatively, Figure 4.1- 4.8 all shows how each mix gain its strength within the time period. As it could be shown from the figure, for each mix there are three points, each point represent the mean value of three cube tests, the tests were carried out as detailed in section 3.2.

Appreciably, all the above figures shows that the density drops for each mix with the time period. Specifically, each point in density of figures above represents the mean densities that were calculated using equation for three cubes and three beams.

The figure shows, the density of each mix drops with time. Two factors control this drop, the first is that when the hydration process start the water of the concrete start to evaporate because of the heat that is produce of the chemical reaction, and that factor is common in any concrete that been air-cured. The second factor is that time increase on Aer-Tech concrete changes its physical shape and dries out.

Obviously, the low strength display of Aer-Tech concrete is attributed to initial inconsistencies in mix and air curing of specimen, as this conforms to findings as discussed in section 2.12.1.

4.8 Effect of mixes proportions to the compressive strength

Considerably, the effect of water cement ratio in Aer-Tech mix brings about a lot changes in strength determination. Clearly, figures 4.9 and 4.10 shows that at lower water-solid ratio ie, at lower consistency the density ratio is higher than unity. The mix is too stiff to mix properly thus causing the bubbles to break during mixing resulting to increased density. Whilst at higher water-solid ratio there is also an increase in density ratio, which causes mix slurry too thin to hold the bubbles, resulting in segregation of the foam from the mix along with the segregation of the mix itself, there by leading to increase in density (Nambair and Ramamurthy,2006),

More so, for concrete water-cement ratio control the strength of the material, as by adding more water reduces strength of concrete, but for Aer-Tech that could be true, but it is not the main factor, figures 4.9 and 4.10, shows the water percentage and the foam percentage against twenty-eight day compressive strength for the first three mixing. Although figure 4.3 and 4.7 shows that by reducing water the material was stronger, the main factor was the foam percentage, as by adding more foam the mix strength reduces. That factor is related to the density as by adding more foam to the mix the density of the mix reduces as its strength reduces.

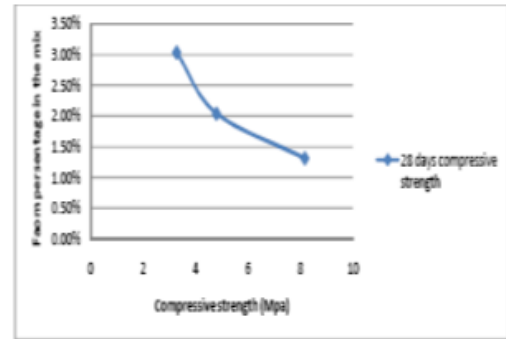
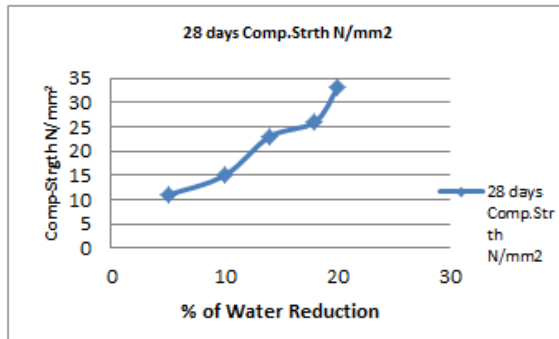


Figure 4.9 Compressive Strength/% water Rdtn Figure 4.10 % Foam/Com Str

4.9 Modulus of elasticity

Figure 4.11 shows how the modulus of elasticity for six Aer-Tech mix increases within the time period.

Apparently, it could be shown from the figure, that for each mix there are four points, each point represents the mean value of three beams tests, which was carried out as detailed in section 3.18. From figure 4.11 it could be notice that the mixes with higher densities have higher elastic modulus. This clearly conforms to literature report that density is a major function of elastic modulus, whereby the E value of conventional concrete as a more dense material is thrice the E value of Aer-Tech material.

In addition, it could be observed that fibre reinforcement didn't have much effect on the elastic modulus, as mix one and mix four have approximately the same elastic modulus.(Neville *et al.*,1978), stated that the modulus of elasticity of aerated concrete is usually between 1.7 and 3.5 Gpa, and from figure 4.11 show that for the twenty-eight days test the modulus of elasticity is in a range of 1.8 to 8.34 GPa

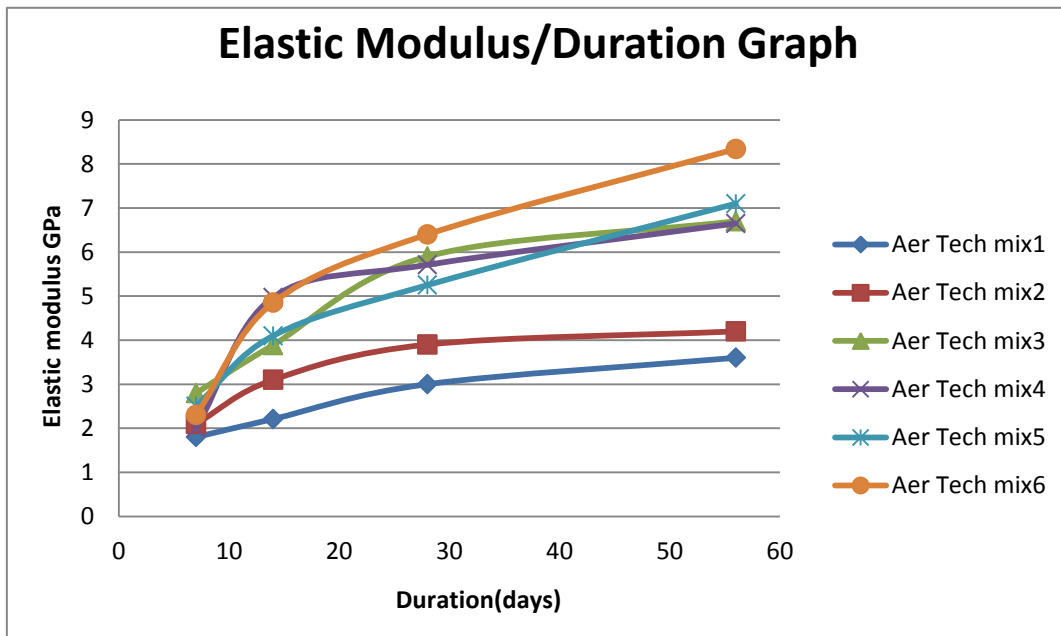


Figure 0.1 Elastic modulus against time

Appreciably, observation made in stress–strain relationship of Aer-Tech materials as shown in figure 4.12 shows that when the load was released the zero reading of the strain wasn't the same as it was before applying the load. This is caused by distortion in air-cells matrix structure of samples.

More so, to confirm if the beams were damaged, an equivalent cube test were carried out after the beams were tested for flexural strength, Figure 4.13 shows the mean value for the cubes test and the mean value for the equivalent cube tests for mix one, and it shows how the sample in mix one was effected, as a sample for all the mixes because they all had the same effect.

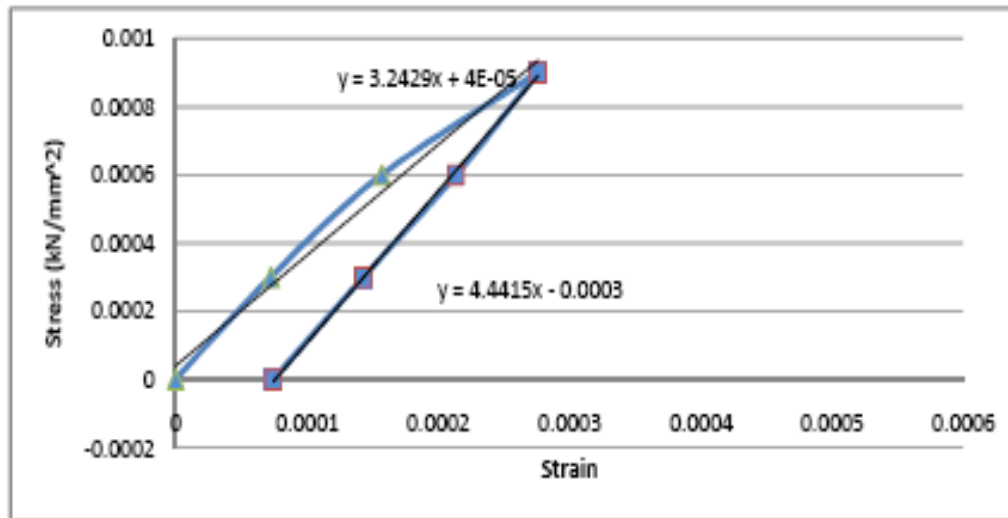


Figure 0.2 Sample of the hysteresis effect

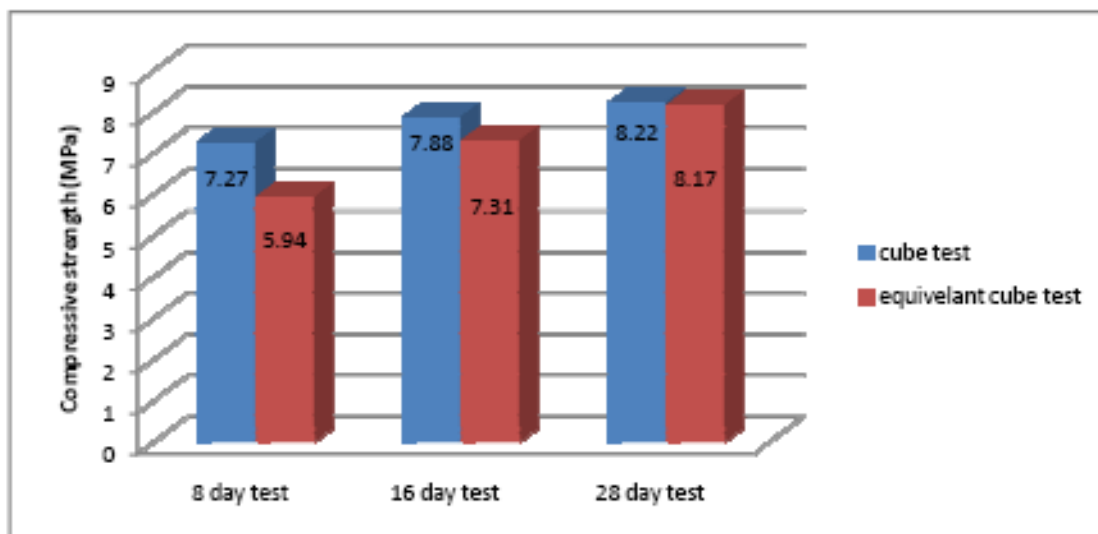


Figure 0.3 Compressive strength for cube tests and the equivalent cube tests

4.10 Flexural strength

The Figure 4.14 shows how each mix gains its flexural strength within the time period. As it could be shown from the figure, for each mix there are three points, each point represents the mean value of three beams tests, the tests were carried out as detailed in section 3.21

From figure 4.14 it could be noticed that mixes with higher density reaches more flexural strength than mixes with lower density. In addition the figure show that the flexural strength increases with increase in age of Aer-Tech material.

Ultimately, Aer-Tech flexural behaviour conforms with findings in literature that moisture gradient, density and curing method within the specimen has a strong influence on the test result (Commite' Euro –international du Beto, 1978).

Furthermore, figure 4.11 show that the Aer-Tech specimen flexural performance from the four different mix, whereby the mixes with fibre reinforced had a higher flexural strength than mixes without a fibre reinforcement.

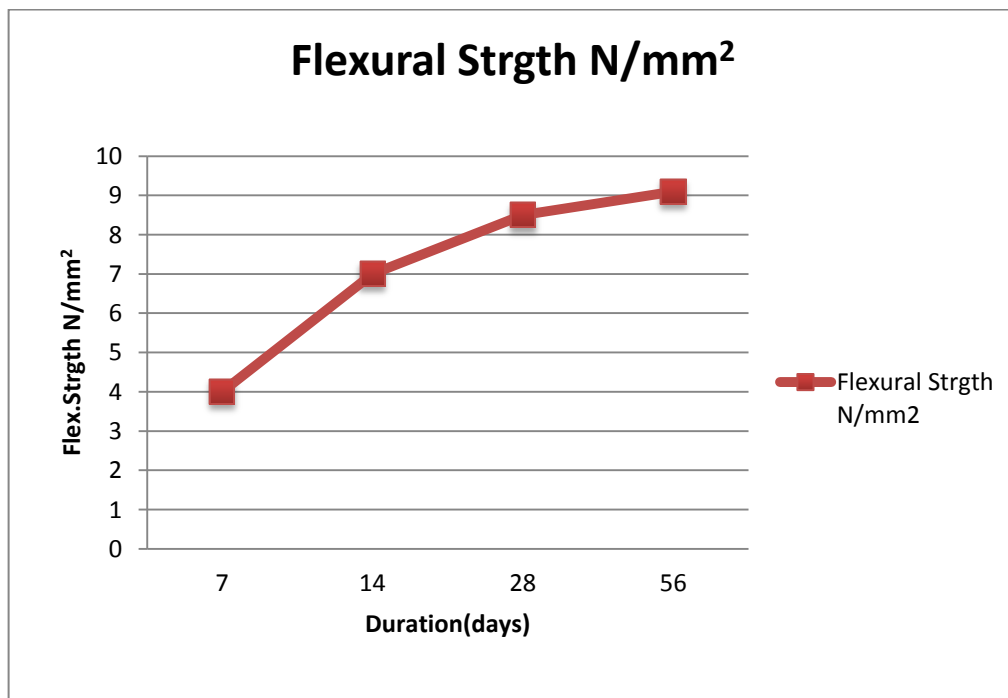


Figure 0.4 Flexural strength against time

4.11 Flexural strength and Compressive strength relationship

Figure 4.15 Shows a relationship between flexural strength and compressive strength as it conforms to findings in literature that the ratio of flexural strength to compressive is $1/4 - 1/6$ (Comite' Euro- international du Beton, 1978).

From the figure 4.15, it could be notice that Aer-Tech material has higher compressive strength than its flexural strength in ratio of 4:1.

More so, from the figure it is clear that, compressive strength and flexural strength gain strength along time.

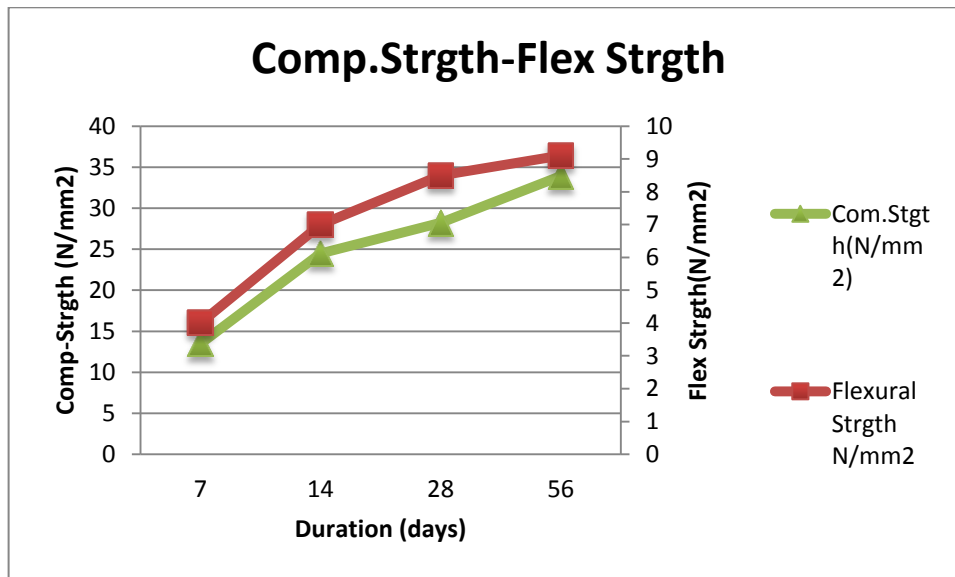


Figure 0.5 Flexural strength and compressive strength relationship

4.12 Structural properties of Aer-Tech reinforced beam

4.12.1 Ultimate moment

Three reinforced beam were tested for each mix as detailed in section 3.18, all the beams had the same reinforcement as shown in figure 3.1. The experiment strains and stresses were calculated as shown in table 4.8 and table 4.9

Table 0.8 Experimental strain

Load	Demec1	Demec2	Demec3	Demec4	Demec5
0	0.00908	0.00916	0.009317	0.00943	0.008814
3	0.009084	0.009148	0.00968	0.009793	0.009184
6	0.008979	0.009124	0.00972	0.009829	0.009608
9	0.008854	0.009076	0.009728	0.009874	0.010087
12	0.008685	0.009019	0.009809	0.009994	0.01068
15	0.008568	0.008971	0.009865	0.010172	0.01099
18	0.008447	0.008902	0.00993	0.010377	0.011296
21	0.008274	0.00883	0.009958	0.010446	0.01151
24	0.008116	0.008773	0.009994	0.010615	0.011703
27	0.007923	0.008644	0.010023	0.010704	0.011969
30	0.007742	0.008616	0.010051	0.010909	0.012231

Table 0.9 Experimental compressive stress

Load	ComStrs d1	Com Std2	Comstd3	Comstd4	Comstrd5
0	0.2360693	0.238165	0.242251	0.245185	0.229154
3	0.2361741	0.237851	0.251682	0.254615	0.238794
6	0.2334498	0.237222	0.252729	0.255558	0.249796
9	0.2302017	0.235965	0.252939	0.256711	0.262264
12	0.2258009	0.234498	0.255035	0.259854	0.277667
15	0.2227623	0.23324	0.256501	0.264465	0.285735
18	0.2196189	0.231459	0.258178	0.269809	0.293698
21	0.2151133	0.229573	0.258911	0.27159	0.299252
24	0.2110269	0.228106	0.259854	0.275991	0.304281
27	0.2059975	0.224753	0.260588	0.278296	0.311197
30	0.2012824	0.22402	0.261321	0.283639	0.318007

The design ultimate moment for each beam were calculated according to BS8110-1:1997 cl 3.4.4.4, as the code propose the following

Equation;

$$M = 0.156 b d^2 f_{cu} \text{-----(4.1)}$$

Where:

- M= Ultimate design moment.
- b = width of the section.
- d = effective depth of the tension reinforcement.
- f_{cu} = compressive strength of the concrete.

4.12.2 Mathematical theory for Aer-Tech Beam Test

The Aer-Tech beam test

A (2T10) beam covered with Aer-Tech material

From Tables $E_c = 26 \text{ kn/mm}^2$, $d = h - 23 = 180 - 23$

$\Phi = 10 \text{ mm}$, $b = 78 \text{ mm}$, $d = 157 \text{ mm}$

$M = E_s / E_c = 200 / 26 = 7.69$

$A_s = [\pi \times 10^2 / 4 \times 2] = 157 \text{ mm}^2$

Now Taking moment about the neutral axis

$$B \times y(y/2) = m \times A_s(d - y) \text{-----(4.2)}$$

$$78 \times y(y/2) = 7.69 \times 157(157 - y)$$

$$39y^2 = 1207.3(157 - y)$$

$$39y^2 + 1207.3y - 189550.1 = 0$$

Solving the above using the quadratic formula.

$$Y = \frac{-b \pm \sqrt{b^2 - 4ac}}{2a} \text{-----(4.3)}$$

$$Y = 37.79 \text{ mm}$$

$$I_{NA} = b \times \frac{y^3}{3} + m \times A_s(d - y)$$

$$I_{NA} = 1.55 \times 10^6$$

$$\text{Where, Moment } m = \frac{Wa}{2} \text{-----(4.4)}$$

Table 0.10 Load and moment

Load(KN)	Moment(KNmm)
3	600
6	1200
9	1800
12	2400
15	3000
18	3600
21	4200
24	4800
27	5400
30	6000

Now to obtain the theoretical compressive stress, substitute the derived moment into the equation below;

$$F = \frac{M \times y}{I_{NA}} \text{-----(4.3)}$$

Table 0.11 Load and theoretical compressive stress

Load	Theoretical Compressive stress
0	0
3	0.01463
6	0.02925
9	0.04388
12	0.05851
15	0.07314
18	0.08777
21	0.10239
24	0.11703
27	0.13166
30	0.14628

4.12.3 Aer-Tech mid span deflection of beam

Using the Macaulay's method of mid- span deflection.
Hence, taking the maximum bending moment at section x.

$$M_x = \frac{wx}{2} - \frac{w}{2}(x - a) - \frac{w}{2}(x - 2a) \text{-----(4.4)}$$

Integrate the above equation $(\int \frac{wx}{2} - \frac{w}{2}(x-a) - \frac{w}{2}(x-2a)$

$$\frac{dy}{dx} = \frac{wx^2}{4} - \frac{w}{4}(x-a)^2 - \frac{w}{4}(x-2a)^2 + A \text{-----(4.5)}$$

Taking 2nd integration to get the deflection $(\int \int \frac{wx^2}{4} - \frac{w}{4}(x-a)^2 - \frac{w}{4}(x-2a)^2 + A)$

$$\frac{dy^2}{dx^2} = \frac{wx^3}{12} - \frac{w}{12}(x-a)^3 - \frac{w}{12}(x-2a)^3 + Ax + B \text{-----(4.6)}$$

Boundary condition

$$X=0; \delta=0;$$

$$X=L; \delta=0; X=3a$$

By substitution:

$$0 = \frac{w}{12}(3a)^3 - \frac{w}{12}(3a-a)^3 - \frac{w}{12}(3a-2a)^3 + A(3a) \text{-----(4.7)}$$

$$27 \frac{w}{12}(a)^3 - 8 \frac{w}{12}(a)^3 - \frac{w}{12}(a)^3 + A(3a) = 0 \text{-----(4.8)}$$

$$\frac{18}{12}wa^3 = -(3a)A \text{-----(4.9)}$$

$$A = -\frac{18}{36}wa^2 \text{-----(4.10)}$$

$$\text{And when } x = \frac{l}{2}; a = \frac{l}{3}$$

$$y = -\frac{1}{EI} \left[\frac{w}{12} \left(\frac{l}{2} \right)^3 - \frac{w}{12} \left(\frac{l}{2} - \frac{l}{3} \right)^3 - \frac{w}{12} \left(\frac{l}{2} - 2 \frac{l}{3} \right)^3 - \frac{18w}{36} \left(\frac{l}{3} \right)^2 \frac{l}{2} \right] \text{-----(4.11)}$$

$$y = -\frac{1}{EI} \left[\frac{wl^3}{96} - \frac{w}{12} \times \frac{l^3}{216} - \frac{w}{12} \left(-\frac{l}{6} \right)^3 - \frac{18wl^3}{648} \right] \text{-----(4.12)}$$

$$y = -\frac{1}{EI} \left[\frac{wl^3}{96} - \frac{18wl^3}{648} \right] \text{-----(4.13)}$$

$$Y = \frac{45wl^3}{1342EI} \text{-----(4.14)}$$

Thus, deflection Y for the Aer-Tech beam = $\frac{45wl^3}{1342EI}$

Thus, table 4.12 shows values of experimental deflection

Table 0.12 Load vs central deflection and theoretical stress

Load (KN)	Central deflection (experimental Defln) mm	Theoretical deflection mm
0	0	0
3	0.5	0.889
6	0.91	1.779
9	1.36	2.669
12	1.87	3.56
15	2.28	4.45
18	2.77	5.33
21	3.48	6.22
24	3.93	7.11
27	4.59	8.01
30	5.22	8.00

The theoretical ultimate deflection is $\left[\frac{span}{250}\right]$ and for this experiment $\left[\frac{1500}{250}=6\text{mm}\right]$.

Therefore, ultimate deflection = 6mm.

Calculating the ultimate load using BS8110

Taking the following from tables;

$$F_{cu}=30\text{N/mm}^2, f_v=460\text{N/mm}^2, f_{cm}=30+1.64=43.12$$

$$B=78\text{mm}, A_s=157\text{mm}^2 \text{ and } d=157\text{mm}$$

Hence,

$$M_u = 0.156 F_{cu} b d^2 \text{ -----(4.15)}$$

$$= 0.156 \times 30 \times 78 \times (157)^2 = 8.421 \times 10^6 \text{Nmm}$$

Now substituting m_u in

$$W = \frac{2m_u}{a} \text{ (where } a=500) \text{ -----(4.16)}$$

$$W = \frac{2 \times 8.997 \times 10^6}{500}$$

$$W = 36.0 \text{ kN}$$

Therefore, theoretical ultimate design load = 36.0kN, whereas experimental failure load is 38.7kN

Table 4.12 shows that the experimental moment achieved is higher than the ultimate moment according to British standards that could be because Aer-Tech concrete has lower elastic modulus than normal concrete, thus it is less stiff than normal concrete. It should be observed that the constant 0.156 in the above equation comes out by multiplying the ultimate stress block of the concrete by the lever arm, and the BS 8110-1997 state the following equation to calculate the ultimate stress block:

Table 0.13 Theoretical stress and experimental stress

Load	Theoretical compressive Stress	Experimental Compressive stress for d1	Experimental Compressive stress for demec5
0	0	0.2360693	0.229154
3	0.014628	0.2361741	0.238794
6	0.02925	0.2334498	0.249796
9	0.04388	0.2302017	0.262264
12	0.05851	0.2258009	0.2777667
15	0.07314	0.2227623	0.285735
18	0.08777	0.2196189	0.293698
21	0.10239	0.2151133	0.299252
24	0.11703	0.2110269	0.304281
27	0.131655	0.2059975	0.31197
30	0.14628	0.2012824	0.318007

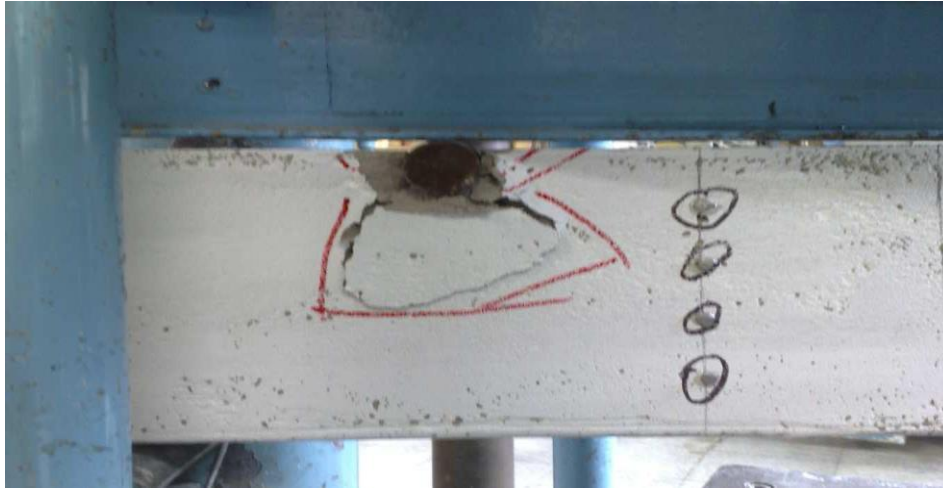


Figure 0.6 Signs of Diagonal failure

4.13 Beam behaviour in service and collapse

Considerable steps had been taking by the researcher to properly access structural performance of Aer-Tech novel material. Interestingly, the Aer-Tech beam test had provided a clearer view of how the material behaves in serviceability and collapse of its reinforced beams. Ultimately, all beams showed typical structural behaviour in flexure. Also, during the test of the three beams no horizontal cracks were observed at the level of the reinforcement, which confirms non-occurrence of bond failure. However, vertical flexural cracks were observed in the constant moment region and final failure occurred due to crushing of compression Aer- Tech material and breaking of steel reinforcement on application of significant amount of ultimate deflection.

4.13.1 Deflection Behaviour Of Aer-Tech Singly Reinforced Beam

The table 4.12 had shown that experimental ultimate deflection is lower than the theoretical ultimate deflection. The illustration in figure 4.17 confirms that the relationship between load and deflection is linear. Which further illustrate that as load increases the beam deflection increases. This is true because tensile stress

increases down the neutral axis to the bottom of the beam, where the reinforced bars are positioned.

More so, from material investigation of Aer-Tech material, this novel material is said to be a less dense and porous material, which practically influences the stiffness of Aer-Tech material. Essentially, these effects had made Aer-Tech to exhibit low modulus of elasticity, which primarily is governed by the stiffness of coarse aggregate in mix. Consequently, the result of deflection of Aer-Tech reinforced beam under the design service load is acceptable, irrespective of low modulus of elasticity, since its values were within the serviceability limit of BS 8110-1:1997 cl 3.4.6.3, as the code specified that the deflection should be less than $[\text{Span}/250]$ and for this experiment $[1500/250 = 6\text{mm}]$.

Comparably, it is observed that Aer-Tech reinforced beam exhibit similar behaviour to that of other lightweight concrete beams (Swamy and Ibrahim, 1975)

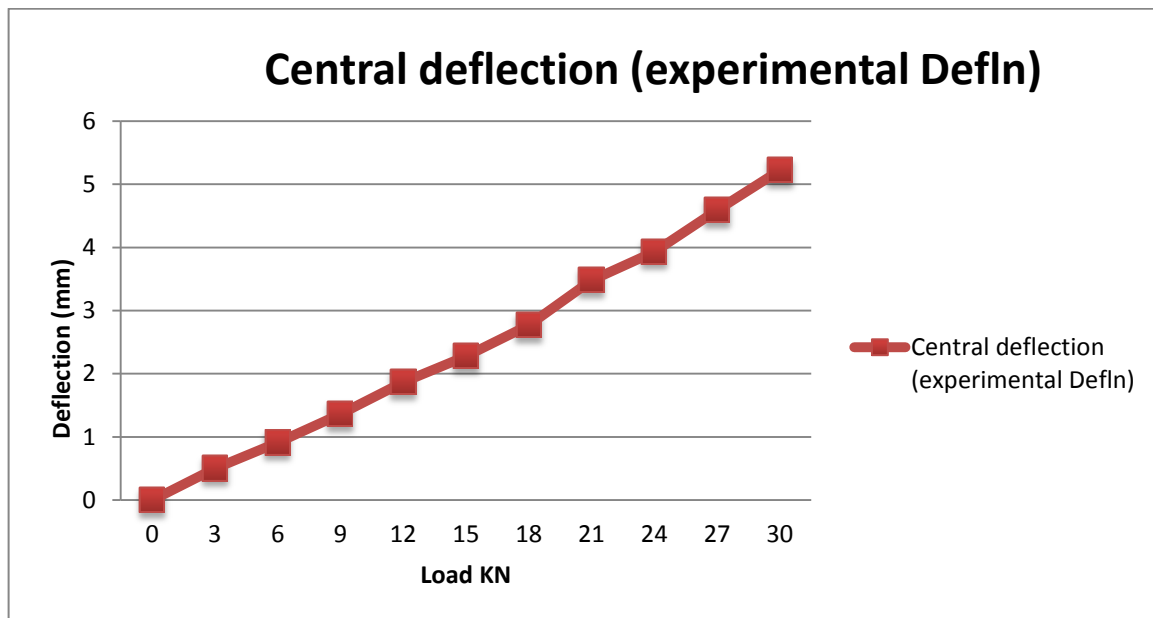


Figure 0.17 Experimental Deflection/Load

4.14 Reinforced Aer-Tech Material Strains and compressive stress

The strain results on reinforced Aer-Tech beam were measured in every load increments. The strain distribution results are presented in table 4.8.

More so, at the given service load of 3KN to 30KN the strain results range from $2283 \times 0.403 \times 10^{-5}$ to $3035 \times 0.403 \times 10^{-5}$. Whilst the measured strain just prior to failure varied from $3198 \times 0.403 \times 10^{-5}$ to $3231 \times 0.403 \times 10^{-5}$ respectively, figure 4.20 shows the strain distribution effect in Aer-Tech material on application of load. The strain diagram confirms that strain occurs across the depth of the beam. The illustration in figure 4.20 show clearly that demec strain reading does reduces at the top on increasing load for demec 1 and 2 , but increases as load increases on demec 3,4 and 5. This behaviour is supported by the bending theory that plane section of a structural member remains plane after straining. Importantly, results obtained are consistent with works of other researchers (Delsye C.L. Teo, Md. Abdul Mannan and John V. Kurian,2006)

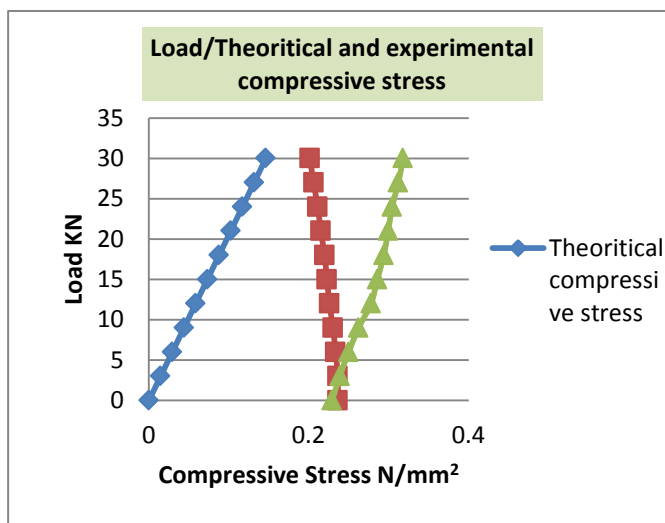


Figure 0.18 Load Against Experimental & Theoretical compressive Stress

The illustration on figure 4.18 shows that the theoretical compressive stress and experimental stress of demec 5 are directly proportional to load application. Explicitly, what happens is that the greater the load application on an Aer-Tech material the higher the compressive stress effect developed.

More so, this significant structural behaviour of Aer-Tech material do lead to first appearance of cracks at the bottom of the reinforced Aer-Tech beam. As the load increases from 3KN to 12KN the initial slight crack appearance becomes more noticeable. These cracks are simply known as diagonal tension cracks. The structural effect of Aer-Tech material conforms with the analogy as stated in (Moseley, Hulse and Bungey.1999) which states that where ever tension occurs in a material, strongly indicates greater chances of crack appearance within same place.

Comparatively, the values from the table 4.13 and figure 4.19 was drawn, using the values of experimental strain at the top surface of the beam (demec 1) and the bottom base of the beam (demec 5) by calculating the theoretical result using $f = E_c \times \epsilon_c$ from the figure and the table, it could be observed that the theoretical results are lower than the experimental ones and that could be because the material matrix is getting disturbed, or it could be because the theoretical values are values without any losses that could be due changing the area of the beam surface or due to shrinkage.

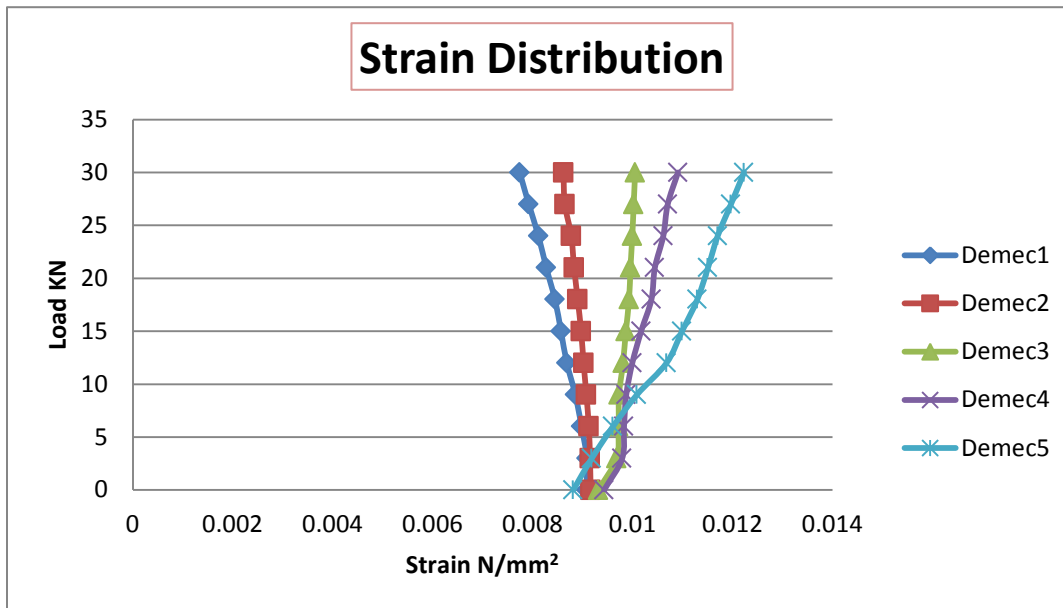


Figure 0. 19 Load Against Strain

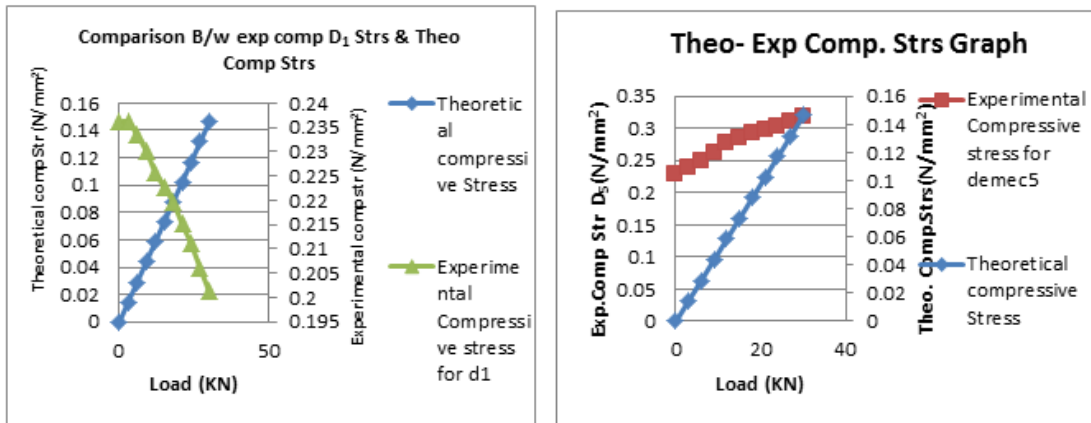


Figure 4.20 Load against compressive stress demec 13& 5

4.14.1 Reinforced Aer-Tech beam Ductility Behaviour

Ultimately, the ductility of reinforced Aer-Tech beam is important in justifying structural capability of the material, because from structural standard it is paramount for a ductile structural material to undergo large deflection at near maximum load carrying capacity, by providing ample warnings to an impending failure. The displacement ductility ratio is taken in terms of $\mu = \Delta_u/\Delta_y$, which is the ratio of ultimate moment to first yield deflection. Where Δ_u is the deflection at ultimate moment and Δ_y is the deflection when the steel yields. In general, high ductility ratio confirms that structural member is capable of undergoing large deflection prior to failure. Consequently, the result of this investigation on Aer-Tech reinforced beam ductility, shows that Aer-Tech material possess relatively good ductile characteristics as beam shows clear signs of cracks on beam long before failure. This can be attributed to its inherent pore structure formation due foam content.

4.15 Modes of failure

The figure 4.22 had shown Aer-Tech reinforced beams mode of failure, whilst Figure 4.21 shows clearly the loading of Aer- Tech singly reinforced beam. Consequently from figure 4.22, the beam failed in total bending. The ultimate experimental failure load of Aer-Tech material is 38.7 KN, whilst the theoretical calculated ultimate load is 36 KN. The nearness of experimental and theoretical failure load confirms structural capability of Aer-Tech material.

Appreciably, the theoretical failure load calculated in accordance to BS8110 is lower than the failure load derived from the lab. Their differences are probably caused by the assumption that the compressive and tensile forces were equal. However, the strain distribution diagram shows that strain at the bottom is greater than the strain at the top. Apparently, what happens is the theoretical failure may not have taken into account that the tensile stress is still subjected to the reinforcement bars after the concrete has cracked. Whilst, in case of the experimental failure load a higher experimental failure load was achieved, since the steel reinforcement in the beam continue taking the tension developed until it reaches its ultimate yielding point where it no longer could with stand any further load increase, it therefore breaks at a higher ultimate failure load as compared to theoretical failure load.

But by measuring the angle of the crack in figures 4.22 it was found to be 35° which indicated that the beam failed in combined mechanism of bending and shear stresses.



Figure 4.21 beam on loading

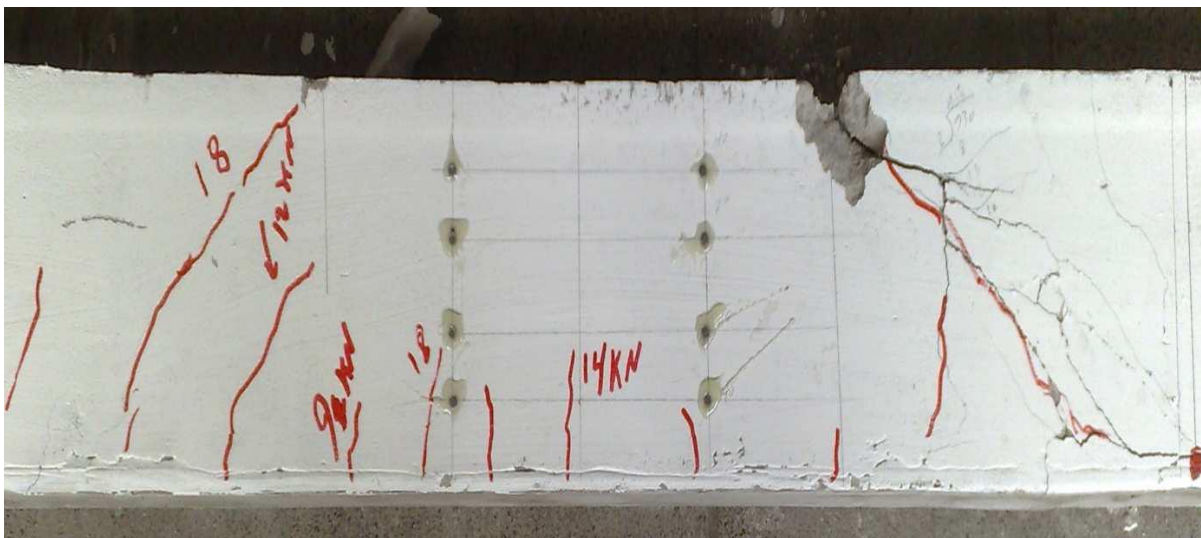


Figure 0.22 Mode of failure for reinforced beam Mix 4

4.16 Analysis of Aer-Tech Neural Network

The Aer-Tech neural network developed in this research is used to predict compressive strength values of 300 Aer-Tech material mix design values. During this process a total of 300 specimen values for 7, 14, 28 and 56 days

compressive strength is passed through the matlab with 280 of them classified as training input and target values. The remaining are graded as testing input and target values. The overall performance of the training values and the corresponding testing set are seen in figure 4.23.

At the end of the training process, the neural network consisted of 2 hidden layers, one input layer and one output layer.

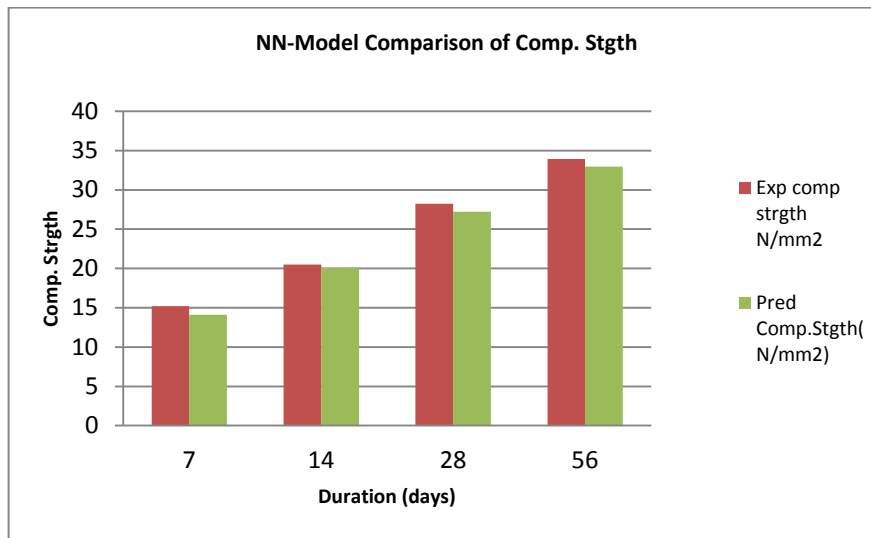


Figure 4.23 Comparison of experimental comp Str& NN Model Pred Comp.Str

Comparatively, the trained network is used to simulate some variable data's of cement, sand, foam, catalyst, and water, in order to subsequently predict the compressive strength and density.

Figure 4.23 clearly shows, that simulated compressive strength is approximately the same values with experimental compressive strength. This is a major breakthrough for Aer Tech NN model to efficiently predicts compressive strength. Appreciably, the results of these simulations and the general performance of the Aer-T neural network have given rise to the following conclusion:

- The simulation analysis has demonstrated the Aer-Tech neural network can effectively be used to predict target compressive strength and density. The simulation process has also pick up some major dependencies of Aer-tech material, which indicate that the binder/water ratio was a key factor influencing strength of Aer-Tech material.
- The trained Aer-Tech neural network model, which was trained with about 300 experimental data's of Aer-Tech constituent material and corresponding output of compressive strength and density, can make better and realistic prediction of varying mix compressive strength and density.

4.17 Analysis for the scanning electronic microscopy

4.17.1 Void Characteristics Of Aer-Tech using the SEM

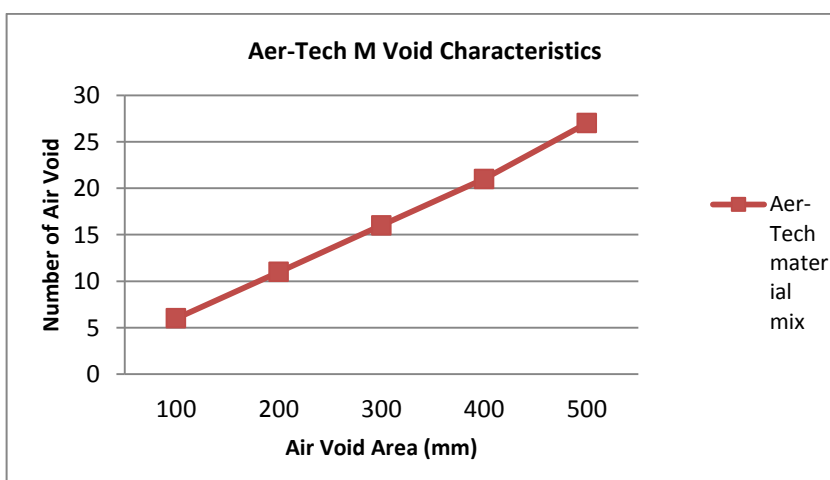


Figure 0.24 Aer-Tech Void characteristics

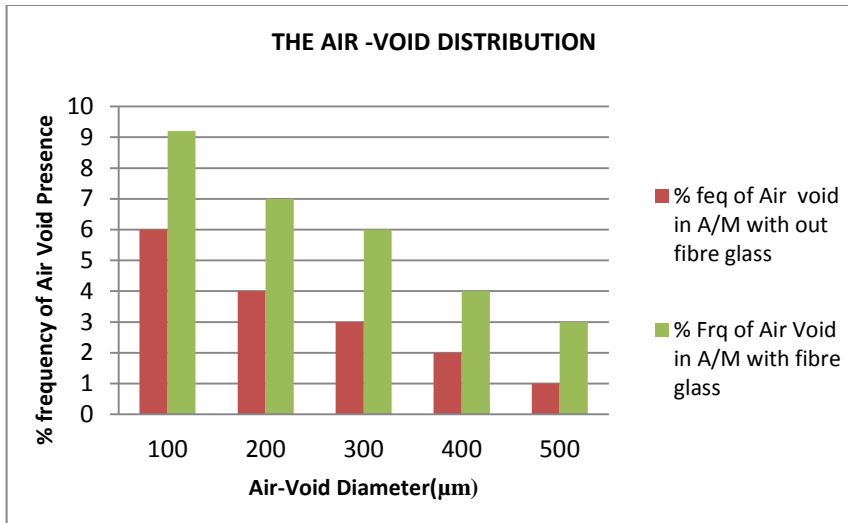


Figure 0.25 Air Void Distribution

The number of visible air-void sizes in figure 4.24 shows that the billions of the Aer-Tech air void are of uniform size, embedded in close microstructure of the material. There are a few bigger sized pores present and their number also increases with an increase in foam volume, which may be due to the possibility of merging and overlapping of pores at higher foam content.

Also, referring to distribution of air void in figures 4.24 and 4.25, at low dosage of foam volume the air-void distribution is more uniform than at high foam volume content. This material behavior of Aer-Tech specimen conforms to findings in literature that says that uniformity is relatively predominant in foam concrete with cement–fly ash mixes as compared to cement–sand mixes such that at higher foam volume, merging of bubbles results in wide distribution of voids sizes leading to lower strength. (Nambiar and Ramamurthy, 2007).

Comparatively, figure 3.16 and fig 3.17 had shown that images of scanning electronic microscopy of Aer-Tech material specimen with and without fibre mesh contains air void.

This comparison is further illustrated in figure 4.25, where percentage frequency of air void distribution is shown to be higher for Aer-Tech mix with fibre glass, hereby confirming clear signs of merging and overlapping of air bubble due to presence of fibre glass.

Whilst in a similar fashion a more uniform distribution is observed in the images of Aer-Tech mix without fibre glass and reduced percentage of air –void present in Aer-Tech mix without fibre glass, confirming evidence that Aer-Tech product has a pore structure which consist of gel pores, capillaries, and millions of air – entrained and entrapped pores which do not collapse, but coalesce on application uni axial force.

4.17.2.Air-void shape parameter

For a cellular material like Aer-Tech the shape is an important parameter in strength determination. The shape factor defines the geometry of the voids and is a function of outer perimeter and surface area for each void obtained through image analysis and is given by

$$\text{Shape factor (SH)} = \frac{\text{Perimeter}}{4\pi} \text{Area}$$

Shape factor equals unity for a perfect circle and is larger for irregular shaped voids.

Considerably, from the figure 3.16 and figure 3.17 it is evident that shape of the voids present is similar, appearing in an ellipsoidal oriented pores shape. Whereas only negligible number of voids are having irregularity due to merging of air voids at higher foam volume.

4.17.3 Air-void spacing factor

The SEM had also measured the smallest distance through the matrix between two voids in both figures 3.16 and 3.17. This air void spacing parameter is an important factor in determination of strength and density of Aer-Tech material as it gives a clear range of vicinity where the air void are located. From the images It is observed that for mix without fibre the air void space are seen to be very high, whereas for mix with fibre the air void spacing are relatively very small as compared to the former. This particular observation confirms reason why strength of Aer-Tech material with fibre glass tend to be low, following evidence of close proximity in air void spacing.

It is important to note that as the pore volume fraction of foam increases, the structure progresses from closed cell to reticulated as windows (perforations between cells) form and widen. The important observation is that even with the porosity above 90%, the foam is almost entirely closed cell.

4.1 Particle size Analysis data for Aer-Tech material composition

Figures 4.26 to 4.28 show particle size analysis for the Aer-Tech material for two set of mixes. Figure 4.26 and 4.27 shows clearly the graphic behavior of a mix without fibre glass. It is imperative to say that from the graph the particle size distribution had shown that the highest sieve volume for maximum material size within the ranges of 100-1000micrometre did not exceed a percentage volume presence of 5. Intrinsically, this had confirmed that lack of fibre glass in mix allows a homogeneous size distribution.

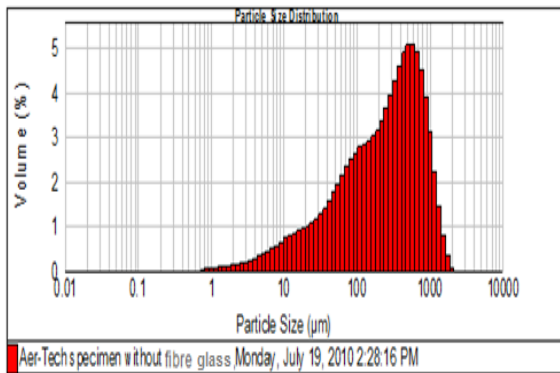


Figure 4.26 Mix without Fibre glass

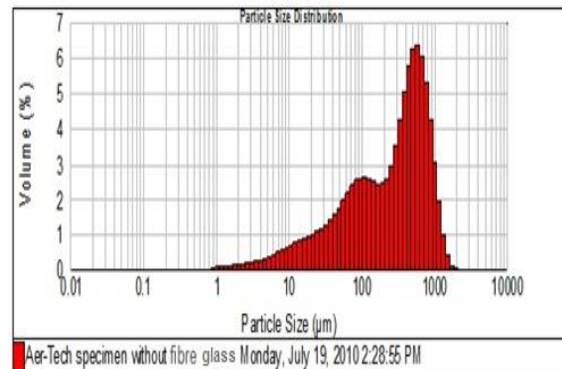


Figure 4.27 Mix without Fibre glass

Whilst, figure 4.28 and 4.29 are Aer Tech mix with fibre glass, their particle size distribution analysis has graphically shown that the mix has higher percentage volume maximum material size through sieve than that of the Aer- Tech material mix without fibre glass. Precisely, while the Aer-Tech mix without fibre glass do not exceeds 5 in its particle size distribution by percentage volume of material within a range of 100-1000micrometre, its corresponding mix with fibre glass exceeds 5 towards 7 by percentage volume of material passed through the sieve.

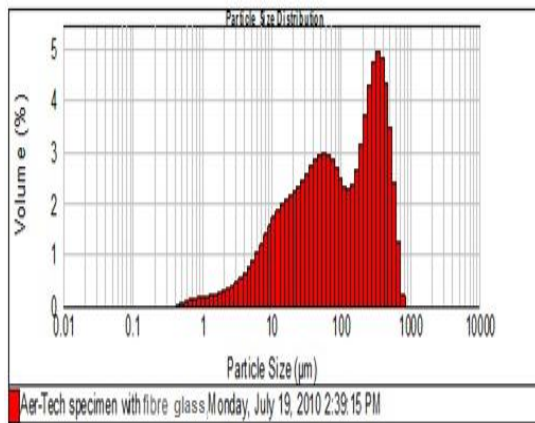


Figure 4.28 Mix with Fibre glass

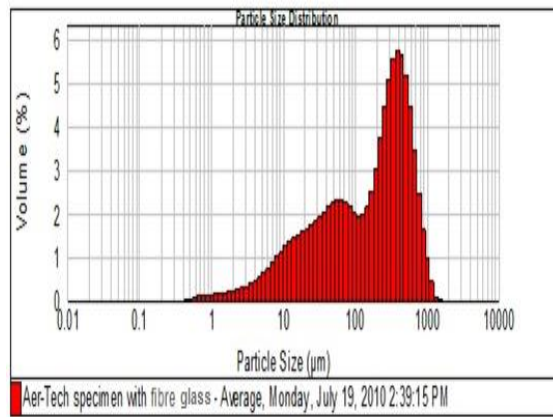


Figure 4.29 Mix with Fibre glass

5 Chapter five: Conclusion

The main intention of this thesis was to investigate the material and structural properties of Aer-Tech material through the use of experimental methods and computational methods.

Intrinsically, researcher commitment to achieving overall research objectives and aim for this research work. Using his experimental findings has shown that all the proposed objectives were achieved and several findings emerged, bringing with them new ideas about this novel material called Aer-Tech.

Precisely, chapter four of this thesis present the findings of laboratory experiment carried out using Aer-Tech concrete specimen. Generally, it comprises of more than seven hundred specimen from eighty different mixes.

More so, the enormous number of specimen taken in this research is aimed at deriving better understanding of the material properties and structural behaviour of Aer-Tech material. The author with a clear objective had structured this research work into three basic segments, the first segment focuses in describing the material properties of Aer-Tech material and overall literature review for aerated concrete, the second part aimed at critically accessing the material and structural properties of the material, through experimental methods. Whereas, the third section focuses on results, findings and calculations for the research work on Aer-Tech novel material.

Apparently, the first segment through the under listed laboratory test on Aer-Tech specimen, had critically accessed the material behaviour of Aer-Tech material.

The tests are as follows;

- Compressive strength test- Aimed at testing the compression capability of material.
- Flexural test- Aimed at accessing the flexural performance of the material.
- Scanning Electronic Microscopy.
- Particle size analysis test.

Ultimately, the findings from the above mentioned test had brought to limelight some outstanding scientific contribution to material behaviour of a cellular concrete.

5.1 Overall Material Behaviour Of Aer-Tech Novel Material

From this chapter the following could be concluded:

- Overall, test result has shown that density of the material controls all of its properties such as fresh state properties, mechanical properties, functional and acoustic properties, as the density of the material is controlled by changing the foam proportion and the water content in any given mix composition of Aer-Tech material.
- The Aer- Tech material density decreases as time increase, thus it is said to be inversely proportional to time, whilst its corresponding compressive strength is directly proportional to time.
- The initial low compressive strength was due to poor machine calibration

- Overall studies from compressive strength experiment had shown that Aer- tech material strength increase as ages increases.
- The Aer- Material had given up to 33N/mm^2 compressive strength for a 56days test. This is a very outstanding result as material strength is comparable to conventional concrete.
- The material has a higher elastic modulus than normal cellular concrete.
- Aer-Tech material with fibre glass, has a higher flexural strength than the Aer-Tech material without fibre glass.
- Fresh state of Aer-Tech material is more workable than normal concrete which made of aggregate.
- The scanning electronic microscopy test had shown images of the micro structure and pore structure of Aer- tech material with fire glass and that without fibre glass, the analysis of these captured internal structure of Aer Tech material had confirmed that the presence of fibre glass in material mix greatly distort the micro structure of the material. The effect leads to merging and overlap of air cells.
- Findings had shown that records of low compressive strength in Aer- Tech mixes with fibre and plasticizers are due to distortion in micro structure and reaction of plasticizers with foam.
- The particle size test had confirmed that Aer-Tech material without fibre glass do not exceeds 5 on the percentage by volume of particle size distribution, whilst the Aer-Tech material with fibre glass spans above 5 and 6.

- Aer- tech material NN- Model had predicted compressive strength and density similar to corresponding experimental compressive strength and density

5.2 Overall Structural Behaviour Of Aer- Tech Reinforced Beam

The experimental investigation of reinforced Aer-Tech beam has shown that Aer-Tech structural behaviour is comparable to other lightweight concrete. Below are some of the conclusions made, based on current experimental results.

- Structural assessment Aer-Tech material has shown that the Aer-Tech beam suffered tension at the bottom and compressive forces at the top, which resulted in the diagonal tension cracks being produced mid-span at the bottom of the beam.
- Also result of reinforced Aer-Tech beam had shown that as load application increases on beam the tension on the steel reinforcement increases until failure occurs.
- The experimental performance of 28 days Aer –Tech beam test, has shown that the experimental ultimate moments of Aer-Tech reinforced beam is 3.62% higher than the theoretical ultimate moments.
- The deflection of Aer-Tech material calculated using BS8110 under service load can be used to give reasonable predictions. Precisely, the deflection under the service load for singly reinforced beams, were within their allowable limit provided by BS8110.

- Importantly, the Aer-Tech reinforced beam test gave a high elastic modulus of 9.23 MPa, an indication Aer-Tech material has flexural capability.

5.3 Over All Scientific contribution of Thesis

These scientific contributions are as follows;

- Material density is a key determining factor in Aer-Tech material behaviour.
- Recent results of Aer-Tech material compressive strength had shown proved that consistent water-cement ratio of mix 4.78:1 gives rise to higher compressive strength.
- Aer- Tech material had shown high compressive strength of about 33N/mm² higher than any known cellular material.
- From the Scanning electronic microscopy, pictures showing microscopic structure of Aer-tech material with fibre mesh and that of Aer-tech material without fibre mesh had confirmed that the presence of fibre in Aer-Tech mix clearly distort the expected closed cell structure of air void in the mix.

- The presence fibre in Aer-tech mix, mostly result into reduction in compressive capability in the material.
- The particle size test had confirmed that Aer-Tech material composition is greater within the particle size range of 100-1000µm.
- Reinforced Aer-Tech material is confirmed as a good structural material. The singly reinforced beam had deflected within the serviceability limit criteria in accordance to BS8110.
- Reinforced Aer-Tech material is a good ductile material to have displayed pending failure before, it finally ruptured.

5.4 Recommendations for future research

The author recommends for the future researches which will continue from this research to check the following areas:

- It is recommended to investigate the consistency in compressive strength of Aer-Tech material.
- Investigate the Aer-Tech material with different mixes, such as fly arch and fibre (steel and glass).
- Investigate structural behavior of Aer-Tech material by undertaking flexural tests of beams.
- In the literature review it was mentioned that the curing method affect the properties of cellular concrete, so it is recommended to investigate the behaviour of Aer-Tech concrete using different method of curing. Specifically, the autoclaving method of curing.

- It is recommended to test the material after the machine get calibrated, and check the different in results with the results that is presented in this research.
- It is recommended to test slabs that are made of Aer-Tech material, be critically investigated for its structural behaviour.

Reference

- V. Deligiannis, S. Manesis, J. Lygeros, (2005). Global automata: a new formal method for modeling industrial systems, *International Journal of Industrial and Systems Engineering*, underscience, in print.
- Deligiannis and S. Manesis, J. Lygeros.(2005).Automata composition for modeling large industrial systems, *CIMCA Proceedings of the International Conference on Computational Intelligence for Modeling Control and Automation*, IEEE Computer Society Press, Vienna, Austria (2005) (November 28–30).
- R.C. Valore. (1954). Cellular concrete part 2 physical properties, *ACI J***50** pp. 817–836.
- ACI Committee 213.2003
- Mc Cormick FC.(1967). Rational proportioning of preformed cellular concrete *ACI Material Journal*;8(3)111-
- M.R. Jones and A. McCarthy.(2005). Preliminary views on the potential of foamed concrete as a structural material, *Mag Concr Res***57** pp. 21–31
- M.R. Jones and A. McCarthy, (2005). Utilizing unprocessed low-lime coal ash in foamed concrete, *Fuel***84** pp. 1398–1409.
- Durack JM, Weiqing, L.(1998). The properties of foamed air cured fly ash based concrete for masonry production. In: Page A, Dhanasekar M, Lawrence S, editors. In: *Proceedings of 5th Australian masonry conference*. Australia: Gladstone, Queensland; p. 129–38.
- Aldridge D, Ansell T.(2001). Foamed concrete: production and equipment design, properties, applications and potential. In: *Proceedings of one day seminar on foamed concrete: properties, applications and latest technological developments*. Loughborough University;
- S. Van. Deijk, (1991). Foam concrete, *Concrete* (August) pp. 49–53.
- O.P. Shrivastava. (1977), Lightweight aerated concrete – a review, *Indian Concr J* **51** pp. 10–23.
- Jones MR. (2001). Foamed concrete for structural use. In: *Proceedings of one day seminar on foamed concrete: properties, applications and latest technological developments*. Loughborough University; p. 27–60.
- W.H. Taylor.(1969). *Concrete technology and practice*, Angus and Robertson, London

- T.G. Richard.(1977). Low temperature behaviour of cellular concrete, *ACI J***74** pp. 173–178
- C.T. Tam, T.Y. Lim and S.L. Lee.(1987), Relationship between strength and volumetric composition of moist-cured cellular concrete, *Mag Concr Res***39** pp. 12–18
- E.P. Kearsley and P.J. Booyens(1998). Reinforced foamed concrete, can it be durable, *Concrete/Beton***91** pp. 5–9.
- Kyle D. (2001). Manufacture and supply of Ready mix C4 top foamed concrete. In: Proceedings of one day seminar on foamed concrete: properties, applications and latest technological developments. Loughborough University; p. 19–26.
- M.R. Jones and A. Giannakou.(2002). Foamed concrete for energy-efficient foundations and ground slabs, *Concrete* pp. 14–17
- M. Madjoudj, M. Quenendec and R.M. Dheilly (2002). Water capillary absorption of cellular clayed concrete obtained by proteinic foaming. In: R.K. Dhir, P.C. Hewelett and L.J. Csetenyi, Editors, *Innovations and development in concrete materials and construction*, Thomas Telford, UK pp. 513–521.
- P.J. Tikalsky, J. Pospisil and W. MacDonald.(2004). A method for assessment of the freeze-thaw resistance of preformed foam cellular concrete, *Cem Concr Res***34** (5) pp. 889–893.
- E.K.K. Nambiar and K. Ramamurthy.(2007), Sorption characteristics of foam concrete, *Cem Concr Res***37** pp. 1341–1347
- H. Weigler and S. Karl.(1980), Structural lightweight aggregate concrete with reduced density – lightweight aggregate foamed concrete, *Int J Lightweight Concrete***2** (), pp. 101–104.
- M.S. Hamidah, I. Azmi, M.R.A. Ruslan, K. Kartini and N.M. Fadhil. (2005). Optimisation of foamed concrete mix of different sand – cement ratio and curing conditions. In: R.K. Dhir, Newlands, MD and A. McCarthy, Editors, *Use of foamed concrete in construction*, Thomas, London
- C. Hall. (1989), Water sorptivity of mortar and concretes: a review, *Mag Concr Res***41** pp. 51–61.
- M.A. Wilson, W.D. Hoff and C. Hall. (1991).Water movement in porous building materials- Absorption from a small cylindrical cavity, *Build Environ***26** pp. 143–152.
- R.C. Valore. (1954). Cellular concretes—Part I. Composition and methods of preparation, *J Am Concr Inst***25** (9), pp. 773–795.

- A. Short and W. Kinniburgh. (1978). *Lightweight concretes*, Applied Sciences Publishers, London
- Durack JM, Weiqing L.(1998). The properties of foamed air cured fly ash based concrete for masonry production. In: Page A, Dhanasekar M, Lawrence S, editors. *Proceedings of 5th Australasian Masonry Conference*, Gladstone, Queensland, Australia,. p. 129–38.
- E.P. Kearsley and M. Visagie. (1999). Micro properties of foamed concrete, *Proceedings of congress on creating with concrete (conference on specialist technology and materials for concrete construction)*, Dundee, Thomas Telford, UK, London pp. 173–184.
- P. Prim and F.H. Wittmann (1983). Structure and water absorption of aerated concrete. In: F.H. Wittmann, Editor, *Autoclaved Aerated Concrete, Moisture and Properties*, Elsevier, Amsterdam pp. 43–53.
- S. Tada and S. Nakano.((1983). Microstructural approaches to properties of mist cellular concrete. In: F.H. Wittmann, Editor, *Autoclaved Aerated Concrete, Moisture and Properties*, Elsevier, Amsterdam pp. 71–88.
- M.S. Goual, F. de Barquin, M.L. Benmalek, A. Bali and M. Queneudec. (2000). Estimation of the capillary transport coefficient of clayey aerated concrete using gravimetric technique, *Cement and Concrete Research***30** pp. 1559–1563
- M. Madjoudj, M. Queneudec and R.M. Dheilly. (2002). Water capillary absorption of cellular clayed concrete obtained by proteinic foaming. In: R.K. Dhir, P.C. Hewlett and L.J. Csetenyi, Editors, *Innovations and Development in Concrete materials and Construction*, Thomas Telford, U.K pp. 513–521
- Giannakou and M.R. Jones, Potentials of foamed concrete to enhance the thermal performance of low rise dwellings. In: R.K. Dhir, P.C. Hewlett and L.J. Csetenyi, Editors, *Innovations and Development in Concrete Materials and Construction*, Thomas Telford, U.K (2002), pp. 533–544
- M.R. Jones and A. McCarthy. (2005). Utilizing unprocessed low-lime coal ash in foamed concrete, *Fuel***84** pp. 1398–1409
- S. Kolas and C. Georgiou (2005). The effect of paste volume and of water content on the strength and water absorption of concrete, *Cement and Concrete Composites* **27** (pp.211–216.
- Andrew Short and William Kinniburgh. (1978). *lightweight concrete*, 3rd edition.

Paul J. Tikalsky, James Pospisilb, William MacDonald (2004). A method for assessment of the freeze–thaw resistance of preformed foam cellular concrete. INSTORN Material testing solution (2008). <http://www.instorn.com/> [20/may/2008].

JONES, M. R. & MCCARTHY, A. (2005). Preliminary views on the potential of foamed concrete as a structural material. *Magazine of Concrete Research*, 21-30.

KEASELY, E. P. & VISAGIE, M. (1999) Micro-properties of foamed concrete R.K. Dhir, N.A. Handerson (Eds.), *Specialist techniques and material for construction*, ThomasTeford.

ORCHARD, D. F. (1979) *Concrete Technology*, Applied science publishers LTD

ACI -116 (2000). *Cement and concrete terminology*, ACI Manual of concrete practice.

ACI Committee 213.(2003). *Guide for structural lightweight aggregate concrete*, American concrete institute.

AMZIANE, S., FERRARIS, C. F. & KOEHLER, E. P. (2005).measurement of workability of fresh concrete using a mixing truck. *National institute of standards and technology*.

ANON (1970) an introduction to lightweight concrete. *Cement and concrete association*.

Autoclaved Aerated concrete CEB manual of design and technology (1978): the construction press.

British Standards (1984): *Testing concrete – part 105: method for determination of flow BS1881*.

British Standards (1997): *Structural use of concrete – Part1: Code of Practice for Design and Construction. BS 8110-1*.

British Standards (2000): *Testing hardened concrete – Part4: Compressive strength –Specification for testing machines. BS EN 12390-4*.

British Standards (2000): *Testing hardened concrete – Part5: Flexural strength of test, specimens. BS EN 12390-5*.

British Standards (2003): *Testing hardened concrete – Part3: Compressive strength of test specimens. BS EN 12390-3*

British Standards (2006): *Products and systems for the protection and repair of concrete structures – Test methods – Determination of the modulus of elasticity in compression.BS EN 13412*.

Mosely W.H, Hulse R and Bungey J.H (1999). *Reinforced Concrete Design*. 5th edn

Swamy, R.N and Lambert,G. H.(1984). "Flexural behaviour of reinforced and prestressed solite structural lightweight concrete beams".

Demuth, H., Beale, M. and Hagan, M. (2008) Neural Network Toolbox™ 6 User's Guide.

Ahmet Oztas, Murat Pala, and M. A Bhatti. (2005). Predicting the compressive strength and slump of high strength concrete using neural network.

Lee SC.(2003) Prediction of concrete strength using artificial neural networks.

BAI J, WILD S,WARE JA, SABIR BB). *Using neural network to predict workability of concrete.* (2003)